Master's thesis

NTNU
Norwegian University of Science and Technology
Faculty of Engineering
Department of Energy and Process Engineering

Jason Gordon Foulkes

Future Low Emission Oil and Gas Platforms

Master's thesis in Natural Gas Technology
Supervisor: Petter Nekså, EPT
Co-supervisor: Rahul Anantharaman, SINTEF Energy Research
Sturla Sæther, Equinor ASA

June 2021

NTNU
Kunnskap for en bedre verden

Jason Gordon Foulkes

Future Low Emission Oil and Gas Platforms

Master's thesis in Natural Gas Technology
Supervisor: Petter Nekså, EPT
Co-supervisor: Rahul Anantharaman, SINTEF Energy Research
Sturla Sæther, Equinor ASA
June 2021

Norwegian University of Science and Technology
Faculty of Engineering
Department of Energy and Process Engineering

NTNU
Norwegian University of
Science and Technology

Norwegian University of Science and Technology

Faculty of Engineering Science and Technology
Department of Energy and Process Engineering

EPT-M

NTNU

MASTER WORK

for

Student Jason Foulkes

Spring 2021

Future low emission oil- and gas platforms

Fremtidens lavutslipps olje- og gass plattformer

Background and objective

There is an increasing concern related to climate change due to emissions of greenhouse gases. This has led to clear international and national targets for emission reductions. In Norway a major part of the emissions from the industry relates from offshore production of oil- and gas at the Northern Continental Shelf.

The governmental targets on emission reductions have led to ambitious reduction plans also from the oil- and gas companies. In January 2020, Equinor announced an unprecedented set of ambitions to reduce absolute greenhouse gas emissions from its operated offshore fields and onshore plants in Norway by 40% by 2030, 70% by 2040 and towards near zero by 2050. The ambition can be realised through electrification projects, energy efficiency measures and new value chains such as carbon capture and storage and hydrogen.

Offshore oil- and gas plants are complex process plants where certain duties related to power, heat and cooling must be satisfied. The duties may vary both on a short hourly timescale and over the lifetime of the production, as well as from platform to platform. Robustness in the process equipment and solutions is crucial, since down-time is very costly.

Introduction of low- or zero carbon solutions, e.g. combined cycle gas turbines or electrification, may to a very large extent influence the system design on the platform, overall energy efficiency, as well as cost of the operations.

The aim of this Master thesis work is to develop and apply a computer model that enables to evaluate how different modifications will influence the overall efficiency, CO_2 emissions as well as the ability to satisfy the required duties on oil- and gas platforms.

The following tasks are to be considered:

1. Literature survey related to offshore oil and gas production processes and options for low carbon power generation, including "green fuels".

Address
N-7034 Trondheim
Norway

Location
K. Hejes vei 1b

Tel. +47 73 59 38 60
Fax +47 73 59 35 80
Org. no. NO 974 767 880

2. Further development of a full platform model in Hysys to incorporate more detailed component models, e.g. related to glycol dehydration and pseudo-component physical properties, and prepare the model for evaluation of other generic platforms that may be both brown- and greenfield cases. The model should also be prepared to evaluate operation during the lifespan, e.g. with varying well compositions and operating conditions.
3. Define and implement calculation of Key Performance Indicators, KPIs, related to e.g. energy efficiency, CO_2 emissions and cost related parameters, e.g. parameters related to complexity; number of components and number of external interfaces or simplified cost functions found in the literature, as well as indicators related to weight and volume.
4. Perform simulations for two model platforms and verify the results towards data from real operation to the extent available.
5. Use the model to explore at least one possible scenario for a future low emission configuration and perform a sensitivity analysis based on assumptions made.
6. Make a draft scientific paper based on the work performed.
7. Propose a plan for further work.

-- “ --

Department for Energy and Process Engineering, January 15, 2021

_____

Adjunct Prof. Petter Nekså
Supervisor

Co-Supervisor(s):
Rahul Anantharaman, SINTEF Energy Research
Sturla Sæther, Equinor ASA

Abstract

This thesis investigates the use of energy-efficient technologies to reduce the quantity of CO_2 emitted by offshore platforms. To do this, an offshore oil and gas platform is modelled on a process simulation software called Aspen HYSYS.

The main emissions from offshore platforms arise from the use of gas turbines, which accounts for 85 % of the total emissions on the Norwegian Continental Shelf (NCS). Thus, the focus of this analysis was to investigate methods to recover waste energy on a typical platform on the NCS and to make the power generation units more efficient and emit fewer quantities of CO_2. A review of exergy analyses, conducted over the processing facility solely, recognised the production manifold, the recompression, and gas treatments trains as the largest sources of exergy destruction. Aside from energy losses within the processing system, the gas turbine exhaust gas was viewed as the most substantial waste stream on the platform. To recover and prevent the aforementioned losses, technologies such as bottom cycling, multi-phase expanders, waste heat CO_2 Rankine cycles, H_2 fuel blending, and wind energy are suggested.

The model was based on two platforms that are currently in operation on the NCS, Platform A and B. After development, the model was validated against real data for both scenarios. In each case, minimal deviations were illustrated. Hence, the output data from the model was deemed to be accurate. To compare the various impacts of the model modifications, key performance indicators (KPIs) were defined. These focused on the carbon footprint, energy efficiency, and operational costs (CO_2 tax and fuel cost).

To analyse the model, a platform lifespan scenario was developed. This was based on Platform B and was extended over a 30-year duration. Several combinations of the aforementioned technologies were analysed. Within the context of this platform, the use of steam bottoming cycles, H_2 fuel and wind energy was shown to be the most effective. Using these systems, a low emission scenario was developed. For the first 15 years of operation, a smaller more efficient gas turbine with a steam bottoming cycle and wind energy was implemented. Following the fifteenth year, H_2 fuel was introduced and the blend fraction was increased from 50 molar % to 90 molar % in the last period analysed. Over the entire 30 year lifespan, compared to the worst case, this scenario reduced CO_2 emissions by 2.7 Mtonnes and saved 6.0 billion NOK, translating to a 54 % and 48 % reduction respectively.

For further work on this topic, the addition of KPIs which consider capital cost and platform weight is recommended. Aside from this, an investigation into the use of a central power distribution hub is suggested.

Preface

This master thesis was written in spring 2021 at the Norwegian University of Science and Technology (NTNU) within the Department of Energy and Process Technology (EPT), as a fulfilment of a Master of Science in Natural Gas Technology. This project was within the HighEFF research group and was in conjunction with Equinor ASA and SINTEF Energy Research.

I would like to thank my main supervisor, Adjunct Professor Petter Nekså for help and guidance over the last year, it has been invaluable. In addition, I would like to thank Sturla Sæther and Lars Thuestad from Equinor; Rahul Anantharaman, Monika Nikolaisen, Mari Voldsund, and Juejing Sheng from SINTEF. The knowledge gained from our various meetings has been interesting and irreplaceable.

Contents

List of Figures

List of Tables

Acronyms

BC Bottoming Cycle. 47, 50, 52, 56, 67

BOE Barrel of Oil Equivalent. 40

CCS Carbon Capture and Storage. 17

CS Chao Seader. 25, 28

EOS Equation of State. 25, 28

GT Gas Turbine. 11

HP High-Pressure. 23

HRSG Heat Recovery Steam Generator. 10

KPIs Key Performance Indicators. 40, 41

LKP Lee-Kesler-Plocker. 25

LP Low-Pressure. 23

MEA Monoethanolamine. 18

MW Molecular Weight. 28–30, 32

NCS Norwegian Continental Shelf. 1

NG Natural Gas. 44, 45, 50

OE Oil Equivalent. 40

OTSG Once-through Steam Generator. 10, 56

PR Peng-Robinson. 25

RKS Redlick-Kwong-Soave. 25, 28, 29

ST Steam Turbine. 11

TEA Triethanolamine. 18

TEG Triethylene Glycol. 26

Nomenclature

$\dot{m}_{NG}$ Mass flowrate of the natural gas

$\dot{W}_{AUX}$ Power requirement of the auxiliary units in the BC (e.g. pumps)

$\dot{W}_{cc}$ Power output of a combined cycle

$\dot{W}_{compressor}$ Power requirement of the GT compressor

$\dot{W}_{GT,gross}$ Gross Power output of a gas turbine

$\dot{W}_{gt,net}$ Net Power output of a gas turbine

$\dot{W}_{H_2O/CO_2 turbine}$ Power output of either the steam of CO_2 turbine in the BC

$\dot{W}_{recovered}$ Power recovered by various energy-efficient technologies

$\dot{W}_{st}$ Power output of a steam turbine

$\dot{W}_{tot,compressors}$ Power requirement of all the platform compressors

$\dot{W}_{tot,heating}$ Total heating duty on the platform

$\dot{W}_{turbine}$ Power output of the GT turbine

$\eta_{CC,net}$ Net efficiency of the combined cycle

η_G Generator efficiency

η_{np} Efficiency of the unit

η_{TOT} Net efficiency of platform, related to the energy supplied to the system

ρ_{liq} Ideal liquid density

$C1$ Combination 1

$C_{CO_2\ Tax}$ Cost of carbon tax

C_{H_2} Cost of hydrogen

C_{NG}	Cost of natural gas
C_{Total}	Total operational costs
m_{hrsg}	Mass of the HRSG
P_c	Critical pressure
T_c	Critical temperature
T_{BP}	Boiling point temperature

Chapter 1

Introduction

1.1 Background and Motivation

Carbon emissions from the Norwegian Continental Shelf (NCS) account for appropriately one-quarter of the total emissions in Norway [1]. A direct result of the growing concern of climate change throughout the world, the Norwegian government has set strict emission reduction goals for the oil and gas sector. To align with these policies, Equinor has announced its ambition to reach carbon net-zero production by 2050 [2]. In addition, they have set a more recent goal to produce a barrel of oil that emits less than 8 kg of CO_2 [2].

To comply with these strict goals, energy-efficient measures, techniques and technologies must be employed. However, this is no simple feat, offshore platforms are complex facilities that require constant heating, cooling and power duties. These requirements shift from month-to-month and from platform-to-platform. Thus, solutions that are robust and compatible with many different scenarios are necessary.

1.2 Aim and Objectives

This thesis aims develop a computational simulation model of an offshore oil and gas platform and to apply various process modifications to determine how this influences overall efficiency and the respective CO_2 emissions. To satisfy this aim, the following research question was matured:

"What are the benefits and implications of implementing carbon-efficient technologies on offshore oil and gas platforms?"

To satisfy this research question, the following objectives were set:

1. Formulate a literature survey of various offshore platform production processes, and display

how their respective efficiencies can be improved. Additionally, the possibility of "green fuels" should be investigated

2. Further development of an offshore oil and gas platform on Aspen HYSYS with more detailed components, such as glycol dehydration units and more accurate pseudo-components. This model should be made as general as possible, with the aim of applying it to either brown or greenfield cases.

3. The model should be able to evaluate performance over the field lifespan, i.e. with varying well composition and operating conditions.

4. Perform simulations for two model platforms and validate the results with data from 'real' operation

5. Define and implement additional Key Performance Indicators that relate to the added cost of the technology

6. Explore at least one scenario for a future low-emission configuration with the developed model

7. Perform a sensitivity analysis based on the assumptions made throughout the development of the model

8. Identify and propose areas for further work

1.3 Limitations and Assumptions

To develop a sufficient and comprehensive model within the given time-frame, the following assumptions and simplifications are made:

- The important presumption of this analysis is the assumption that the platform units (i.e. compressors) are electrified. This means that no gas turbine drives a compressor. Instead, power is generated centrally and distributed amongst the components. In reality, smaller gas turbines are on the same shaft as larger compressors on offshore platforms.

- To compare the accuracy of the developed model, the analysis is limited to platforms where there are no acid gas removal processes present

- A constant electricity and heating demand for general platform use is assumed to be constant over the lifespan of the platform

- The capital costs of the process modifications are not studied. Initially, it was decided that capital costs would be included in this report - in the form of an added weight or volume component. However, upon discussion with the thesis supervisors, it was decided that this

would not be included. Rather the cost analysis would be focused on the operating costs of the added systems

- The CO_2 emission analysis is limited to the power generation units. Aspects such as flaring and downstream emissions are not included. An exception is concerning the use of hydrogen as a fuel, as production emissions are considered in the overall analysis
- In the case of the platform lifespan analysis, the process conditions and well stream composition is updated every 5 years. Dynamic changes between this 5 year period are not considered
- In the case of wind energy, an average load factor is utilised. Essentially, this means that dynamic changes in wind supply and how this impacts the gas turbine load is not investigated

1.4 Report Structure

A general outline of the thesis structure is as follows:

- A summary of the Norwegian oil and gas industry will be discussed, focused on identifying where the future of this industry lies. Additionally, from a general perspective, offshore platform energy losses will be analysed
- Following this, a literature review on the available methods of reducing carbon emissions will be conducted
- A description of the model system will proceed this. A focus will be put on how the model was developed and subsequently validated against data from real operation
- An explanation of the chosen Key Performance Indicators will then be given, with a summary of how they are relevant and how they are applied to the developed model
- A results and discussion section will follow, where the key outcomes from the model are thoroughly analysed
- Lastly, there will be a general conclusion based on the whole investigation and recommendations for future work will be given

1.5 Risk Assessment

As this project was limited to the development of a computational model, there were no laboratory tests. Thus, a risk assessment of this project was not completed.

Chapter 2

Norwegian Petroleum Industry

The petroleum industry is one of the most important industrial sectors in Norway. It accounts for approximately 35 % of the countries exports, and just over 10 % of the state's revenue [3]. Looking at Figure 2.1, it is seen that the quantity of petroleum that is produced is expected to rise over the next 5 years. This is due to new field discoveries, especially that of Johan Sverdrup which is anticipated to produce for the next 50 years and accounts for almost 30 % of the total oil production [4].

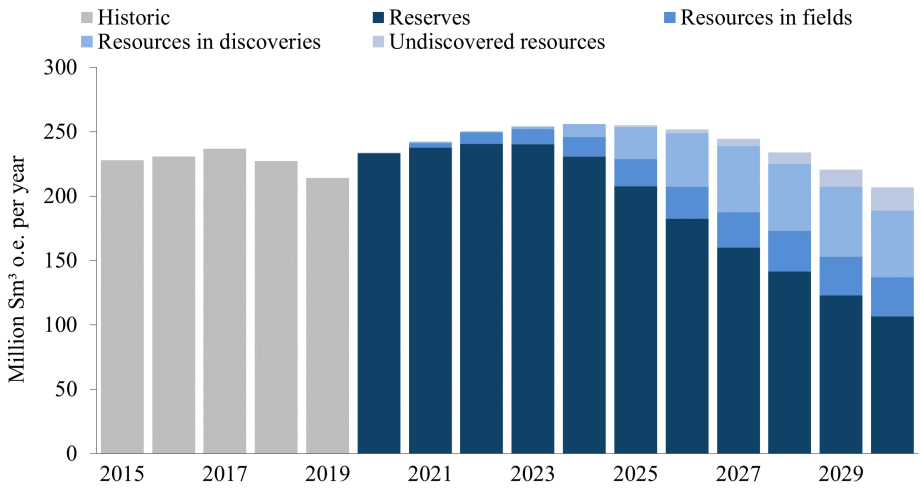

Figure 2.1 Forecasted and historical production from the Norwegian petroleum sector [4]

2.1 Carbon Emissions

As the petroleum industry is not predicted to slow down over the next decade, it is important to consider the modifications that can be made to this sector in the context of carbon emissions. Looking at Figure 2.2, it is seen that the carbon emissions are set to increase in correspondence with the increased production rate, then decrease slightly as carbon mitigation strategies are im-

plemented. However, this decrease is minimal and it is not sufficient to align with the international climate change accords and the further prevention of the greenhouse effect.

To mitigate the rate of greenhouse gas emissions, the Norwegian government introduced carbon taxes on all petroleum operations on the NCS in 1991 [5]. The current rate for 2021 is NOK 1.27 per standard cubic metre of gas or litre of condensate or oil. In the context of the combustion of natural gas, the tax rate is equivalent to NOK 493 per tonne of CO_2 [5]. Aside from the Norwegian state carbon tax, companies operating on the NCS are subject to the Greenhouse Gas Emission Trading Act. This means that companies will pay approximately NOK 700 - 800 per tonne of CO_2 emitted, and this is only expected to increase over the coming years [5].

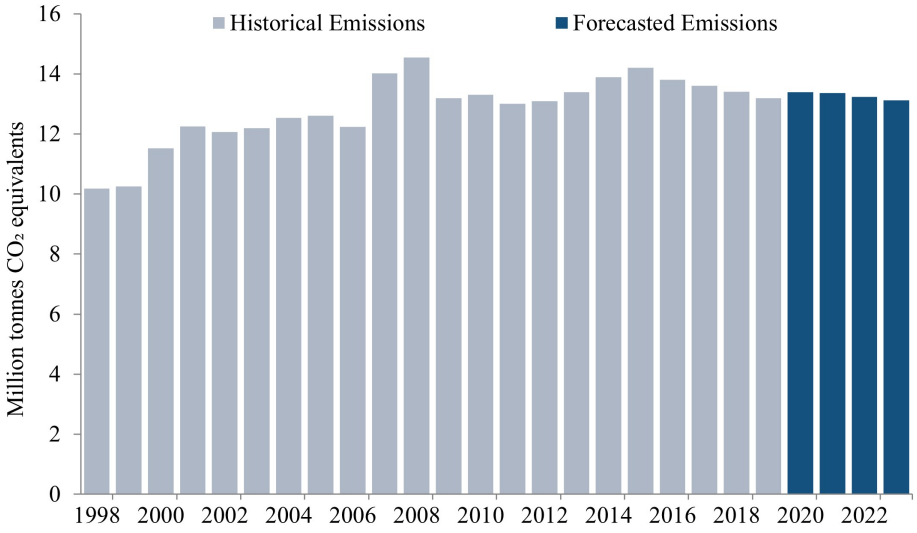

Figure 2.2 Forecasted and historical carbon emissions from the Norwegian petroleum sector [5]

To comply with the international climate change accords, and to minimise the substantial cost of carbon taxes, it is important to analyse where the largest portions are emissions arise from during typical operation. From Figure 2.3 it is seen that the majority of the emissions are directly from the use of natural-gas fired turbines with the purpose of generating electricity. Thus, for the sake of this report and analysis, it is important to consider this as the main point of reduction. In terms of generating power and making the use of it on the platform more efficient.

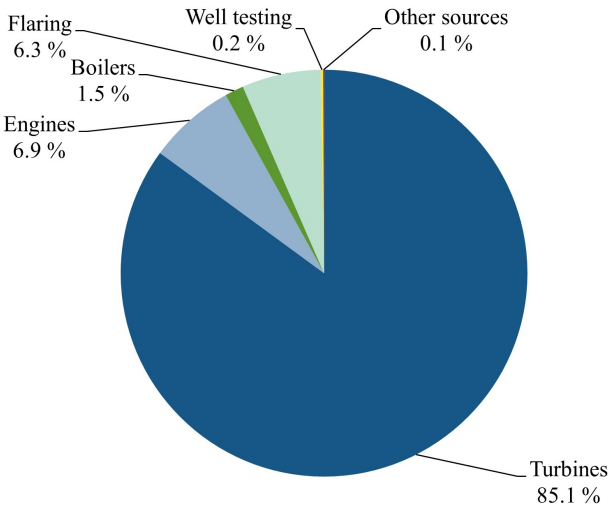

Figure 2.3 CO_2 emissions by share in the Norwegian petroleum industry in 2019, on a mass basis [5]

2.2 Offshore Platform Energy Losses

To analyse in particular what processes need to be improved in terms of energy efficiency, an energy analysis must be considered. A viable way of viewing the various energy losses throughout the system boundary is via the use of an exergy analysis. Exergy is defined as the maximum theoretical work that is obtainable when the system in question interacts with the surrounding environment in order to reach an equilibrium state [6]. To determine which processes in particular are inefficient, the term exergy destruction can be considered. Exergy destruction refers to the thermodynamic inefficiencies within a system that arise from entropy generation [6]. Essentially, in this context, this is the quantity of energy within a system that can be recovered.

Following the exergy analyses conducted in [6], [7], a typical production platform can be broken up into 7 sectors. These being: production manifold; separation train; recompression train; gas treatment section; oil/condensate export; fuel gas system; and in some cases a seawater injection sector. This can be viewed in Figure 2.4 with the exception of seawater injection which is not illustrated.

The well streams enter through the production manifold where the various pressures and temperatures are adjusted accordingly. Following this, the stream is transferred into the separation train, where the three phases present (gas, aqueous and liquid) are separated from one another. There are typically 3-phase and vapour/liquid flash separators in series in this sector. During this train, the pressure is reduced to further liberate gas from the process stream. The gas recovered in this sector needs to reach the same pressure as the gas from the first 3-phase separator, thus, it must undergo recompression. The gas streams are then dehydrated and compressed to a higher pressure with the purpose of injection into the transport pipeline.

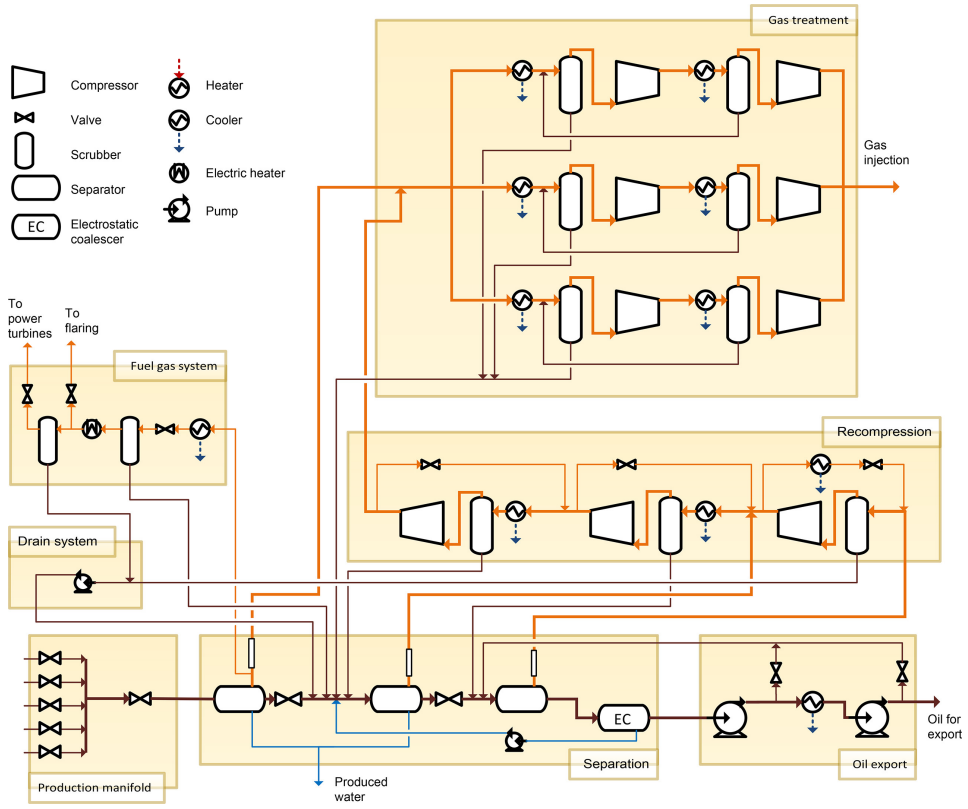

Figure 2.4 Typical platform layout. The gas, water, and oil streams are orange, blue, and brown respectively [6]

A key figure from an exergy analysis performed in [7] is shown in Figure 2.5. This analysis is conducted over 4 Norwegian offshore platforms based upon their typical operational conditions. It must be noted that this analysis only considers losses arising from the use of process machinery, hence, inefficiencies arising from the use of gas turbines is not included.

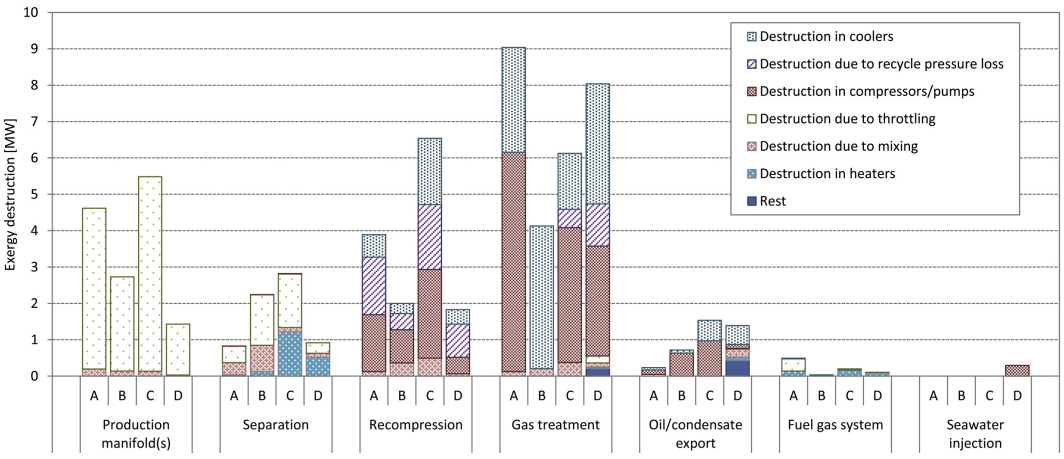

Figure 2.5 Breakdown of the destroyed exergy on four offshore platforms in Norway [7]

It is shown here that there is a substantial quantity of exergy destruction in the production manifold and gas treatment section. In the production manifold, the main energy losses come from the use of throttling valves that are used to reduce the pressure from the well stream into the plat-

form. In the gas treatment section, the main losses come from two separate aspects: compressor inefficiencies; and the use of either inter or aftercoolers. The compressor inefficiencies may be caused by the inadequate sizing of the compressor or from the mode of operation. As the oil field matures, the well outlet composition changes. This typically implies that there is a reduction in the gas to water ratio, meaning that over time the quantity of gas recovered from a well is decreased. When a compressor is initially sized it is based on the original gas flowrate obtained from the well. After time progresses, there will be less power required by the compressor which means that it will operate in an off-design range - with lower efficiency. Aside from the efficiency aspect, to prevent compressor surging with the lower gas flowrates, there is typically a portion of gas after the compressor which is throttled and recycled back into the compressor entrance. Thus with both these considerations, exergy destruction arises.

The exergy destruction arising from the compressor coolers is due to the use of cooling water. It is common to cool between compressor stages as lower temperatures increase the stage efficiency of the compression process. In almost all offshore operations, the cooling is completed via the use of seawater, where the thermal energy is irreversibly transferred to the ambient environment. This is a large proportion of energy that is essentially being wasted, as these streams often have large mass flowrates in the gas treatment sector. The same factors mentioned for the loss of energy in the gas treatment sector can be said for the recompression stage as well. However, the flowrates here are far smaller, so the effect is far less noticeable; however, still present.

Chapter 3

Methods of Reducing CO_2 Emissions

This section will outlines techniques for reducing CO_2 emissions on offshore platforms. These methods will be within the following categories: reducing electricity consumption from the production processes; providing carbon-efficient or neutral electricity; using alternative fuels; utilising technology to recover wasted energy; or implementing processes such as carbon storage and sequestration. The technology used to recover waste energy is investigated in three areas: gas turbine exhaust gas; compressor intercooler/aftercooler; and the inlet well stream energy [8].

3.1 Gas Turbine Resizing

Gas turbines typically operate with a fraction of their design power load. As the part-load percentage increases, the efficiency decreases - as seen in Figure 3.1. This means that the majority of gas turbines operate at lower efficiencies than they are designed to operate at. Thus, given this, a method of increasing the platform energy-efficiency could be to resize the gas turbines in operation so they operate closer to their optimum design point [8].

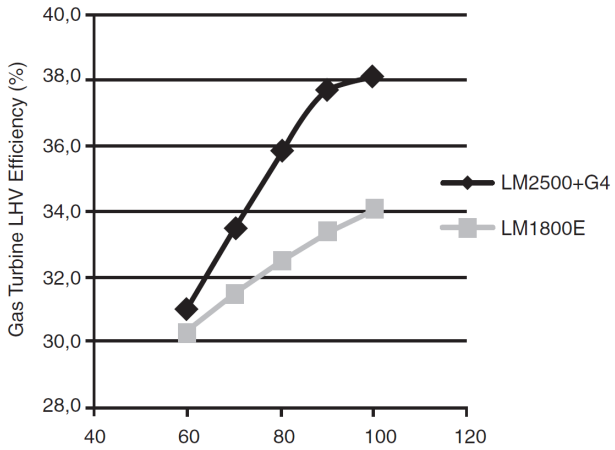

Figure 3.1 Gross efficiency vs part load percentage for two separate gas turbines [8]

The part-load efficiency is also very dependant on the gas turbine utilised. This is illustrated in Figure 3.1. Here, the LM2500+G4 (31.5 MW) and the LM1800E (15 MW) turbines are compared. At full-load, the larger turbine has a far higher efficiency than the smaller turbine; however, this efficiency value rapidly drops as the part-load percentage increases. This change is far more gradual in the case of the smaller turbine. Looking at a case study performed by [8], it is shown that if the part-load efficiency is changed from the 0.6 range to the 0.9 range and the turbine is adequately changed, there can be a 2.0 % reduction in the platform CO_2 emissions. However, a point from this case analysis is that it is conducted over an 18-year period and the majority of the emission reductions come towards the end of the field's lifespan. This mitigation strategy does not present radical changes; however, there will be minimal revisions to the platform size and weight constraints.

3.2 Bottoming Cycles

Given that gas turbines account for the largest majority of carbon emissions on the NCS, it is important to consider available technology to improve their efficiency and mode of operation. The gas turbine exhaust gas is viewed as the largest source of thermal energy that can be utilised for power recovery on offshore platforms [8]. A study performed by [9] illustrated that the gas turbine exhaust gas accounts for approximately 60 % of the total exergy losses. On onshore installations, combined cycle systems are used to recover a large proportion of available thermal energy from the turbine exhaust gas. Despite this, there are only three offshore platforms that utilise bottoming cycles: Oseberg; Eldfisk; and Snorre B [10]. This is mainly due to the size and weight limitations that exist for offshore installations [11]. The bottoming cycles in operation use once-through heat recovery steam generators (HRSG) as they are generally more compact and therefore take-up less space [11]. Aside from steam bottoming cycles, cycles that use CO_2 as a working fluid present promising results.

3.2.1 Steam Bottoming Cycles

As previously mentioned, steam cycles are already present on some offshore installations. This is a somewhat mature technology, which has been tried and tested. Strictly for offshore activities, once-through HRSG technologies are viewed as the most viable option. In comparison to multiple-pass steam generators, there is only one pressure level present; thus, steam drums are not required.

The once-through steam generator (OTSG) is far simpler than typical HRSGs, as there are no defined sections for the economiser, evaporator, or super-heater [10]. An outline for this process can be viewed in Figure 3.2. Here, the exhaust gas interacts with the working fluid in the OTSG. The high-pressure steam is then expanded in the steam turbine, condensed and then pumped back to the steam level pressure. A comparison between the different steam cycles can be seen in Table 3.1.

Table 3.1: Comparison between 2-drum, 1-drum and OTSG steam cycle technology [10]

		2P Drum	1P Drum	OTSG
GT gross power out	$\dot{W}_{gt}$ *(MW)*	32.1	32.1	32.1
GT gross efficiency	η_{np} *(%)*	38.2	38.2	38.1
ST gross power out	$\dot{W}_{st}$ *(MW)*	13.7	11.2	11.3
CC net power out	$\dot{W}_{cc}$ *(MW)*	45.3	42.8	42.9
CC net efficiency	η_{np} *(%)*	53.8	50.9	51.0
HRSG weight estimate	m_{hrsg} *(kg)*	340	145	110

In any case scenario, it is seen that the efficiency of the combined cycle is drastically higher than that of the gas turbine efficiency. The two drum cycle produces approximately 2.5 MW more electricity than the OTSG cycle; however, the weight required is more than threefold more. Thus, for an operation with stringent space and weight requirements, the multiple pressure level arrangement is an unnecessary addition when viewing the benefits. For this comparison, the live steam pressure and temperature were 25 bar and 450 °C respectfully [10].

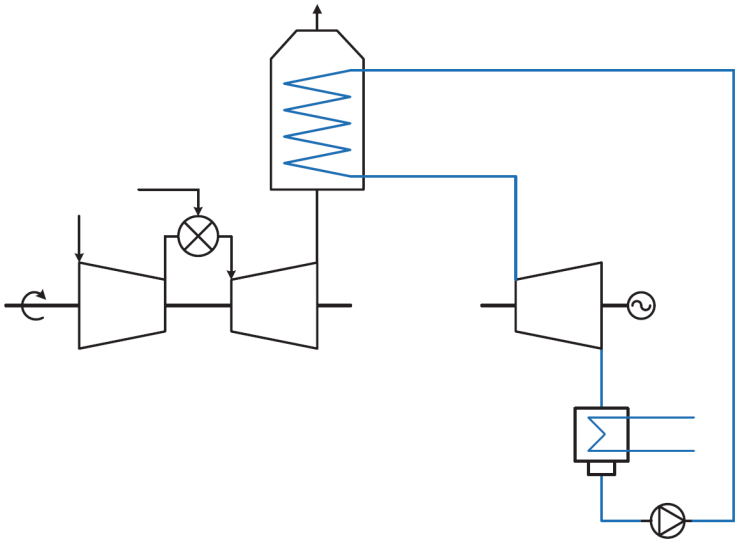

Figure 3.2 Basic schematic of a once-through steam bottoming cycle [10]

With the respective benefits, there are some challenges with this technology. On offshore facilities, it is difficult to obtain freshwater. This water has to be supplied from onshore, or from costly desalination plants [10]. With multiple pressure steam cycles the water contaminants, such as salts, are removed with drum blow-downs. However, as these are not present, water with minimal contaminants are needed for the OTSG system to avoid unwanted material build-up [10]. Apart from this, deaerator units would be required to eliminate dissolved gases (oxygen, carbon dioxide, argon, and nitrogen) from the cycle water.

3.2.2 CO_2 Bottoming Cycles

An alternative to steam bottoming cycles is the use of CO_2 as a working fluid in a somewhat similar cycle. The advantage here is that this cycle has a high working pressure, hence, the process units

could be more compact in comparison to a normal bottoming cycle [12].

This cycle will operate at pressures above the critical pressure of CO_2 (73.8 bar) [12]. Compared to a steam cycle, the exit temperature from the turbine is much higher. For higher operational efficiency, it is beneficial if this heat is recovered. This is done by employing a heat exchanger between the low-pressure side of the turbine, and the high-pressure side of the pump [12]. There are two main layouts that are reported in literature, but for the sake of keeping consistent with the steam bottoming cycle, only a single pressure level cycle will be investigated. A schematic illustration of this process is seen in Figure 3.3.

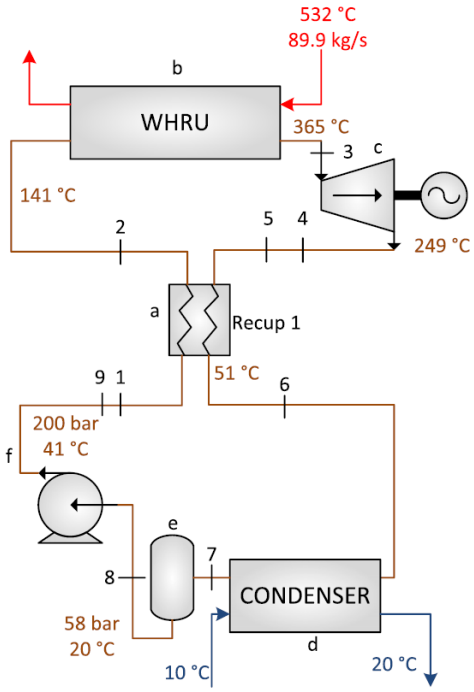

Figure 3.3 Schematic of a CO_2 bottoming cycle, showing key cycle temperatures and pressures [12]

The efficiency and power output values for the respective cycle can be seen in Table 3.2. In comparison to the steam cycle (Table 3.1), the combined cycle efficiency is slightly lower, along with the net power output value.

Table 3.2: Comparison between simple, 1-stage, and 2-stage CO_2 bottoming cycle [12]

		Simple Cycle	Combined Cycle - Single Stage	Combined Cycle - Dual Stage
GT gross power out	*MWe*	32.5	32.1	32.1
BC net power out	*MWe*	-	9.5	10.4
Net power out	*MWe*	32.2	41.1	42.0
CC net efficiency	%	38.3	48.9	50.0

3.3 Compressor Resizing and Control Strategy

Compressors are one of the most important units on offshore platforms. They are responsible for the majority of the power demands on a platform. However, despite this, compressors are often

run with low efficiencies due to their poor part-load conditions [13]. In addition to this, as the well stream flowrates and composition changes over the field lifespan, a certain portion of gas needs to be recycled to avoid compressor surging. This technique is called anti-surge recycling. Here, some of the compressed gas is split, throttled, and sent back into the compressor entrance. This unnecessarily increases the compressor power and subsequently cooling duty. It is estimated that there is an additional 10 - 15 % power demand due to this technique [13]. Figure 3.4 shows a case study where four separate platforms are analysed. From this figure, it is evident that there are large energy losses that result from this concept.

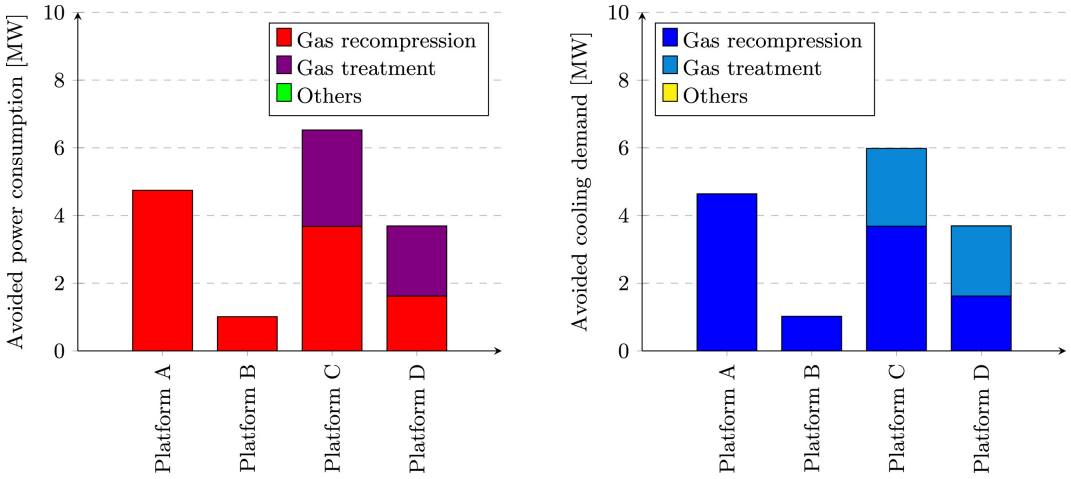

Figure 3.4 Avoided power and cooling demands where anti-surge recycling does not take place [14]

The main issue is that many of the compressors offshore do not have variable speed drives, and they are not adequately sized for their current operation. This means that there is a limited range to where the compressor can operate; thus, to deal with this fact anti-surge recycling is implemented. [14] suggests three separate methods to limit the use of anti-surge recycling: (i) utilising multiple compression trains in parallel - however, this requires additional space on the platform; (ii) employing smaller compressors, or re-wheeling the existing compressors; (iii) adjusting and optimising the control strategy - which is not feasible in all case scenarios. In the case where it is applicable, other control strategies such as pre-throttling and after-throttling can be considered. There are also associated energy losses with these strategies; however, they are not as substantial as with anti-surge recycling.

3.3.1 Compressor Waste Heat Recovery

As previously discussed, and illustrated in Figure 2.5, there is a large quantity of exergy that is destroyed in the recompression and gas treatments sectors. Aside from compressor inefficiencies and losses due to surge recycling, the losses resulting from inter and after cooling is the next largest source of exergy destruction in these sectors. The cooling is needed to decrease the power demand of the compressors, as compression efficiency increases with lower operational temperatures, and to satisfy the transport pipeline requirements [14]. This is most prevalent on platforms with large

gas processing capabilities [8]. Steam Rankine Cycles cannot be utilised in this scenario as the operating temperature of the cycle would be too low. Thus, Rankine Cycles with organic working fluids must be utilised [14].

[15] investigates the possibilities of different working fluids for waste heat recovery from export gas compressors. A schematic of the proposed process is shown in Figure 3.5. This process focuses on using the waste heat from the outlet stream of the last export gas compressor. Here, the high pressure stream is available at 125 °C, and must be returned at a temperature lower than 100 °C.

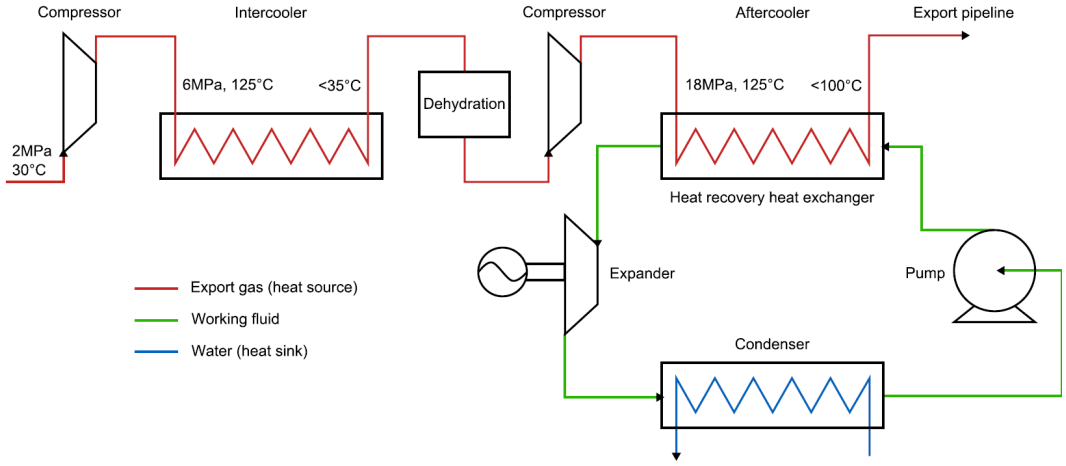

Figure 3.5 Export compressor waste heat recovery schematic [15]

This study looks at three different working fluids: a transcritical hydrocarbon mixture; a subcritical propane mixture; and a transcritical CO_2 mixture. All fluids have gliding temperature profiles in the heat recovery exchanger and condenser, which minimises the approach temperature and reduces the quantity of exergy destruction. The hydrocarbon mixture is seen to recover the most power from the heat sink. However, the differences between the three fluids are not large, with all fluids outputting a net power of 3.5 MW. Putting this into context, it is about 10 % of the compressor work [15]. For offshore applications, one may view the CO_2 Rankine Cycle as the most viable. This being due to several reasons. Firstly, this cycle would operate at a much higher pressure than the other fluids, at 135 bar. This is a similar pressure to the heat sink stream (180 bar), thus, the required system would be much more compact with the higher densities. Secondly, if there is an acid gas separation plant on the platform, CO_2 would not be needed to be provided from onshore - which would be the case for the other fluids. Lastly, one of the most important aspects of offshore activity and technology is safety. Both the propane and hydrocarbons mixtures are volatile and flammable, adding an increased risk to the operation.

The issue with this cycle is that it would require additional space on the platform. So other technologies which recover greater quantities of energy may first be prioritised. Additionally, as the operation of offshore platforms is rather dynamic, it is unsure how this system would behave in off-design situations [15].

3.4 Production Manifold Multi-phase Expander

The production manifold is a large source of exergy destruction, as seen in Figure 2.5. This energy loss comes from the use of well inlet throttle valves which reduces the temperature and pressure of the incoming feed streams from the respective well. In the case of high pressure wells, the quantity of destroyed exergy is substantial. [14] states that if the valves in the production manifold are substituted with multi-phase expanders, then the power generated would cover 6.5 % and 16 % of the total power demand on two separate platforms, assuming an expander efficiency of 30 % [14]. These numbers are quite high, even with the conservative expander efficiency estimate. In reality, the efficiency value can vary between 30 % and 70 %. However, this technology is under-developed, and there is much room for progress.

The use of expanders would cause a slight drop in temperature into the platform, which would reduce the inlet vapour fraction. This does not have a major impact on the downstream units. The largest difference would be that the recompression stages will have to recover more portions of gas at the lower-pressure stages [14]. However, as mentioned, this change is not substantial. The main point of concern with this technology is with regard to operability. As this is at the front-end of the platform, whatever technology is used will have to be extremely reliable. One way of dealing with this issue is implementing a by-pass line which would lead to a throttle valve and a cooler to reduce the temperature to the slightly lower expander temperature. Another point of concern is with regard to corrosion. As this is the first unit in contact with the well stream, it will encounter impurities and multi-phase conditions which will negatively impact the lifespan of the process components [7]. One major benefit to this technology is that it will not occupy a large amount of space of the platform, thus, conforming with the stringent size and weight constraints.

3.5 Platform Electrification

Electrification of platforms is a prevalent topic in the Norwegian oil and gas industry, and it is especially gaining large amounts of political support. Essentially, power is transferred from renewable sources onshore (such as hydroelectric power stations) to the offshore platform via the use of sub-sea cables. This notion depends upon the premise that power is generated more efficiently onshore, even if thermal power-producing facilities are utilised [16]. Aside from utilising onshore electricity, electricity from offshore wind farms and tidal energy are also promising topics.

Strictly considering power supplied from onshore facilities, the platforms that are considered viable for electrification projects are to be within a reasonable distance to the shore, and also must not be largely deep water. [16] utilised the Utsira High area in the North Sea as a case study. This area is expected to produce for the next 40 years and contains large fields such as Johan Sverdrup, Gina Krog, Edvard Grieg and Ivar Aasen. This area is approximately 200 km from the shore, and the water depth ranges between 100 and 120 m. These fields are the basis for a large electrification

project which started in 2019 [16]. This case study analyses two main concepts: full electrification; and partial electrification. The partial electrification concept will be a combination of onshore power generation and the use of offshore gas turbines. In this scenario, the four producing fields are set to have a central power generation hub that supplies energy to all platforms simultaneously.

As power across Europe is an integrated system, the aforementioned case study considered a model which predicted the impact on the European power system [16]. The study found two different effects that could result. The marginal effect over the entirety of the field lifetime illustrates that with the increased power demand on the integrated power system, CO_2 emissions associated with the offshore platforms could increase up to 40 % [16]. This may seem like a strange result, however, this is due to the increased reliance on coal-fired power plants onshore. In the case where the average effect is looked at, it is seen that with the utilisation of electrification projects that CO_2 emissions associated solely with the offshore platform can decrease in the range of 48 % and 90 %. However, this largely depends upon the geographical region considered [16].

Figure 3.6 illustrates a general potential set up for an electrified platform. Both full and partial electrification scenarios are shown. Here it is displayed that onshore generated power can be either be from combined cycles, or from hydroelectric plants. The transmission losses are assumed to be approximately 8 % [17]. In the case of full electrification, the heating demand can be satisfied by offshore grid electric heaters. Where partial electrification is considered, gas-fired heaters are utilised in conjunction with the onshore supplied power.

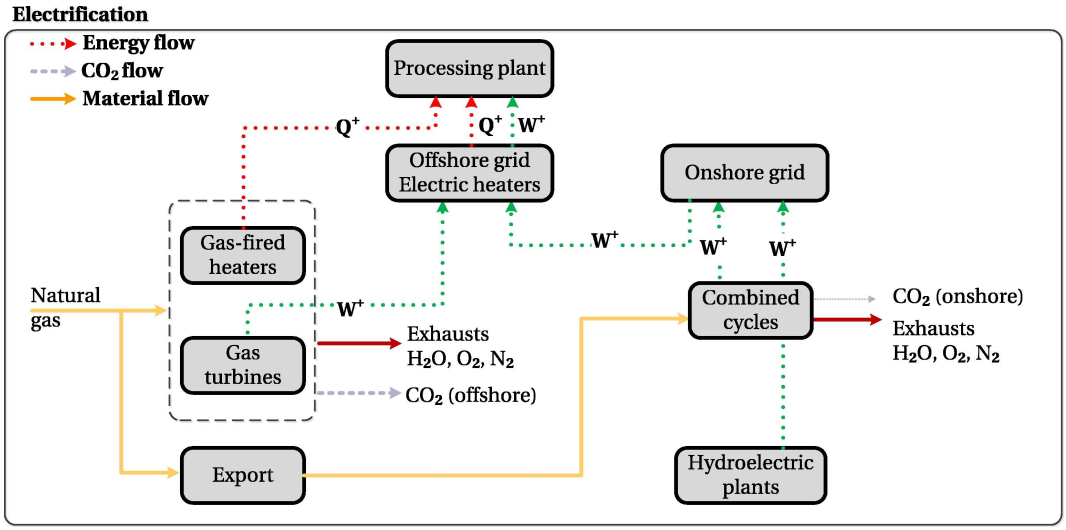

Figure 3.6 Schematic illustration of the proposed integrated offshore electrification system [17]

3.5.1 Renewable Energy Implementation

Offshore wind energy has developed rapidly over the last ten years, both fixed-bottom and floating wind turbines are now utilised commercially [18]. Wind energy presents a strong basis for supplying energy to offshore oil and gas platforms. The vast majority of the platforms present of the

NCS have water depths ranging between a hundred metres to several hundred metres. In addition, there is typically higher than average wind speeds with lower turbulence in close proximity to the existing fields.

Equinor is set to implement a 88 MW wind farm in the Norwegian North Sea. This wind farm will supply the Snorre and Gullfaks offshore fields with power. This is estimated to supply almost 35 % of both the fields electricity demand. The project is due to start up in 2022 and will result in a reduction of 200 ktonnes of CO_2 per annum [19]

Case studies performed in [18], [20] illustrates that in conjunction with subsea cables from onshore facilities, the use of floating wind farms could be extremely beneficial for providing power to offshore platforms. As wind farms have an unpredictable power output, it is important that an energy source that can be scaled up or down is also used. Thus, in the cases where subsea cables are not a viable option, it is recommended to use wind energy in combination with gas turbines to provide a stable power output.

Aside from utilising wind energy, several research papers have investigated the use of wave energy for supplying power to offshore platforms. As previously mentioned, the sporadic nature of wind energy is the main challenge for offshore applications. [21] suggests that to overcome this challenge without additional reliance on gas turbines, wave energy converters (WEC) could be utilised. The biggest issue with this technology is that it is not commercially available, and thus, the associated costs are high. However, despite this, there is huge potential for wave energy as the biggest opportunities are between 30 and 6° latitude, where the majority of the Norwegian offshore facilities are located [21]. A case studies shown in [21], [22] illustrate that is large promise in utilising tidal energy. [21] reviews different WEC technologies and states that half the gas turbines could be replaced by wave farms and 141 ktonnes of CO_2 could be saved per year. However, [22] shows that the quantity of wave energy recovered is highly dependant on the season, with summer resulting in far lower recoveries - as would be seen for wind energy.

3.6 Carbon Capture and Storage

Carbon capture and storage (CCS) is seen as an alternative to replacing fossil fuels for offshore and onshore activities. Renewable energy technology may put a high strain on the precious metal industry and will be hugely costly for a '100 %' swap [23]. Thus, instead of completely transferring to renewable energy sources that are not carbon-based, CCS is utilised to separate the emitted CO_2 from the exhaust gas of the fossil-fuel-based power generator. This technology has been already put to test on the NCS, with Sleipner West being in operation since 1996, capturing almost 1 million tonnes of CO_2 per annum [24].

There is a large variety of technologies available, such as absorption; adsorption; membrane separation; and cryogenic distillation [17]. The majority of current work looks at absorption

methods. Here, acidic gases (such as CO_2) are bounded either physically or chemically to an organic solvent [17]. In cases where CO_2 has a low concentration, and hence a low partial pressure, chemical absorption via the use of monoethanolamine (MEA) as a solvent is the utilised technology. For cases of higher CO_2 partial pressures (greater than 7 bar), triethanolamine (TEA) is the preferred solvent for chemical absorption. Physical absorption is also a strong option for this case [17].

[17] outlines three main pathways for CO_2 capture. These being: pre-combustion; oxy-combustion; and post-combustion. Pre-combustion refers to converting the carbon-based fuel into a non-carbon-based fuel (methanol, hydrogen, ammonia, etc ...) prior to its combustion. During the conversion stage, the CO_2 will be separated (in the reforming step in the case of hydrogen production) and then subsequently stored. In this scenario, there will be much higher concentrations of CO_2 in the gas to be separated. Thus, either chemical absorption via TEA or physical absorption is used. The issue with this pathway is that it required substantial capital costs, and the combustion methods are largely based on the use of hydrogen - which is a new and immature technology with several developmental issues [17]. Post-combustion instead refers to separating out CO_2 from the exhaust gas of the fossil-fuel-based power generator. This pathway results in lower CO_2 partial pressures, thus, chemical absorption via MEA is preferred. A proposed structure for both pre and post-combustion pathways for offshore applications is shown in Figure 3.7.

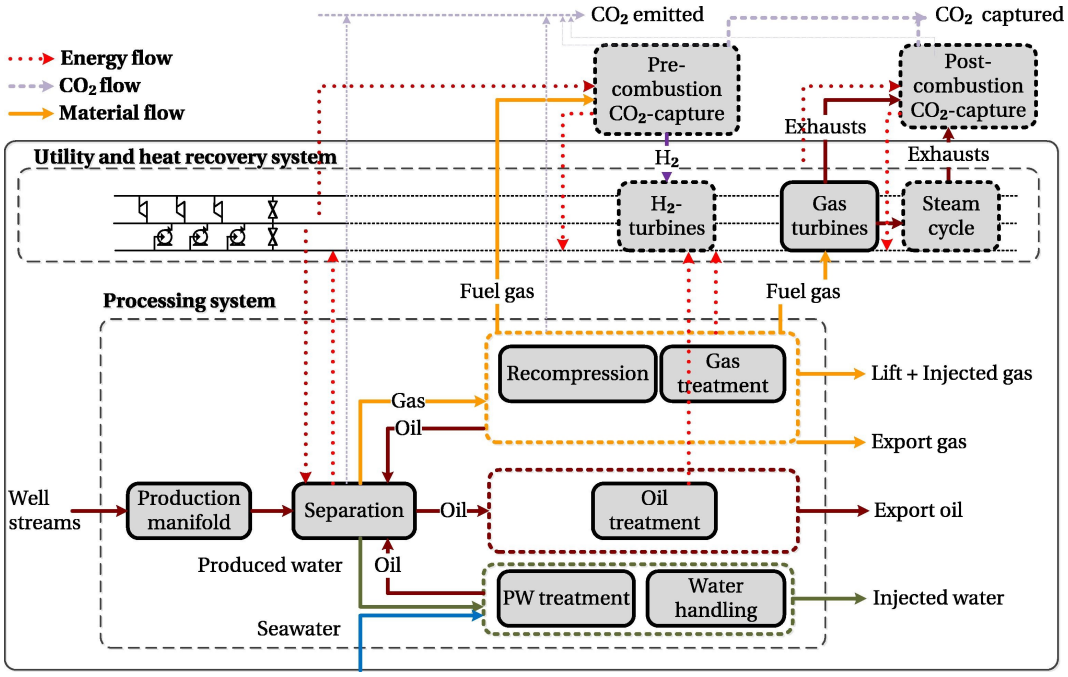

Figure 3.7 General schematic of the proposed CCS pathways for offshore oil and gas platforms [17]

Aside from the cost, size and weight constraints for CCS technology, there is a large energy penalty that results from its use. Considering the post-combustion pathway for offshore use, there will be a low CO_2 partial pressure in the gas turbine flue gas. This means that a large amount of energy will be required when regenerating the chemical solvent in the stripping section of the acid-gas

removal loop. A study performed by [23] quantifies this to 13 % power loss that is strictly associated with the use of CCS.

3.7 Alternative Fuels

This section will investigate the possibility of alternative fuels for providing power for offshore installations. There are a large number of alternative fuels that can be utilised in order to reduce the carbon emission intensity of the power generation processes, ranging from biofuels to hydrogen. [25] highlights three main types of fuel that can be utilised in gas turbines, these being: fatty acid methyl esters; biogas based fuels; and industrial gases rich in hydrogen. Strictly concerning offshore power generation, hydrogen is viewed as the most promising possibility. This is due to the fact that the hydrogen value chain is rapidly expanding, and within the coming years it will become more readily available for commercial use. Thus, based on the aforementioned, this review will largely focus on hydrogen as an alternative fuel to natural gas.

3.7.1 Hydrogen Fuel

The use of hydrogen for generating power is becoming a prevalent topic in today's society. The key advantage of hydrogen is that it releases neither CO_2 nor CO when combusted [26]. One of the main issues associated with H_2 fuels is that there is a larger potential for more severe NOx emissions, due to the higher combustion temperatures. Aside from this, there are issues related to combustion flame stability, and further issues related to the lack of materials available to cope with the excessively high temperatures which result from the burning of H_2. However, these are the main issues when pure H_2 is used as the primary fuel. A way of avoiding, or reducing these issues without a complete redesign of gas turbine technology, would be to mix in the H_2 with more conventional fuels such as natural gas.

One study analysed the use of pure H_2 and natural gas for a 50MW gas turbine [27]. Here, it was found that both thermal and exergy efficiency favoured the use of H_2 fuels over that of natural gas. However, when the economics were considered, despite the previously mentioned advantage, natural gas fired turbines were found to be more advantageous with respect to the price per unit of power produced [27]. Aside from using pure H_2, a separate study analysed the use of natural gas-hydrogen mixtures in gas turbines. [28] performs a 3D numerical study analysing the effects of varying H_2 and natural gas concentrations in a micro gas turbine. This study found that with just a 10 % addition of H_2 to the fuel mixture, that there was a significant reduction of 60 % and 15 % for CO and NOx respectively. This result relates more to the use of hydrogen to minimise the prevalence of incomplete composition. [29] found similar results when injecting small concentrations (4 %) of H_2 into the primary combustion zone of a gas turbine. [30] states that several combined cycle plants utilise portions of H_2 in their fuel gas, ranging from 9 % vol to 60 % vol. The most complicated issue in these scenarios is keeping the flame temperature down,

and this is possible by the use of advanced cooling methods and fuel diluents.

Chapter 4

Model Platform Development

This chapter will focus on the development of a comprehensive offshore oil and gas platform. A model was inherited from a former summer student at SINTEF and Equinor, which was used as a foundation for this project [31]. Two separate platforms, Platform A and B, were used as a basis for the development of the model. Platform A was the basis for the model taken over.

The key reason for utilising two platforms is to make the model more applicable to a range of operating conditions and scenarios - with the ultimate goal of making the model as generic as possible. Making the model entirely generic is not practically feasible, as no platform is the same and the set-up heavily depends upon the production field. However, if the model is flexible and automated, this is highly beneficial for various analyses and future use.

4.1 System Description

The purpose of an offshore oil and gas platform is to process and separate the lighter hydrocarbons from the heavier hydrocarbons, with the aim to prepare the lighter hydrocarbons (export gas) for transport in a pipeline to an onshore facility for additional processing.

4.1.1 General System Overview

A general schematic of this system can be seen in Figure 4.1. The various inlet streams from the different production wells enter the system at the production manifold. These streams have a range of temperatures and pressures. The purpose of the production manifold is the reduce the pressure and mix the streams. The pressure is reduced in order to separate out the lighter hydrocarbons in the subsequent separation steps. Here, there is a train of three-phase and flash separators. Between each separation unit, the pressure is reduced to further liberate and recover more vapour from the mixed liquid stream. This recovered vapour is then recompressed back to the respective pressure and sent to the gas treatment sector. The water is separated from the oil and gas via the use of the aforementioned three-phase separators. This produced water is then

adequately treated and discharged back into the environment.

In the gas treatment sector, the inlet gas is first dehydrated via the use of a glycol absorption column. The dry gas stream is then sent for compression. In this case scenario, there are no acid gas removal steps as the well streams do not have a high CO_2 or H_2S content. If this were not the case, acid gas removal would occur again in an absorption column with an amine-based solvent.

The dry gas is compressed in multiple stages with inter-cooling to obtain lower compression duties. A portion of the production gas is compressed to higher pressures and reinjected back into the well to maintain the pressure. A fragment of the treated gas is taken from this section and is used as a fuel to drive the gas turbines to provide electricity for the platform. The rest of the gas is then compressed to the required pressure and is then sent to an onshore facility via a pipeline.

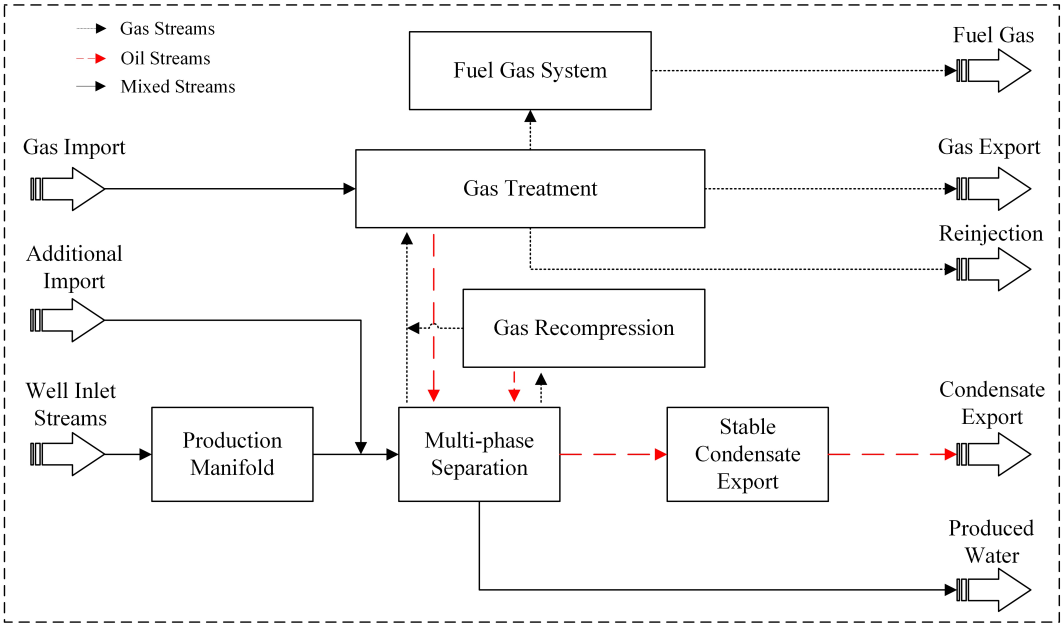

Figure 4.1 Basic schematic of the oil and gas platform system, adapted from [7]

4.2 Studied Platforms

This section will give a summary of the important information and inlet conditions for each of the studied platforms. It should be noted that for the inlet streams the pressures and temperatures are those after the production manifold has received them from the respective wells. Essentially, these are the conditions after inlet well stream throttling. The values before the well stream throttling can be viewed in Table 4.17. It should be also noted that additional inlet refers to streams that do not fall within the HP or LP bracket, and may be present as a well test stream.

4.2.1 Platform A

This offshore platform is in the Norwegian North Sea and has been in operation for over 30 years. It is one of the largest platforms in operation on the NCS when looked at in terms of produced

volume. This platform receives from multiple fields, which generally have a high reservoir pressure but a more moderate inlet temperature. Pressure is maintained through water and gas injection into the various fields. This platform does not contain an acid-gas treatment section. The inlet streams can be seen in Table 4.1. It should be noted that the numbers for this model are not strictly exact, they are more general and represent the range in which the wells would produce at.

Table 4.1: Platform A: Inlet streams

Stream Name	Mass Flowrate (kg/s)	Pressure (bar)	Temperature (°C)
HP Inlet	109.5	60.0	43.1
LP Inlet	89.0	19.0	49.9
Additional Inlet	232.8	58.0	56.2
Gas Import	2.78	34.5	13.0
Additional Import	25.3	43.0	33.9

The constraints of the system are shown in Table 4.2. These values are mainly the requirements for the export (rich) gas that is to be sent in the export pipeline. Requirements that relate to H_2S are not shown as it is not present to a significant degree within the process streams.

Table 4.2: Platform A: System constraints and requirements for the export gas pipeline

Requirement	Specification
Maximum operating pressure (barg)	210
Minimum operating pressure (barg)	112
Maximum operating temperature (°C)	60
Maximum cricondenbar pressure (barg)	110
Maximum cricondentherm temperature (°C)	40
Maximum water dewpoint at 69 barg (°C)	-18
Maximum carbon dioxide (mol %)	2

4.2.2 Platform B

This facility has been in use for just over 10 years. It has a high reservoir pressure and temperature, and the outlet streams have a high gas-to-oil ratio. This platform has a relatively low power demand in comparison to Platform A, as there is a lower compression demand. A research paper focusing on exergy destruction utilised this platform - here it is known as platform C [7]. This platform does not possess either glycol dehydration or acid-gas removal units.

The inlet streams can be viewed in Table 4.3. In comparison to Platform A, fewer streams are received, as there is not additional import. The system constraints are the same as that of Platform A, this can be viewed in Table 4.2.

Table 4.3: Platform B: Inlet streams

Stream Name	Mass Flowrate (kg/s)	Pressure (bar)	Temperature (°C)
HP Inlet	242.9	46.0	61.4
LP Inlet	3.27	7.22	68.7
Additional Inlet	0.828	12.9	63.0
Gas Import	1.87	110.2	4.40

4.3 Process Simulation

The development of the model took place using a process simulation software called Aspen HYSYS, this being the same software on which the inherited model was built. The student based the simulation on a provided simulation from Equinor. This simulation from Equinor was developed on Honeywell UniSim - also a process simulation software.

This inherited model did not have a rigorous gas turbine design, nor did it have compressor maps to estimate the compressor's isentropic or polytropic efficiencies at off-design conditions. In addition, there were no controls present to ensure that the simulation met the constraints shown in Table 4.2. Aside from this, there was a large amount of 'hard-coding' that went into each simulation. Essentially meaning that the simulation was not automated.

4.3.1 Model Development Procedure

As previously mentioned, two platforms were used to develop the final model. To complete this process the inherited model was first developed to include additional and more detailed components for Platform A. The inclusion of the power generation and energy-efficient components was the most important aspect of this development. For accurate and reliable results, power generations units that can simulate off-design situations were essential for this study. The method and explanation of these units will be discussed in further detail later on in this chapter.

After Platform A was developed to an acceptable level, the output results were validated against the provided simulation from Equinor for the same platform. The most crucial aspect in the validation method relates to the outlet stream composition and conditions. Following the validation of the Platform A model, the next step was to convert the model to be able to solve Platform B reliably and efficiently. To complete this, 'logic manipulators' were employed. The term 'logic manipulators' is used to describe the use of logic functions to manipulate the simulation. The use of this is to reroute the different pressure streams to the appropriate separator - being most important in the gas recompression/multi-phase separation systems (see Figure 4.1). The reason why this is important within these sections is that between the platforms there is a variety of different pressure streams which should belong to certain separators. If these 'logic manipulators' were not employed then the recompression demand would be erroneous, and the use of the model would not be automated in any sense.

After the improvements and modifications to the model were employed, the results were verified with real data from Platform B. The verification data for Platform B was obtained from a doctoral thesis that utilised this platform for an exergy analysis [7]. Although changes were made to the model when applying it to Platform B, the model does not have to be verified again for Platform A. The reason for this is because of the previously mentioned logic manipulators. As these are utilised, the core structure of the Platform A model is not altered. Rather when the same conditions

for Platform A are put back in, there is almost no difference from the unchanged model that was verified.

The fact that the final model was developed utilising two separate platforms with contrasting operating pressures is important. It means that the model is set-up to handle various conditions which it may face during its operational lifespan, which is a key focus in the later parts of this study.

4.3.2 Equation of State Selection

The selection of the Equation of State (EOS) is one of the most important aspects of a simulation. Changing an EOS severely impacts how the model will predict densities, fluid interactions and other important physical properties. When selecting an EOS, there are four essential features that need to be considered: (i) the temperature and pressure range; (ii) the type of properties in question; (iii) the mixture composition; and (iv) the parameter's accessibility [32]. A decision tree, shown in Figure A.1, was first utilised to pick an EOS. Considering that non-polar, real components are used at high pressures, the following EOSs could be used: Peng-Robinson (PR), Redlick-Kwong-Soave (RKS), or Lee-Kesler-Plocker (LKP). However, given that at times there are pseudo and real components present, Chao Seader (CS) could also be utilised. Pseudo-components were used to adequately model the oil and condensate in the system. Given the aforementioned, as a starting point, RKS was chosen for both of the models to be developed, with an exception for the glycol dehydration unit. To cope with the pseudo-components, customised binary interaction parameters are employed.

It should be noted that Platform A and B utilise different pseudo-components. The reason for this is that the validation data for these platforms comprises of different data sets. So to compare the model to 'real' data, different sets of pseudo-components must be used. However, after the validation steps, only the pseudo-components from Platform B will be used for the model. This is due to two reasons: firstly, Platform A has a substantial amount of components - unnecessarily complicating the system; secondly, this set of pseudo-components is not listed for public use. Whereas the set of pseudo-components for Platform B has been published for public use [7]. When defining pseudo-components the most important variables are the critical properties (temperature and pressure) and the acentricity factor.

4.3.3 Compressor Maps

Compressor maps were implemented for all situations where it was possible. These maps were extracted from the UniSim model, and then subsequently implemented in the HYSYS model. As maps from manufacturers are strictly confidential and are not published, the used maps were more general for a compressor of the same size. A sample of one of the compressor maps can be seen in Figure A.2. These maps gave much more realistic power outputs and efficiencies in

comparison to the inherited model, where these values were guessed and were constant for any given flow rate. This is important because the compressors dictate the power requirement of the platform, and subsequently the carbon emissions.

4.3.4 Dehydration Unit

Dehydration is an important process for treating natural gas on offshore platforms. Excess water needs to be removed to prevent corrosion, and more importantly the formation of hydrates in the export gas pipeline. In commercial practice, there are three main methods of dehydration: absorption; adsorption; and condensation [33]. The preferred method for offshore platforms is absorption via the use of a glycol solvent.

The utilised solvent is typically triethylene glycol (TEG). In this process, lean TEG is contacted with the wet gas stream. The TEG essentially strips the wet gas process stream of water. The now dry process gas then leaves the column and is sent to the subsequent process steps. The rich TEG, full of the absorbed water, is then stripped in a column, cooled and sent back into the absorption column - completing the TEG loop. Within the TEG absorption column, stripping gas can be utilised to aid the removal of water from the rich TEG stream. The stripping gas can be any inert gas, however, on offshore platforms, it is typical to use process gas. An overview of the process is shown in Figure 4.2.

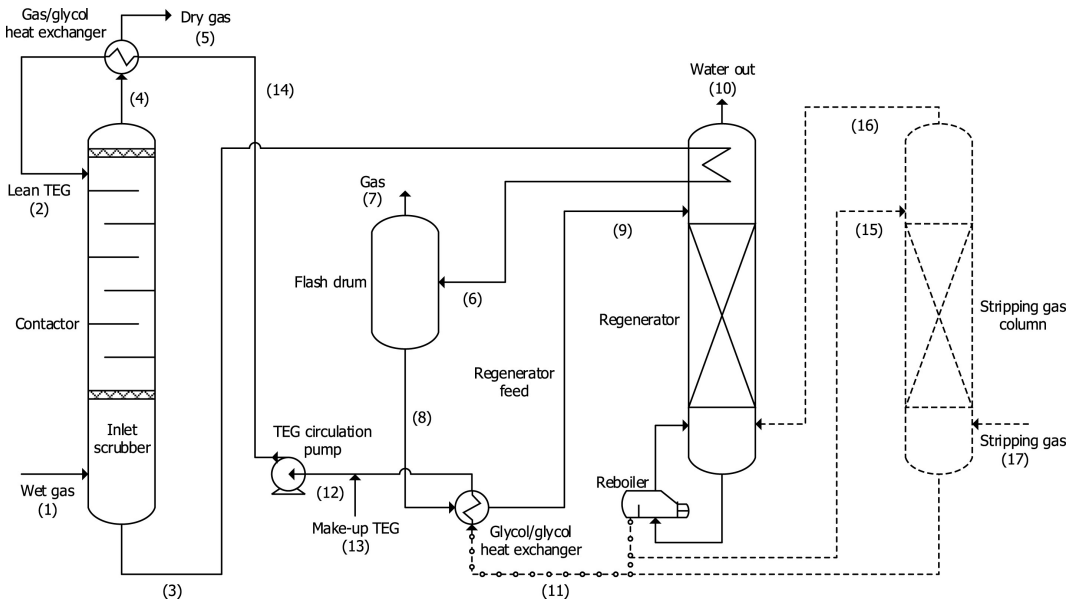

Figure 4.2 Schematic of a natural gas dehydration system using TEG as a solvent, taken from [34]

To set-up the dehydration unit on HYSYS, the local glycol property package was selected to simulate the behaviour of the system. One of the most important factors when designing a dehydration system is the selection of the minimum concentration of TEG (lean) which will enter the absorber [33]. There are two key variables in this decision: the equilibrium dewpoint temperature; and the contactor temperature. The equilibrium dewpoint temperature is dependant on the requirements

of the dry gas. The export pipeline restrictions state that the maximum water dew point should be -18 °C (at 69 barg). Given this, and the desire to keep the incoming wet gas stream at the receiving temperature (30 °C), a TEG concentration of 99.0 wt % is chosen. The figure dictating this concentration can be seen in Figure A.3.

Aside from the parameters that dictate the performance of the process gas/TEG absorber, the design of the TEG regeneration loop is very important. The main design parameters for this subsystem is the reboiler pressure and temperature, these factors will determine the quality of the TEG that is fed back into the initial absorber. The selection of these parameters is based upon the design procedures illustrated in [33]. A summary of all the design variables utilised for this model can be seen in Table 4.4.

Table 4.4: TEG dehydration system design parameters

Design Variable	Unit	Value
TEG circulation flowrate	kg/s	1.00
Lean TEG concentration	w.t. %	99.0
Regenerator column pressure	barg	0.80
Regenerator reboiler temperature	°C	180
Regenerator pump efficiency	%	75.0

4.3.5 Simulation Model Assumptions

- An ambient temperature of 15 °C was chosen, e.g. the air enters the gas turbine compressor at this temperature
- When sea-water is used as a coolant, it is assumed to be available at 10 °C and the maximum return temperature is set to 20 °C.
- When relevant, the minimum approach temperature in heat exchangers is set to be 10 °C.

4.4 Validity of the Model

In order to determine the validity of the developed HYSYS model, the obtained results were compared against "real" data from the respective platforms. As previously discussed, this involves two validation procedures. Initially, the first model is compared against data from Platform A. After the various modifications are implemented, the results are then validated for Platform B. The real data for Platform A is taken from the received model from Equinor, which is developed on Honeywell UniSim. Henceforth in the upcoming sections, this model will be referred to as the "UniSim Model". The validation data for Platform B was taken from [7], where a study comparing this platform was conducted.

This section will compare the input and output variable from both simulations, and comment on any explainable key differences and/or similarities.

4.4.1 Platform A Validation

Equation of state

The UniSim model was developed using a Redlich-Kwong-Soave (RKS) equation of state. In order to model the condensate in the system, pseudo-components were utilised. To accurately simulate the interaction between the aforementioned condensate and the additional components, customised binary interaction parameters are employed. These same binary interaction parameters were utilised for the HYSYS model, as previously mentioned. The EOSs discussed in subsection 4.3.2 are compared in Table 4.5. Three key streams were chosen for the comparison: oil export; natural gas export; and the vapour outlet of the first 3-phase separator. The reason the vapour outlet stream from the 3-phase separators is chosen is because this is a situation where there is an interaction between the liquid, aqueous and vapour phases - which is a key feature for an EOS to predict. The Molecular Weight (MW) of the respective stream was chosen as a comparison variable as there are many components that are difficult to completely compare, so to aid in the comparison this value is utilised. It essentially illustrates whether or not the composition of the compared streams are similar or not.

Table 4.5: Comparison between the different equation of states for Platform A

Stream	Variable	HYSYS Model - RKS Variant	HYSYS - Peng Robinson	HYSYS - Chao Seader	UniSim Model
Oil Export	Mass Flowrate (kg/s)	94.78	94.56	94.47	94.78
	MW (g/mol)	188	187.7	187.4	187
Gas Export	Mass Flowrate (kg/s)	87.83	88.08	88.03	87.94
	MW (g/mol)	19.4	19.39	19.4	19.4
3-phase separator	Mass Flowrate (kg/s)	66.25	66.33	65.56	66.11
	MW (g/mol)	18.93	18.95	18.89	18.91

From Table 4.5 it is seen that the HYSYS RKS and UniSim model have very similar output flowrates for the oil stream. There is a difference in the MW, with the Chao Seader package having the closest value to the UniSim model. However, the CS mass flowrate is off by a much large portion. Looking at the export gas, the mass flowrate for RKS and CS is essentially within the same range as the UniSim model. The MW value of the RKS model is identical to the UniSim model though. Finally, looking at the vapour outlet stream of the 3-phase separator, the RKS model is the closest for the mass flowrate value. There is minimal difference between the RKS and CS models with regard to the MW (when comparing to the standard model). In almost all cases, the Peng-Robinson model is the furthest away at predicting the behaviour seen in the UniSim model. This is a possibility due to the fact that this EOS has no appropriate method of dealing with pseudo-components - which is a factor more prevalent in both the RKS and CS models.

Reflecting on the aforementioned differences, there is no clear indicator to tell whether CS or RKS suits the system better, each has their own benefits. However, it can be said that the most

important stream is the export gas. The RKS model accurately predicts this stream with regard to the MW, which is an important feature as this represents the composition of the export gas. In addition, the RKS model has the closest mass flowrate values for both the oil and 3-phase separator streams. Thus, the RKS model can be said to fit the data presented by the UniSim model with the highest accuracy.

Outlet streams

To determine how accurately the HYSYS system predicts the platform behaviour, the outlet streams of the standard model is compared against the developed model. This is shown in Table 4.6, with the full comparison illustrated in Table A.1. It is seen that there are minimal differences between the two models. Thus, it can be said that in the context of validating the outlet streams, that the HYSYS model appropriately simulates Platform A.

Table 4.6: Comparison between developed model and the control model outlet streams for Platform A

Stream	Variable	HYSYS Model	UniSim Model	Percentage Difference
Gas Export	Mass Flowrate (kg/s)	87.74	87.94	0.232%
	MW (g/mol)	19.4	19.4	0.0526%
Oil Export	Mass Flowrate (kg/s)	94.82	94.78	0.0431%
	MW (g/mol)	188	187	0.267%
Gas Reinjection	Mass Flowrate (kg/s)	75.83	75.86	0.0430%
	MW (g/mol)	19.4	19.4	0.0492%
Fuel Gas	Mass Flowrate (kg/s)	6.41	6.41	0.0480%
	MW (g/mol)	18.7	18.7	0.00657%
Produced Water	Mass Flowrate (kg/s)	194.45	194.44	0.00226%
	Temperature (°C)	57.4	56.9	0.9034%

Compression requirements

As previously stated, the power requirements of the process compressors are one of the most important aspects of the simulation, thus, it is important that reasonable and accurate values are obtained. The comparison between the developed and standard model is shown partially in Table 4.7 and in full in Table A.2.

Table 4.7: Comparison between developed model and the control model compressor requirements for Platform A

Unit	Variable	HYSYS Model	UniSim Model	Percentage Difference
1st Gas Recompressor	Duty (kW)	1082	969	10.4%
	η_{np} (%)	67	63	5.02%
2nd Gas Recompressor	Duty(kW)	588	635	7.93%
	η_{np} (%)	43	42	1.68%
3rd Gas Recompressor	Duty (kW)	2914	2860	1.8%
	η_{np} (%)	64	60	6.2%
Export Pipeline Compressor	Duty (kW)	33237	33207	0.09%
	η_{np} (%)	80	78	2.86%
Gas Reinjection Compressor	Duty (kW)	15125	15202	0.51%
	η_{np} (%)	70.9	71	0.51 %
Total	Duty (kW)	52945	52874	0.14%

Compared to the previous table, the differences between the two models are far more notable. The differences between the first three compressors can be explained by the fact that the compression duty is entirely dependant on the pressure levels in the recompression train. In the HYSYS model, the pressure level of the second last separator is slightly higher than in the UniSim model. Thus, the first compressor will have to do slightly more work than the others. This is seen when Table A.2 is viewed, as the pressure ratio is higher in the HYSYS model, whilst the mass flowrates are similar. This subsequently impacts the compressor efficiency which is lower in the case of the UniSim model. If the duty of all three compressors in the recompression train is summed up, the value will be similar for both models.

The pipeline compressor has very similar duties for both models. The polytropic efficiency of the HYSYS compressor is higher than that of the UniSim compressor. A possible reason for this can be attributed to the fact that the HYSYS model has a slightly higher MW at this stage. Looking at the total compression duty, there is minimal difference between the two models. Thus, based on this, the model can be deemed to be accurate for estimating the compressor duty for Platform A - this being an important fact for later analysis.

Heating and cooling requirements

The last important comparison between the two models is with regard to the heating and cooling requirements. This is partially shown in Table 4.8 and fully shown in Table A.3. The difference in the dehydration coolers can be explained by the fact that the total mass flow rate is split across the two coolers. The split between the two coolers is slightly different in the compared models, this is seen by the fact that the total cooling duty and mass flow rate values are similar. The duty of the third suction cooler also differs between the two models. This is due to the HYSYS model having a slightly lower supply temperature than the UniSim model. This difference can be explained by the fact that the supply temperature is completely dependant on the compression ratio of the individual compressors in the recompression train - with the reason for this being explained in Section 4.4.1.

The remaining coolers and heaters illustrate minimal differences between the two models. The units that alter the temperature of the crude streams present a good result for deciding upon the validity of the model. This is because this is where the importance of a well matched equation of state comes into play, as here the simulator will estimate multiple physical properties of the respective streams.

Table 4.8: Comparison between developed model and the control model heating and cooling requirements

Unit	Function	Variable	HYSYS Model	UniSim Model	Percentage Difference
Gas Export Compressor Aftercooler	Cooler	Duty (kW)	42718	42694	0.05%
		Mass Flow (kg/s)	164	164	0.13%
Gas Dehydration Cooler 1	Cooler	Duty (kW)	7385	7033	4.76%
		Mass Flow (kg/s)	113	107	5.47%
Gas Dehydration Cooler 2	Cooler	Duty (kW)	3649	4086	12%
		Mass Flow (kg/s)	56	62	11%
Recompression Aftercooler 1	Cooler	Duty (kW)	706	715	1.3%
		Mass Flow (kg/s)	3.90	3.97	1.7%
Recompression Aftercooler 2	Cooler	Duty (kW)	1003	972	3.1%
		Mass Flow (kg/s)	3.45	3.45	0.15%
Recompression Aftercooler 3	Cooler	Duty (kW)	1417	1610	14%
		Mass Flow (kg/s)	12	12	0.8%
Gas Reinjection Cooler	Cooler	Duty (kW)	15876	15961	0.5%
		Mass Flow (kg/s)	82	82	0.1%
Gas Reinjection Aftercooler	Cooler	Duty (kW)	3848	3886	1.0%
		Mass Flow (kg/s)	82	82	0.1%
Export Crude Cooler	Cooler	Duty (kW)	7869	7889	0.3%
		Mass Flow (kg/s)	95	95	0.04%
Inlet Crude Heater	Heater	Duty (kW)	6035	6111	1.3%
		Mass Flow (kg/s)	95	95	0.3%

4.4.2 Platform B Validation

The developed model does not have the exact same layout for Platform B as is seen in [7]. The key differences between the model and what is seen in the respective literature is the number of units. Meaning that there is a different number of separators, heaters, coolers, and compressors.

This means that the same validation method for Platform A is difficult for this case scenario, as units cannot be compared one-on-one in this instance. Thus, given this, the comparisons will mainly be done by considering the overall requirements. However, this validation method, whilst different, is still relevant. The goal of this model is to predict the power requirements of a platform, and if the model completes this with reliability and accuracy then the objective is met. Additionally, this point further comes across if the model illustrates that it can handle different scenarios, flowrates, pressures and temperatures.

Thus, in this subsection, a validation approach that compares the overall results from the model will be conducted. However, if possible and relevant a one-on-one approach may be applied.

Equation of state

The same equation of state for Platform A is used for Platform B. This does not require further validation as the model developed in [7] also utilises the same EOS. However, as previously mentioned, this model utilises different pseudo-components to predict the behaviour of the heavier hydrocarbons (C7+). These hypothetical components are taken directly from [7] and the respective data is shown in Table 4.9.

Table 4.9: Platform B pseudo-components, adapted from [7]

Component	M (g/mol)	T_{BP} (°C)	T_C (°C)	ρ_{liq} (kg/m^3)	P_c (bar)
Hypo A-1	81	73	247.9	721.2	33.46
Hypo C-1	98.78	85.76	269.3	754.3	35.5
Hypo C-2	141.2	173.9	365.7	816.6	27.19
Hypo C-3	185.8	240.5	434.1	861	22.71
Hypo C-4	241.1	314.5	505.2	902.5	18.54
Hypo C-5	404.5	487.1	647	955.3	10.45
Hypo C-6	907	552.8	710	1007	9.61

Outlet streams

The outlet streams can be seen in Table 4.10. Here, there are minimal differences between the mass flowrates of the respective outlet streams. It can be said that the results are not as precise as the results seen for Platform A. However, given that this model was specifically developed for Platform A and rather adapted to Platform B, the marginal differences for this comparison can be considered acceptable in the context. When the molecular weight is considered, the difference is largest for the oil export sections. The oil export contains a higher proportion of entrained lighter hydrocarbons in the developed model, which subsequently lowers the MW. The most probable reason for this is that the literature model has an additional horizontal separator in comparison to this model. This means that additional gas can be liberated from the oil stream. Simultaneously this explanation also accounts for the differences seen in the gas export mass flowrates.

Table 4.10: Platform B - outlet stream comparison

Stream	Variable	HYSYS Model	Real Data	Percentage Difference
Gas Export	Mass Flowrate (kg/s)	80.10	80.62	0.65%
	MW (g/mol)	18.86	18.93	0.37%
Oil Export	Mass Flowrate (kg/s)	286.90	286.20	0.24%
	MW (g/mol)	293.00	297.30	1.47%
Gas Reinjection	Mass Flowrate (kg/s)	4.82	4.84	0.44%
	MW (g/mol)	18.86	18.93	0.37%
Fuel Gas	Mass Flowrate (kg/s)	2.15	2.15	0.14%
	MW (g/mol)	18.82	19.00	0.96 %
Produced Water	Mass Flowrate (kg/s)	71.46	71.58	0.17%

Additional requirements

The only variable available for comparison is the total compression requirements of the platform. However, this is still sufficient for comparison between the two models. As it can be seen there are no large differences between the respective requirements. This is a positive result given that there are a different number of compressors in the separate systems.

Table 4.11: Comparison of compressor requirements for Platform B

Variable	HYSYS Model	Real Data	Difference
Total Compressor Duty (MW)	24.77	24.62	0.61%

4.4.3 Validity Conclusion

As can be seen from the aforementioned analyses, there are no large differences between the two models, with the HYSYS model being similar to the UniSim model in almost all regards for Platform A. In comparison to the validation method for Platform A, Platform B underwent a far less rigorous check. However, the most important aspects were considered: the outlet streams; and the compression requirements. These previously mentioned variables present the most useful information for further analysis with the model. As was the case with Platform A, there were minimal differences between the developed model and the model presented in [7].

For absolute validation of the developed model, given that more information is available for Platform B, it is recommended that a more rigorous check of the model is completed. However, this is not essential. One of the main goals of this study is to investigate the possibility of reducing carbon emissions in the power generation sector and this can be completed with ease from the information that has been validated.

4.5 Model Modifications

After the validation procedure, the model was then altered to include the power generation and various energy-efficient systems. This section will outline the respective changes made to the model, illustrating the various impacts that arise from the implementation of the aforementioned energy-efficient technologies. A large number of processes are presented in Section 3; however, not all options are viable for this project. Electrification, from onshore energy sources, is not viewed for this particular analysis. The reason for this is that these operations are extremely expensive to effectuate, they need to be installed over a long timescale, and they are not practically possible for all platforms. The same can be said for CCS technology, which is not investigated.

This analysis rather concerns technology that can be installed within a shorter time-period, and focuses on improving existing systems to make them more efficient or more carbon neutral. Given this, the following technologies and/or systems will be covered in this section:

- Resizing of gas turbines
- CO_2 and H_2O bottoming cycles
- Waste heat recovery of compressor heat
- Platform heat integration options
- Addition of multi-phase expanders in the production manifold

Before illustrating the impacts of the above technologies, the method of calculation or estimation will first be elaborated upon.

4.5.1 Gas Turbine Simulation and Part-load Estimation

As discussed in Section 3.1, it is important to appropriately size the utilised gas turbine because as the part-load percentage of the gas turbine decreases, the overall efficiency decreases. In this analysis, two gas turbine models are viewed: GE LM2500+G4 DLE, which is a 32.6 MW turbine; and a GE LM2500 DLE, which is a 21.3 MW turbine.

One of the most important aspects of simulating a gas turbine is estimating the off-design performance, as these units are almost always operated with a load lower than that of their design load. Accurately simulating the off-design performance is a rigorous process, and it is commonly performed using niche software specifically aimed for this purpose, such as Thermoflow GT PRO. This software will contain the appropriate compressor and turbine maps that are necessary for these calculations. Obtaining these maps outside of the software is not possible, as they are not published. Thus, in order to accurately simulate off-design performance outside of this software and rather in HYSYS, an alternative method had to be developed. To do this, a data set published by [35] was utilised. This resource contains the exhaust gas temperature, mass flow rate, and heating rates at design and off-design conditions. From this, correlations were developed to estimate these values at different load conditions, which the HYSYS model could then solve for. These correlations are illustrated in Figure 4.3 and 4.4.

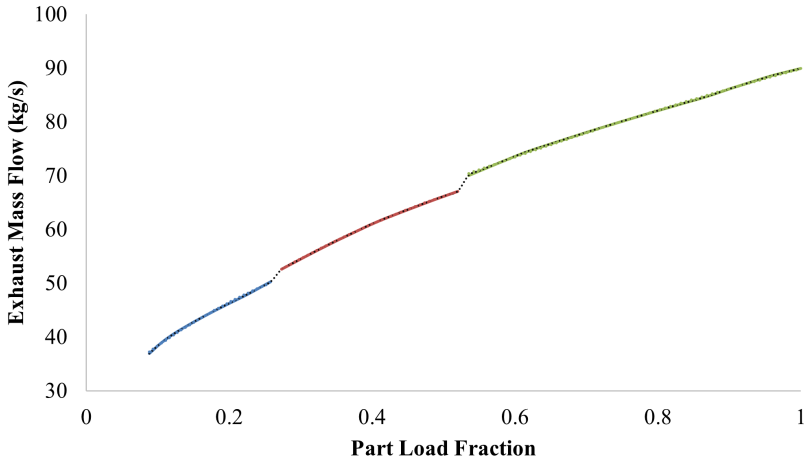

Figure 4.3 Exhaust gas mass flowrate variation with part-load fraction, for a GE LM2500+G4 gas turbine [35]

Looking at these figures, it can be seen that lines can be split up into three intervals. With this, three equations can be developed per variable. The practical reason for these intervals is that this gas turbine uses dry low emissions (DLE) technology for the combustor. This means that the combustor contains separate zones and burners which fire at different rates dependant on the load of the gas turbine. The use of different zones and burners means that the flame temperature can be kept below 1200 °C - prohibiting the formation of NOx. A Conventional combustor will have a far higher internal flame temperature, with a much higher NOx formation rate.

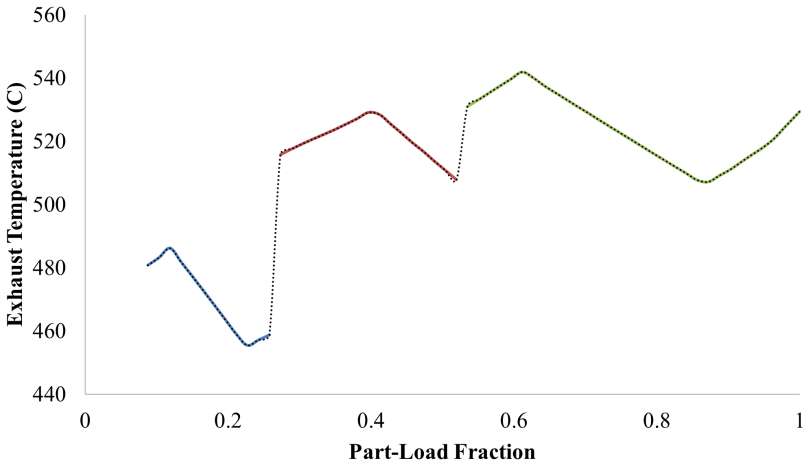

Figure 4.4 Exhaust gas temperature variation with part-load fraction, for a GE LM2500+G4 gas turbine [35]

When the aforementioned correlations were implemented into HYSYS, Figure 4.5 resulted. From here, it is illustrated that the same trends seen in Figure 4.3 and 4.4 are obtained. Note that different part-load ranges are shown in the below figure in comparison to the above figures.

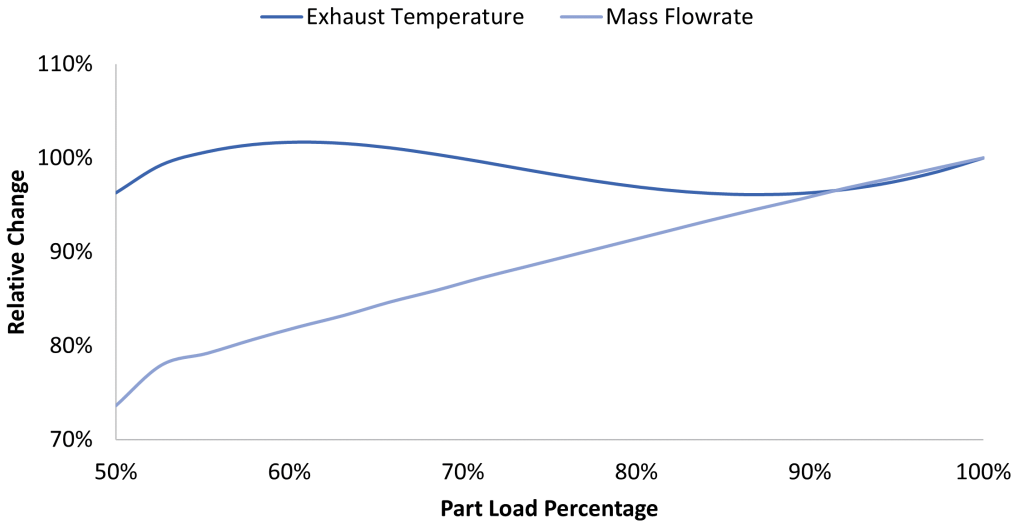

Figure 4.5 Exhaust gas mass flow and temperature relative variation with part-load fraction, from HYSYS

This was completed with the following assumptions:

- Isentropic efficiency for both the turbine and compressor is constant, with values of 84 % and 89 % used respectfully
- A constant generator efficiency value of 97.5 % is used
- Ambient temperature of the air into the compressor is constant, using a temperature of 15 °C

- Air humidity is not considered in the model
- A pressure drop of 1 % is assumed across the combustor

4.5.2 Bottoming Cycle

Here two cycles were simulated, a steam and a CO_2 bottoming cycle. For both the cycles it was assumed that with part-load performance the pressure levels will not change, with the adjusted variable rather being the mass flowrate of the working fluid in question.

Steam bottoming cycle

Only once-through steam bottoming cycles were considered in this analysis. The method outlined in [10] was followed. The variables that were assumed and used throughout the simulation are shown in Table 4.12. A schematic of the utilised system is previously illustrated in Figure 3.2.

Table 4.12: Steam bottoming cycle assumed variables

Variable	Value
Live steam pressure (bar)	25
Live steam temperature (°C)	450
Exhaust Gas Outlet Temperature (°C)	170
Condenser Pressure (bar)	0.05
Steam Turbine Efficiency (%)	88
Water Pump Efficiency (%)	70
Cooling Water Supply Temperature (°C)	10
Cooling Water Exit Temperature (°C)	20

CO_2 bottoming cycle

Once again, only a single-stage CO_2 bottoming cycle was modelled in this analysis. The procedure outlined by [12] was followed, with the various assumed variables shown in Table 4.13. A basic schematic of the followed system can be seen in Figure 3.3.

Table 4.13: CO_2 bottoming cycle assumed variables

Variable	Value
Superheated CO_2 pressure (bar)	200
Superheated CO_2 temperature (°C)	365.2
Exhaust Gas Outlet Temperature (°C)	170
Condenser Pressure (bar)	58.1
CO_2 Turbine Efficiency (%)	85
Condensed CO_2 Pump Efficiency (%)	80
Cooling Supply Water Temperature (°C)	10
Cooling Water Exit Temperature (°C)	20

4.5.3 Compressor Waste Heat Recovery

To recover the waste heat that is lost to the environment when the compressor discharge stream is cooled, a transcritical CO_2 cycle is utilised (similar to that of the CO_2 bottoming cycle). One of the most important variables for this technology is the supply temperature, as this must be

high enough for the cycle to be viable. Given this, only coolers with supply temperatures over 100 °C are considered. Following this, the target temperature must be higher than the bubble point temperature of the considered working fluid at the outlet pressure of the turbine. Thus, only target temperatures above 30 °C are considered.

To illustrate how the streams will be selected for this technology and how much energy can be recovered from this system, Platform A will be considered as an initial example. The streams seen in Table 4.14 were considered for this process. Following the aforementioned criteria, only two coolers are considered viable for this process: the gas export aftercooler; and the gas reinjection cooler. Both these streams have high pressures, which is a beneficial feature with regard to the compactness of the cycle's heat exchanges. As space is in limited supply on the offshore platform, only one stream was considered viable for replacement. Given that gas export aftercooler has a duty almost threefold larger than that of the reinjection cooler it was selected for this analysis.

Table 4.14: Available streams for waste heat recovery

Unit	Duty (kW)	T_{supply} (°C)	T_{target} (°C)	Mass Flow (kg/s)
Gas Export Compressor Aftercooler	42718	137	50	164
Gas Dehydration Cooler 1	7385	54	30	113
Gas Dehydration Cooler 2	3649	55	30	56
Recompression Aftercooler 1	706	111	30	3.90
Recompression Aftercooler 2	1003	152	30	3.45
Recompression Aftercooler 3	1417	77	30	12
Gas Reinjection Cooler	15876	113	53	82
Gas Reinjection Aftercooler	3848	44	33	82

The procedure outlined in [15] was followed, with the general schematic illustrated in Figure 3.5. The basic assumptions and obtained results are seen in Table 4.15.

Table 4.15: Assumed values and obtained results for the transcritical CO_2 cycle

Variable	Value
Superheated CO_2 pressure (bar)	170
Superheated CO_2 temperature (°C)	127
Outlet Stream Temperature (°C)	50
Condenser Pressure (bar)	41.2
CO_2 Turbine Efficiency (%)	85
Condenser CO_2 Pump Efficiency (%)	80
Cooling Supply Water Temperature (°C)	10
Cooling Water Exit Temperature (°C)	20
Turbine Power (kW)	7633
Pump Power (kW)	3474
Gross Power (kW)	4160
Net Power (kW)	4056

4.5.4 Platform Heat Integration

It is important to utilise all heat available on a platform to avoid the unnecessary use of heaters. Once again, as with the previous section, Platform A will be used as an example to illustrate the heat integration procedure. Looking at Table 4.8, the only cold stream available for heat integration

on the platform is the crude heater. This means that for this scenario a pinch analysis will not be necessary, as all viable hot streams can be integrated with the single aforementioned cold stream. The criteria for matching with the crude heater should be the following:

1. The heat exchange should be conducted in as few units as possible, i.e. a minimum amount of hot streams should be matched with the cold stream - aiming to cover the entirety of the duty
2. The exchange must not violate the minimum approach temperature, nor must it cause temperature cross over
3. The stream already considered for the waste heat recover CO_2 cycle should not be considered for heat integration possibilities

Thus, given the aforementioned criteria, there is only one real possibility of integration. This will be matching the stream from the gas reinjection cooler with the crude heater. This exchange is summarised in Table 4.16. Another possibility for integration that is not considered in this analysis is the use of the hot flue gas that exits the bottoming cycle at a temperature of around 170 °C.

Table 4.16: Platform heat integration summary

Variable	Reinjection Cooler	Crude Heater
Function	Hot Stream	Cold Stream
T_{supply} *(°C)*	113	50
T_{exit} *(°C)*	99.1	101
mCp (kW/°C)	312	82
Duty (kW)	4164	

4.5.5 Production Manifold Expanders

As mentioned in Section 3.4 there is huge promise for utilising the pressure reduction in the production manifold to generate power for use on the platform via the use of expanders. In the base scenario, the choke valves decrease the pressure of the incoming streams, and the energy from this pressure reduction is lost irreversibly.

Using Platform A as an example for the purpose of illustration, the viable incoming streams are shown in Table 4.17. It should be noted that these streams have different names and pressures to those shown in Table 4.1. In the previous representation, the high pressure (HP) streams were grouped together after the inlet well throttling. Here, to present the potential of recovering energy from the production manifold, they have been reverted back to their original pressures before the aforementioned grouping. It can be seen from these streams that all scenarios are possible. They have large mass flowrates and pressure reduction ratios. However, as these streams are essential with regard to the operation of the platform, not all streams will be utilised in this analysis. The streams that require the greatest reduction in pressure will be viewed. Thus, given this, streams HP1, HP2, and HP3 will be considered.

The efficiency range of multi-phase expanders range between 30 % and 70 %, for the sake of this analysis, an isentropic efficiency value of 70 % will be utilised. This is chosen as given that the appropriate technology is commercially viable, this analysis will show the promise that is available.

Table 4.17: Available streams in the production manifold for implementing expanders

Stream	Pressure In (bar)	Pressure Out (bar)	Mass Flow (kg/s)
LP1	40.0	19.0	89.0
HP1	145	60.0	62.7
HP2	156	60.0	46.8
HP3	142	58.0	233

Using these three streams, the power recovered is shown in Table 4.18. It is seen that a large amount of energy is able to be recovered with a combined total of 12.4 MW being generated. Here it is assumed that the expanders will drive a generator and not compressors or other turbomachinery units on the platform - for the sake of operability. As reliability is the main concern when it comes to these units, it is important that there is a fail-safe mechanism present to keep the platform running in the case of issues with the expanders. Thus, by-pass lines leading to choke valves should be utilised. As the temperature reduction is greater when utilising an expander than when using a valve, a cooler must be placed down stream from the by-pass valve to compensate for the temperature difference. This will ensure that there is no change to the rest of the downstream process units.

Table 4.18: Implemented expanders for the production manifold with key results

Stream	Pressure In (bar)	Pressure Out (bar)	Temp In (°C)	Temp Out (°C)	Mass Flow (kg/s)	Power (kW)
HP1	145	60.0	76.8	33	63	4100
HP2	156	60.0	54.0	12	47	2307
HP3	142	58.0	61.0	47	233	6052

Chapter 5

Key Performance Indicators

Key performance indicators (KPIs) are important parameters used to compare different scenarios quantitatively. In this report, the main emphasis is on the reduction of CO_2 emissions, increasing energy efficiency, and the associated operational costs incurred; thus, this will be the main focus of the implemented KPIs.

5.1 CO_2 Footprint

The following equation was used to measure the carbon footprint of the compared processes:

$$CO_2\,(kg/BOE) = \frac{CO_2\,Emitted\,(kg/s)}{Barrel\,of\,Oil\,Equivalent\,Produced\,(barrel/s)} \tag{5.1}$$

Note that oil equivalent (OE) refers to the total sum of oil, gas, and condensate that is produced from the platform. The conversion factor stated by The Norwegian Petroleum Directorate was utilised, where 1000 Sm^3 of gas relates to 1 Sm^3 OE [36].

Aside from the CO_2 emitted from the combustion of the fuel in the power generation scenario, CO_2 emissions from the production of H_2 will be included in the scenarios where H_2 is blended into the combustion fuel. The reason why this is included is that it would be an inaccurate assumption to state that H_2 is completely carbon neutral. In terms of large scale production, H_2 is typically produced via the reforming of natural gas. The CO_2 intensity of the utilised hydrogen is taken from a study that considers the production of H_2 via reforming of natural gas with CCS [37]. This value was taken as **0.8 kg CO_2/kg H_2**.

5.2 Energy Efficiency

The below equations were utilised in defining the KPIs that relate to system energy efficiency:

$$Power\ Requirement\ (kW) = \dot{W}_{tot,compressors} + \dot{W}_{tot,heating} - \dot{W}_{recovered}$$

$$\dot{W}_{GT,gross}\ (kW) = \dot{W}_{turbine} - \dot{W}_{compressor}$$

$$\dot{W}_{GT,net}\ (kW) = \dot{W}_{GT,gross} \cdot \eta_G$$

The following equations relate to the defined energy efficiency KPIs:

$$\eta_{GT,net}\ (\%) = \frac{\dot{W}_{GT,net}}{LHV_{NG} \cdot \dot{m}_{NG}} \cdot 100 \tag{5.2}$$

$$\eta_{CC,net}\ (\%) = \frac{\left(\dot{W}_{GT,gross} + \dot{W}_{\mathrm{H_2O/CO_2}\ turbine} - \dot{W}_{AUX}\right) \cdot \eta_G}{LHV_{NG} \cdot \dot{m}_{NG}} \cdot 100 \tag{5.3}$$

$$\eta_{TOT}\ (\%) = \frac{Power\ Requirement}{LHV_{NG} \cdot \dot{m}_{NG}} \cdot 100 \tag{5.4}$$

The KPIs relating to η_{TOT} is important because it will include the power recovered by the various energy-efficient processes that are implemented throughout the production facility. It does not relate to the efficiency of the individual process, rather to the system as a whole. It links the power generation requirement to the energy supplied via the combustion of the natural gas; which is essentially the energy input into the platform if electrification is not considered.

5.3 Operational Costs

To compare the various costs associated with the implementation of various technologies the differential operational costs will be considered. In terms of the scope of the term operational costs, the following aspects will be considered: cost of natural gas as a fuel; cost of H_2 as a fuel; and incurred CO_2 taxes. General operational costs such as labour and utilities are not included in this term. Rather operational costs which change with the various energy-efficient technologies are considered. The cost of natural gas and H_2 is taken from [37], whilst the CO_2 tax for 2021 is taken from [5]. These values are shown in Table 5.1.

Table 5.1: Respective costs of the various fuels and the implemented carbon tax

Variable	Unit	Value
CO_2 Tax (2021)	NOK/kg CO_2	493
Cost of H_2	NOK/kg	16.24
Cost of NG	NOK/kg	2.15

The resultant KPI can be seen in the equation below:

$$C_{Total}(NOK) = C_{H_2} + C_{NG} + C_{CO_2 Tax} \tag{5.5}$$

Chapter 6

Model Analysis

After the development and verification of the model, the next step is to analyse the output data. This chapter will first put forward a future scenario for the lifespan of a platform based on one of the previously studied platforms. The various energy-efficient technologies described in the previous chapters will then be applied to this future platform lifespan scenario. The technologies will then be compared against one another utilising the aforementioned key performance indicators as an important tool. Finally, once all the technologies have been adequately compared, a future low emission configuration will be proposed and analysed.

6.1 Platform Lifespan Analysis

This section will outline the applied methodology when determining a future scenario for the lifespan of the platform. This is important for two main reasons. Firstly, it illustrates the flexibility of the model and how it can perform with different operating conditions and flowrates. Secondly, it provides crucial information on how the various energy-efficient technologies operate over a long period of time and additional data with regard to achieved CO_2 and cost savings.

A platform typically produces in three main phases: build up; plateau and decline [38]. In the build up phase, the hydrocarbon production starts slow, whilst there are minimal quantities of water in the feed. As the hydrocarbon feed reaches its highest point the plateau phase is then entered. Between the two phases, the quantity of water produced increases in an exponential fashion. After a certain amount of time, the oil and gas volumes start to decrease as the decline phase is then entered. At a certain point, there will be a higher quantity of water produced than oil and gas. At this point, the field is considered mature. This is illustrated graphically in Figure 6.1. It should be noted that this is a general model of how a field can behave, but this does not imply that every field is the same. Some fields have lower gas to oil ratios and higher contents of water. The takeaway from this figure should be that after a certain amount of certain hydrocarbon production will slow

down and the quantity of water at the platform inlet will increase substantially.

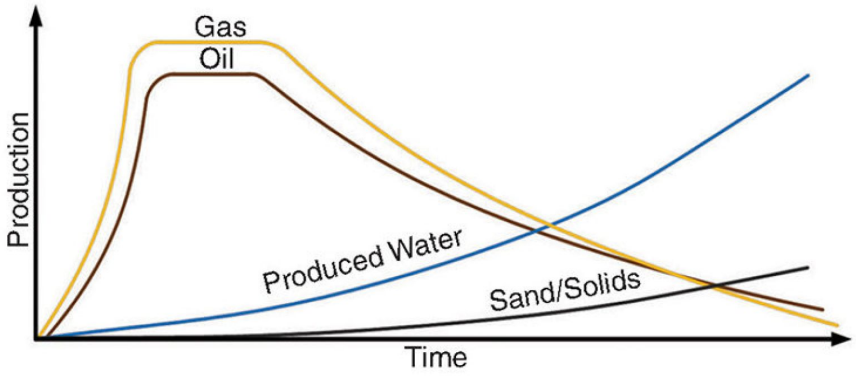

Figure 6.1 Typical oil, gas and water volume flowrates over platform lifespan, taken from [39]

Platform B was chosen as a starting point for the lifespan. One of the key reasons that this was chosen is due to this platform having far fewer components in comparison to Platform A. This means that generating data would be a far simpler task. Another important reason is that the list of pseudo-components has been published publicly, so future work of the developed model can easily continue.

The aim was to mirror the curves seen in Figure 6.1 whilst using Platform B as a basis. The data of Platform B used in the previous chapters was taken after its tenth year of operation. Thus, using this, additional years of operation could be estimated. A thirty year lifespan was selected, with the field composition changing every fifth year. The initial data for Platform B was set as the tenth year. To try to remain as accurate as possible, the hydrocarbon to water and oil to gas ratios were used as the method of scaling. At the same time, the ratios of components within the gas or oil range were kept constant. Essentially this means that the quantity of oil and gas was altered, changing the overall composition and flowrate of each component; however, at the same time, the composition of an oil component was kept constant relative to the oil stream itself. Although this method is not completely accurate, it achieves the goal of obtaining a set of data that simulates the lifespan of a platform, as well as follows the trends that are seen in literature.

The results of this can be seen in tabular form in Table B.1 and graphically in Figure 6.2. Looking at the figure, it can be seen using the aforementioned method, the trends seen in literature are matches to a sufficient degree. Thus, based on this, this lifespan scenario can be deemed to be accurate and sufficient for later use in this chapter. Another assumption made in this analysis is that the quantity of inerts increases over the platform lifespan in a similar manner to that of water. In this case, the term inerts refers to N_2 and CO_2.

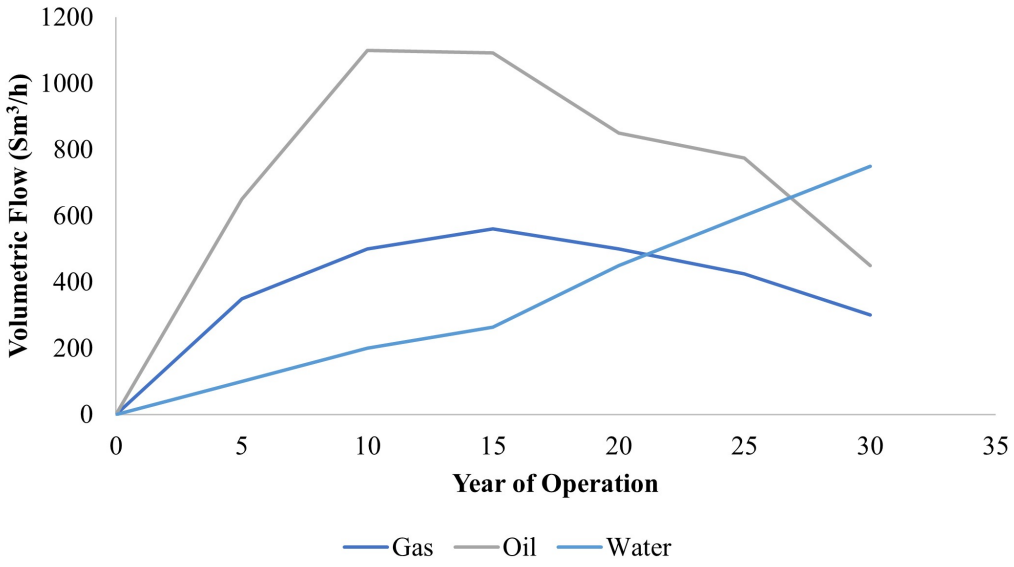

Figure 6.2 Oil, gas and water volume flowrates over platform lifespan

6.2 Analysis Assumptions

Apart from the general model assumptions highlighted in the previous chapters, the following additional assumptions are applied throughout the performed simulations:

- Compressor anti-surge recycling ratios are not adjusted with the changing flowrates, they are rather set at a constant value
- It is assumed that the platform units (i.e. compressors) are electrified. Power is generated centrally and distributed amongst the components
- When wind energy is used, an average load factor of 56 % is utilised throughout the analysis
- If H_2 is used as a fuel, it is blended with the platform fuel gas. A H_2 molar fraction of 50 % is selected for all scenarios
- Additional power requirements that may increase along with the platform lifespan, such as pressure boosting for the well, are not considered
- For general power requirements on the platform, an additional 4000 kW is assumed, this value does not change throughout the entire analysis. This value is assumed based on figures seen in [7]
- The cost of H_2 and NG is considered to be constant for the duration of the lifespan. Whereas, CO_2 tax is assumed to increase 50 % each five year period - inline with reported policies [5]
- The operating costs associated with wind energy are not included as they are assumed to be minimal in comparison to the other costs. These costs are shown in Table B.2

6.3 Initial Comparisons

Before applying the model to the developed platform lifespan, the various energy-efficient technologies must be compared to determine which suits the platform in question. Thus, only one single year of analysis will be considered in this section. The utilised data will be that of year fifteen, which was the data taken from [7] and subsequently verified. The following technologies and energy-efficient practices will be compared:

- CO_2 and H_2O bottoming cycles
- Blending of H_2 with NG as a fuel for power generation
- Waste heat recovery of compressor heat via a CO_2 Rankine Cycle
- Implementation of wind energy

It should be noted that multi-phase expanders are not considered in this chapter's analysis. The reason for this is that despite them illustrating good potential for energy recovery, they may only be viable for certain phases of operation. As in the later stages of the platform lifespan the pressure levels from the production wells will decrease, meaning that there will be less chance of energy recovery in the production manifold. Additionally, the platform in consideration (Platform B) has a different variety of pressure ranges within its inlet streams, in comparison to Platform A, where the initial analysis of multi-phase expanders took place.

Additionally, the use of different gas turbines will not be shown in this section. However, this will be included for further analysis in the later sections. The reason for this is that the initial comparison of the technology does not provide sufficient information for justifying its inclusion. Rather a long-term lifespan analysis is better suited for its comparison as a varying gas turbine load can be applied.

6.3.1 Selected Combinations

To adequately analyse the model, six combinations were developed to illustrate how the various techniques perform with regard to their carbon footprint, operating cost and energy efficiency. These combinations are shown in Table 6.1.

Table 6.1: Description of the combinations for the initial comparison of the model (note that "✓" marks whether the technology is present or not)

Combination	Gas Turbine	Bottoming Cycle	Wind	Hydrogen Fuel	CO_2 RC
A	LM2500G4+	-	-	-	-
B	LM2500G4+	H_2O BC	-	-	-
C	LM2500G4+	CO_2 BC	-	-	-
D	LM2500G4+	H_2O BC	-	✓	-
E	LM2500G4+	H_2O BC	✓	-	-
F	LM2500G4+	H_2O BC	-	-	✓

6.3.2 Model Results

This subsection will present the obtained results from the aforementioned analysis. The complete set of results can be seen in Table B.3. The breakdown of the generated power is shown in Figure 6.3. It should be noted that in each combination the total power requirement of the platform does not change. It is rather a reflection of how each combination produces power for consumption.

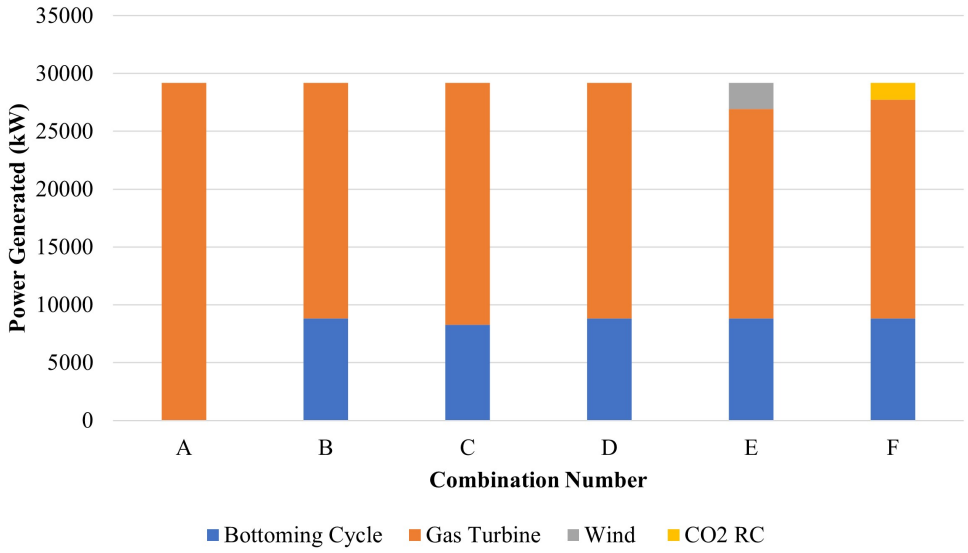

Figure 6.3 Amount of power generated from each technology for each combination

The quantity of CO_2 emitted is shown in Figure 6.4. The combination with the lowest carbon emissions is the one that utilises H_2 fuel. Whilst the highest belongs to the combination that solely uses a gas turbine - which is an expected result.

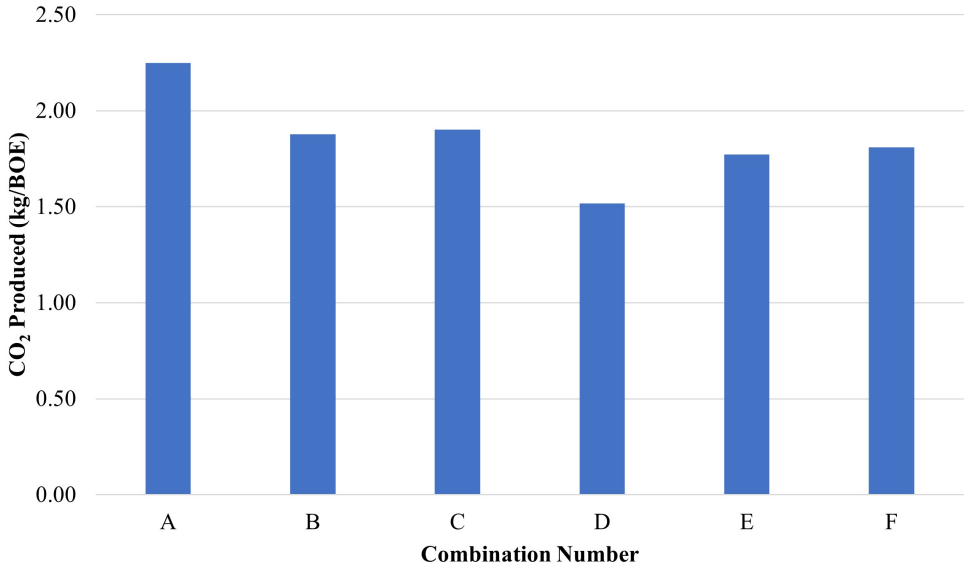

Figure 6.4 Amount of CO_2 for each combination

Figure 6.5 illustrates the breakdown of the operating costs associated with the various combinations. The lowest costs belong to the combinations that use both the CO_2 Rankine Cycle and wind energy. Contrary to the quantity of carbon emitted, the combination that uses H_2 fuels has the joint highest costs (along with the single gas turbine).

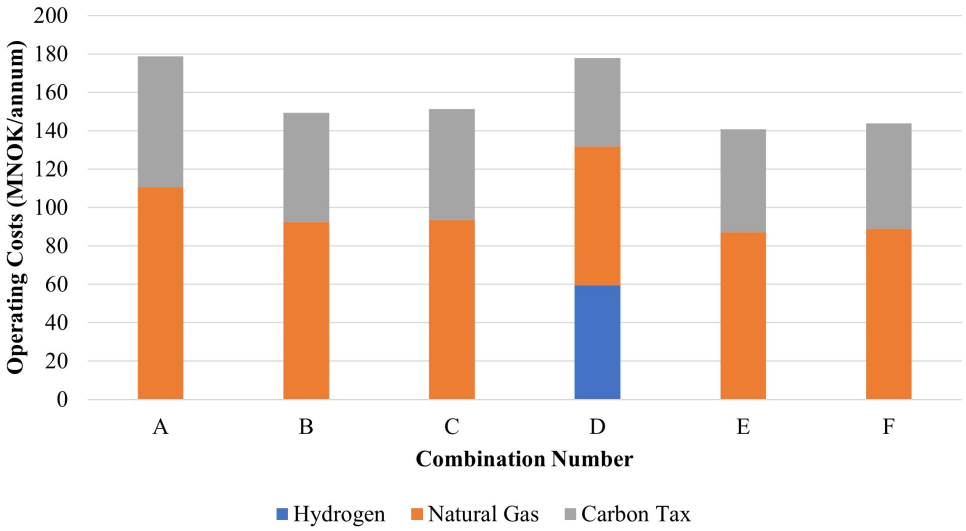

Figure 6.5 Breakdown of the operating costs for each combination

Bottoming cycles

From the previous figures, it can be seen that both bottoming cycles perform in a similar manner with regard to cost, carbon emissions, and amount of power generated. However, when looking further into the results (Table 6.2) it can be seen that the cycle which uses H_2O as the working fluid performs more favourably. The H_2O BC has a higher power output, and a higher overall thermal efficiency value - resulting in lower carbon emissions and lower costs.

Table 6.2: Comparison between CO_2 and H_2O bottoming cycles

Variable	Unit	Combination B	Combination C
BC Working Fluid	-	H_2O	CO_2
Gas Turbine Power	MW	20.3	20.9
BC Power	MW	8.82	8.27
Total Power Generation Efficiency	%	45.5%	44.9%
CO_2 Emitted	$kgCO_2$/BOE	1.88	1.90
Operating Cost	MNOK/annum	149	151

Given that the CO_2 BC is untested commercially and that it shows worse performance than the commercially available H_2O BC, further analysis in this chapter will not consider CO_2 as a working fluid. Outside of the scope of this analysis, there are potential benefits for CO_2 BCs; however, in the context of this investigation, they are not apparent. It should be noted that the worse results for the CO_2 BC are not the key reason for the exclusion. Instead, it is that it presents more issues, concerning operability and design, than benefits. On the other hand, the H_2O bottoming cycle illustrates promising results, thus, this will be considered for further analysis in this chapter.

Hydrogen fuel

The use of hydrogen in the fuel gas results in a substantial decrease in the quantity of CO_2 that is emitted. As downstream emissions are taken into account, this is an extremely promising result. However, despite this, there is still a key issue concerning cost. As can be seen from Figure 6.5, the scenario where H_2 fuel features has the highest operating costs. The aforementioned is solely due to natural gas being far cheaper than H_2.

Despite this being a strong negative, there are other aspects that need to be considered within this analysis. H_2 technology is novel and it currently has high operating expenses. However, this is predicted to be reduced over the coming years. Another important factor to be considered is carbon tax. Carbon tax (especially in the context of operation in Norway) is expected to increase substantially over the coming years. So if these two aspects coincide, then H_2 as a fuel will be economically viable (only considering operational costs). Thus, given this, H_2 fuel will be analysed further in this chapter.

CO_2 Rankine Cycle

The inclusion of a CO_2 Rankine Cycle is beneficial with regard to operational costs and CO_2 emissions. However, despite this, there are some key issues that present themselves. This technology is immature, and it has not been installed on any existing offshore oil and gas platforms. In addition, there are several units in this system that need to be installed on the platform. These all take up a large portion of weight and volume, which is a valuable commodity on offshore platforms. Thus, if they are to be installed they need to be able to contribute and recover significant quantities of power.

A comparison between the scenarios with and without the CO_2 Rankine Cycle can be seen in Table 6.3. The reduction in carbon emissions and operating costs are not largely significant in comparison to other available technologies, which have fewer size and weight issues.

Table 6.3: Comparison between the combinations with and without the CO_2 Rankine Cycle

Variable	Unit	Combination B	Combination F
CO_2 Rankine Cycle	-	x	✓
Total Power Generation Efficiency	%	45.5%	44.8%
CO_2 Emitted	$kgCO_2$/BOE	1.88	1.81
Operating Cost	MNOK/annum	149	144

Given all the aforementioned considerations, the use of the CO_2 Rankine Cycle will not be investigated in future analyses within this chapter. If size and weight are not constraints, then this system should be installed. There are several associated benefits and energy that would typically go to waste can be recovered. However, in this case, the amount of energy that is recovered is not notable. This technology still presents a huge amount of promise if it commercialised and applied to a platform where it can achieve a higher degree of energy recovery.

Wind energy

The use of wind energy results in the combination with the lowest operating costs. Additionally, it has the second lowest CO_2 emissions. A key limitation in the costing analysis is that operating costs associated with the wind farm are not included. This may slightly warp the result of this analysis. However, these costs are not expected to be significant. Thus, the previous statement with regard to the promising operational costs can be deemed to still be accurate.

This technology shows similar values to that of the CO_2 Rankine Cycle. However, the key difference is that the use of wind energy occupies no additional space on the platform. So the same issues cannot be linked between the two systems. Given all these considerations, wind energy can be said to be promising for future scenarios. Thus, further analysis will consider this technology.

6.4 Platform Lifespan Technology Comparisons

After comparing the various energy-efficient technologies and practices over a single year of operation, the comparison will now be extended to multiple platform years. This is an important analysis as it illustrates how the different systems perform with the changing conditions. After narrowing down the various technologies in the previous section, this section will compare the following systems:

- H_2O bottoming cycles
- Blending of H_2 with NG as a fuel for power generation
- Implementation of wind energy
- Adequate sizing of the utilised gas turbine(s)

6.4.1 Selected Combinations

Here, eight scenarios were stipulated in order to investigate how the aforementioned systems performed throughout the platform lifespan. These combinations can be seen in Table 6.4.

Table 6.4: Combinations to compare the various systems throughout the platform lifespan

Combination Number	Gas Turbine	Bottoming Cycle	Wind	Hydrogen Fuel
1	LM2500G4+	-	-	-
2	LM2500 x 2	-	-	-
3	LM2500G4+	H_2O BC	-	-
4	LM2500G4+	-	-	✓
5	LM2500G4+	-	✓	-
6	LM2500G4+	H_2O BC	-	✓
7	LM2500G4+	H_2O BC	✓	-
8	LM2500	H_2O BC	✓	-

6.4.2 Model Results

This subsection will display and discuss the results obtained from the model. The first five combinations (1-5) are compared in Figure 6.6. Here it can be seen that the scenario that emits the largest quantity of CO_2 is the scenario which uses the smaller gas turbine. This is an expected result because here there are two gas turbines, both operating at low efficiencies. Comparing this to the combination with the larger gas turbine (Combination 1), it can be seen that there is a significant decrease in CO_2 produced - highlighting the importance of gas turbine sizing.

Another important result from this figure is with regard to Combination 3. In this situation, a H_2O BC is employed. This results in the scenario that releases the least CO_2 - performing better than the combination with wind energy, whilst having very similar results to the scenario where H_2 fuel is added.

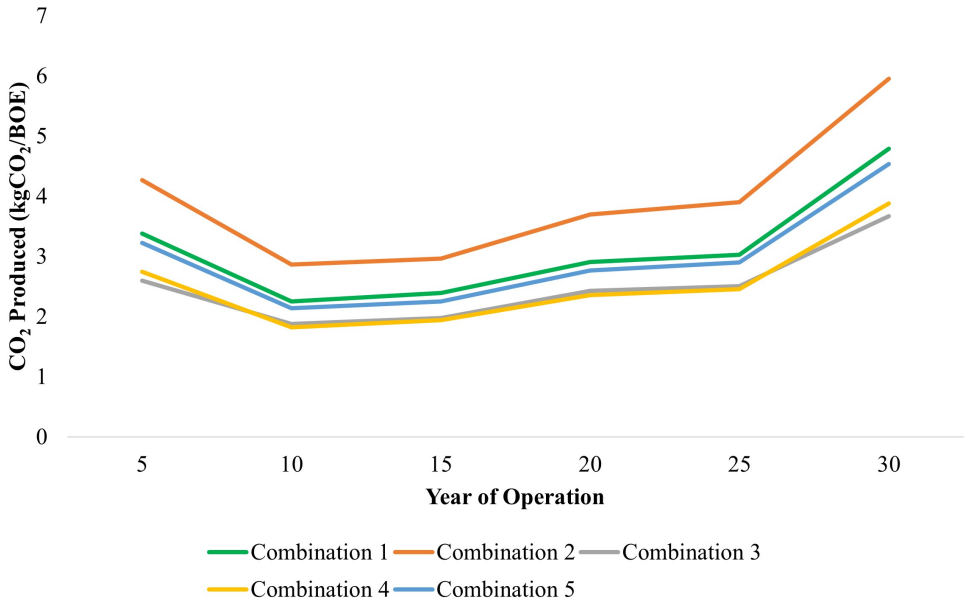

Figure 6.6 Comparison of the carbon emissions from different combinations (1-5) throughout the platform lifespan

Looking further into different KPIs with regard to the same scenarios, Figure 6.7 can be seen. Here the operating costs are compared. Similarly to the previous figure Combination 2 has the highest associated costs, with Combination 3 having the least.

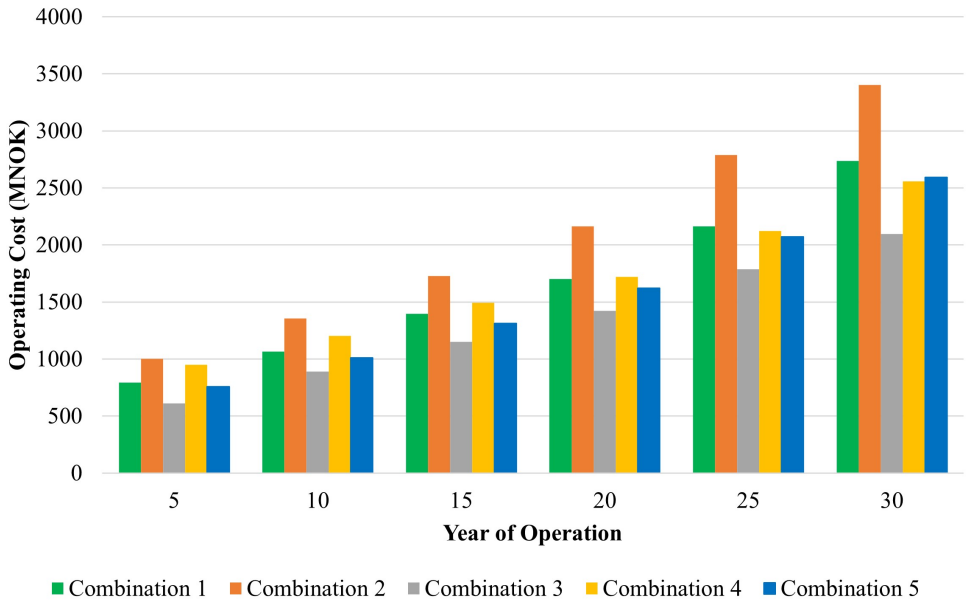

Figure 6.7 Comparison of the operating costs from combinations (1-5) throughout the platform lifespan. Note the costs for each point are a sum of the past 5 years of operation

In contrast to the results in Figure 6.6, Combination 4 has very high costs throughout most of the platform lifespan. This is due to the high costs of H_2, which is a result that has been seen before in previous sections. However, when looking at the whole platform lifespan it seen that the scenario with H_2 starts off with higher costs than Combination 1 and 5, but in the later years it ends up

being the combination with the second lowest costs. This result shows the importance of utilising H_2 fuels when carbon tax rates become exorbitant in the latter years. Aside from this point, these figures show the importance of installing a BC to recover energy from the gas turbine. There are significant savings with regard to CO_2 emitted, as well as costs incurred.

The CO_2 emissions of the remaining combinations (6-8) are compared in Figure 6.8, with combinations 1 and 3 remaining for reference. Aside from Combination 1, all the scenarios illustrated in this figure contain H_2O BCs. These scenarios exist to compare the benefits and implications of using either H_2 fuel or wind energy - given that a BC is already installed. It should be noted that Combination 8 has a smaller gas turbine, and the point of its inclusion is to compare it against Combination 7 - which has the same set-up aside from the gas turbine.

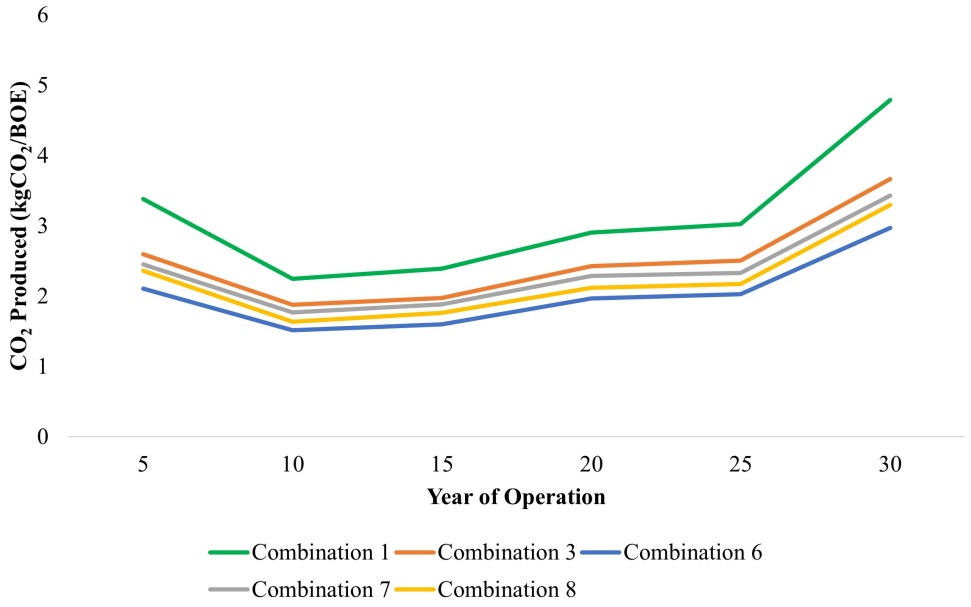

Figure 6.8 Comparison of the carbon emissions from different combinations (1,3,6-8) throughout the platform lifespan

From this figure, it is seen that Combination 6 has the lowest CO_2 emissions, with Combination 1 having the highest. This result demonstrates the important role that H_2 can play in reducing platform emissions. However, it should be reminded that this scheme includes a BC, and as we saw in Figure 6.6, the use of H_2 without a BC is not beneficial in the context of carbon emissions. Another important outcome from this figure is between Combination 7 and 8. All through the analysis, Combination 8 has lower quantities of CO_2 emitted.

Further comparing these systems, Figure 6.9 can be viewed. Here the operational costs are compared. The most cost-efficient scheme is Combination 8 - the system with the smaller gas turbine. As is seen in Figure 6.7, the combination with H_2 starts with high costs, which are then later reduced in comparison to the other schemes. Another important outcome concerns Combination 3. This system only comprises of a BC but it has very similar costs to the other technologies.

Although it is slightly more costly, there is a significant difference when compared to the first combination.

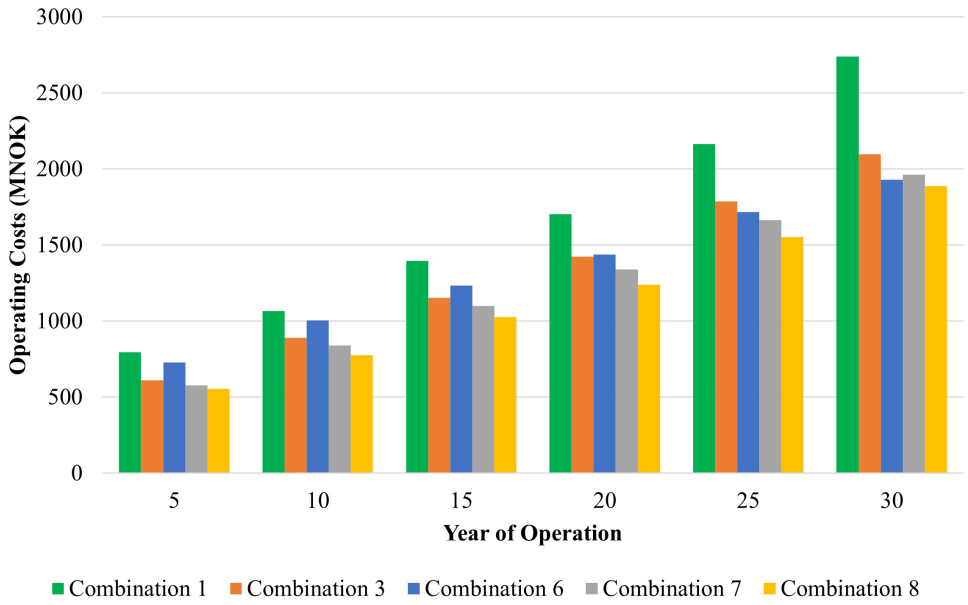

Figure 6.9 Comparison of the operating costs from combinations (1,3,6-8) throughout the platform lifespan. Note the costs for each point are a sum of the past 5 years of operation

Looking further into the analysis of the operating costs, Figure 6.10 can be seen. This figure compares the savings of the various schemes relative to Combination 1, which is seen as a base case scenario. It should be noted that these values are a cumulative sum of the entire platform lifespan. This figure can be utilised as a tool to view the potential payback times of installing various technologies, when capital costs are compared.

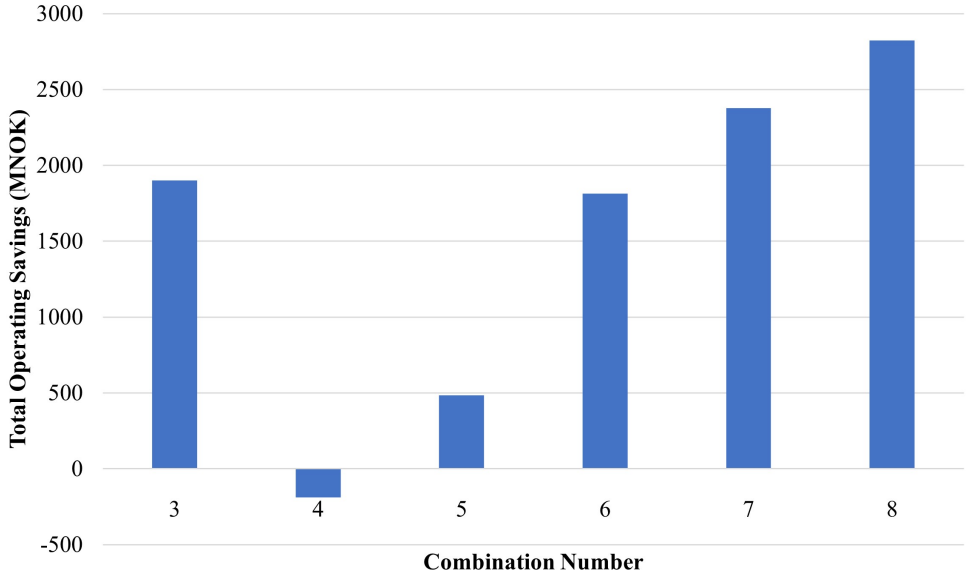

Figure 6.10 Cumulative operational savings relative to Combination 1 after 30 years of operation

One of the most important outcomes of this figure is with regard to Combination 3 - which is something that has been seen throughout this entire analysis. This scenario has very high savings when compared to the other systems; only the systems which additionally employ wind energy generate a high proportion of savings. An interesting comparison can be seen between Combination 3 and 6. Both scenarios use bottoming cycles with the latter utilising H_2 fuel. Here it is seen that Combination 3 has lower operating costs than Combination 6. However, it is worth considering the results in Figure 6.8 again. Combination 6 has the lowest CO_2 emissions which is also an important result. Thus, based on the aforementioned, a scenario that balances both CO_2 emissions and incurred costs needs to be considered.

To gain insight into how a balanced future scenario will look, Figure 6.11 can be considered. This figure is a breakdown of the operating costs for Combination 6. From this diagram, what has been mentioned throughout this analysis is illustrated. As the year of operation progresses the cost of hydrogen becomes far less substantial in comparison to the cost of carbon tax. Hence, there is an important takeaway from this figure - despite the negative aspects that hydrogen fuel presents, these considerations may be eradicated in the future when the cost of carbon tax becomes far more notable.

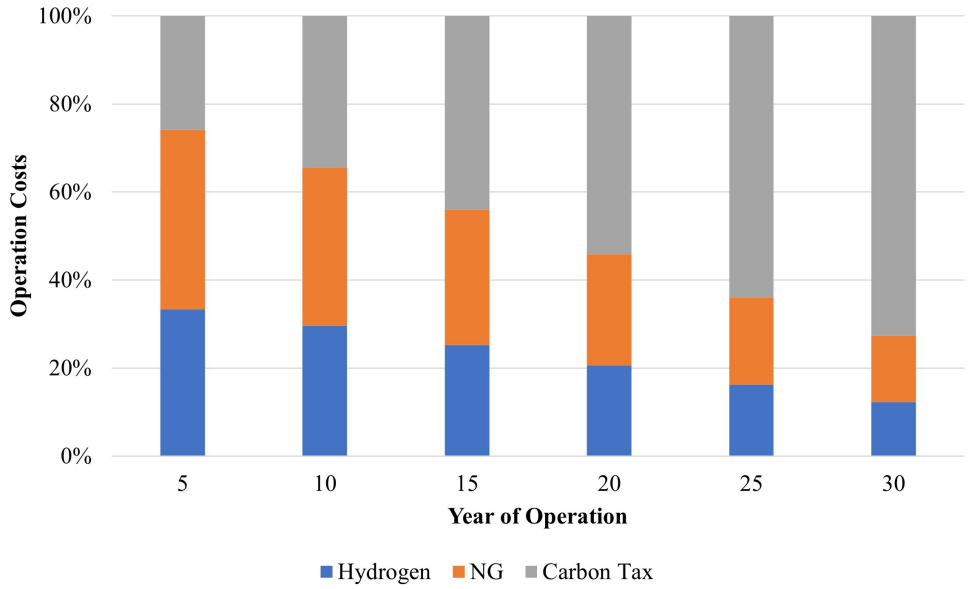

Figure 6.11 Breakdown of the various operational costs throughout the platform lifespan for Combination 6. Note the costs for each point are a sum of the past 5 years of operation

Thus far, aspects concerning the appropriate sizing of the utilised gas turbine have been briefly mentioned. The first two combinations show the difference between using a single larger gas turbine and using multiple smaller gas turbines. In this specific scenario, the smaller gas turbines were operating at low efficiencies and had far greater carbon emissions in comparison to the larger gas turbine (refer to Figure 6.6). Thus, showing that here it was more efficient to run a single larger

gas turbine.

The last figure (Figure 6.12) to be shown in this section compares Combination 7 and 8. In this figure the amount of CO_2 emitted and the overall efficiency of the power generation system is compared.

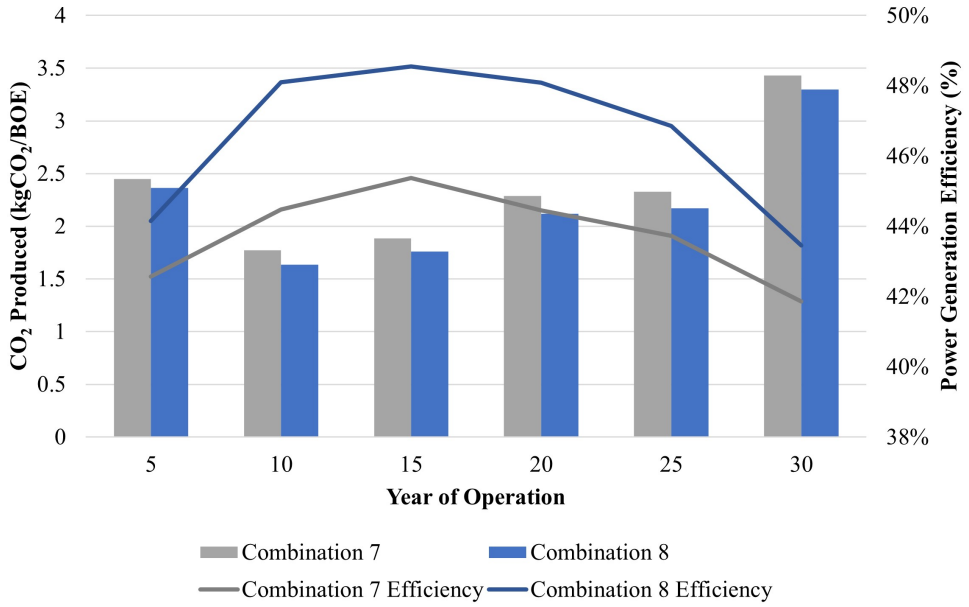

Figure 6.12 Comparison between Combination 7 and 8. Note that the lines relate to the efficiency values on the right vertical axis

It can be seen that Combination 7 has a lower efficiency and a higher quantity of CO_2 produced. The difference in efficiency is significant, with Combination 8 having 2 % points higher than Combination 7 for the majority of operation. This difference is also illustrated in Figure 6.10, where the use of Combination 8 results in far larger savings. This again shows the importance of running the utilised gas turbine at high efficiencies. The purpose of this result is not to show which gas turbine is better; it is rather to show the importance of selecting the appropriate unit for each platform.

6.4.3 General Discussion

This section has compared several scenarios for use over the model platform's lifespan. It is important to note that during the development of the model several assumptions have been made that may not relate to all platforms. Thus, the obtained results may not apply to every platform. The purpose of the various analyses performed in this chapter is to show how the developed model behaves as an analytical tool and to show what information can be obtained.

One of the most important outcomes of this analysis is with regard to the implementation of the H_2O bottoming cycle. In all aspects this system performs favourably, significantly reducing CO_2 emissions and operating costs. The subsequent addition of either H_2 fuel or wind energy is

beneficial only if a bottoming cycle is already present. There may be large capital costs associated with installing a bottoming cycle on an offshore platform; however, the potential savings with regard to operating expenses are also substantial. It should be taken into account that the bottoming cycle that is modelled is a once-through unit. If a system with multiple pressure drums are utilised, the combined cycle net efficiency can increase an approximate 3 percentage points (Table 3.1). This is significant; however, it may not be feasible due to the weight and volume constraints. Nevertheless, despite not being at the top of the range in terms of efficiency, there are important benefits associated with using a OTSG BC.

The lifespan scenario also shows the importance of CO_2 efficient technology near the end of the platform lifespan. The quantity of CO_2 emitted and the associated operational costs both increase notably during the later operating years. This is where the importance of H_2 may be crucial. With high CO_2 tax and emissions, the use of H_2 as a fuel could drastically reduce costs and CO_2 emissions in these years. The use of wind energy is also extremely promising, especially in combination with a bottoming cycle. However, given the results shown in this analysis, it can be said that it only makes sense to implement wind energy once a bottoming cycle is installed. Noting Figure 6.10 and 6.6 as explanations for this statement (comparison between Combination 3 and 5).

Lastly, this analysis displays the importance of selecting an appropriate gas turbine. The first two combinations (1-2) utilised different gas turbines. There were significant cost and CO_2 reductions for the unit operating with lower part-load and higher efficiency. This is also seen for the last two combinations (7-8). Although they have the same technology, the more efficient gas turbine outputted far more favourable results.

The full results for this entire analysis can be seen in Tables B.4 - B.11.

6.5 Future Low Emission Scenario

After analysing the benefits and implications of the various systems throughout the platform lifespan, this section will propose a future scenario to minimise both operating costs and carbon emissions.

6.5.1 Scenario Description

The most important technology to implement for all years of operation is a steam bottoming cycle. This is proven to be efficient and worthwhile in all cases. The smaller gas turbine (LM2500) is selected for all cases, as it is proven to be more efficient in the context of this specific scenario. Aside from this, wind energy is also highly beneficial as there is minimal weight or volume added to the platform.

This is a different case with hydrogen. The costs in the early years of operation are substantial; thus, for the first 15 years of operation it will not be included. For the 20th year, a blend of 50 molar percent will be included, which is inline with the current technological capabilities. For the 25th and 30th years, a molar percentage of 70 and 90 will be used respectfully. These blend ratios may be higher than what is available today; however, within this time frame, technology is assumed to advance in a positive direction. This scenario is utilised to balance the trade-off between operational costs and CO_2 emissions for hydrogen. A summary of what has been described in shown in Table 6.5.

Table 6.5: Future low emission scenario summary

Year	5	10	15	20	25	30
Gas Turbine	LM2500	LM2500	LM2500	LM2500	LM2500	LM2500
H_2O BC	✓	✓	✓	✓	✓	✓
Wind Energy	✓	✓	✓	✓	✓	✓
H_2 Fuel	-	-	-	✓	✓	✓
H_2 Fuel Percentage (mol. %)	-	-	-	50	70	90

6.5.2 Model Results

This subsection will display the results obtained from the future low emission scenario that has previously been presented. Comparisons to certain combinations from the previous section will also be drawn to analyse how well the low emissions scenario fares. The full results can be seen in Table B.12.

The first figure (6.13) shown displays the breakdown of the carbon emissions for the future system. It can be seen that in the latter years where hydrogen fuel is introduced that there is a significant decrease in the amount of CO_2 emitted. In these years, hydrogen contributes small quantities in comparison to the initial use of natural gas. This shows that despite the inclusion of the hydrogen CO_2 intensity figure, the amount of carbon emissions is minimal in comparison to the use of natural gas.

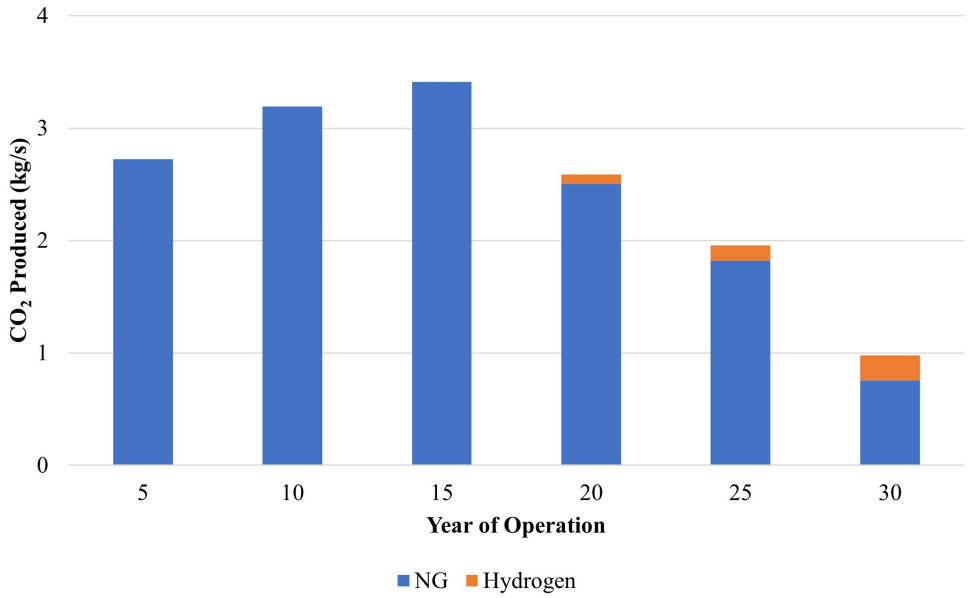

Figure 6.13 Breakdown of the carbon emissions for the future scenario

Still considering CO_2 emissions, the future scenario is then compared against Combination 6 (H_2O BC and H_2 fuel), which was the best performer in the previous section with regard to CO_2 produced. This comparison is seen in Figure 6.14. Initially, Combination 6 has slightly lower carbon emissions. This is because H_2 is yet to be introduced for the future scenario. Once H_2 is introduced, the CO_2 emissions drastically decrease; whilst in Combination 6 the emissions increase. The difference between the two scenarios is substantial after year 20. The large reduction of CO_2 emissions in these years more than makes up for the slightly higher emissions seen in year 5 to 15.

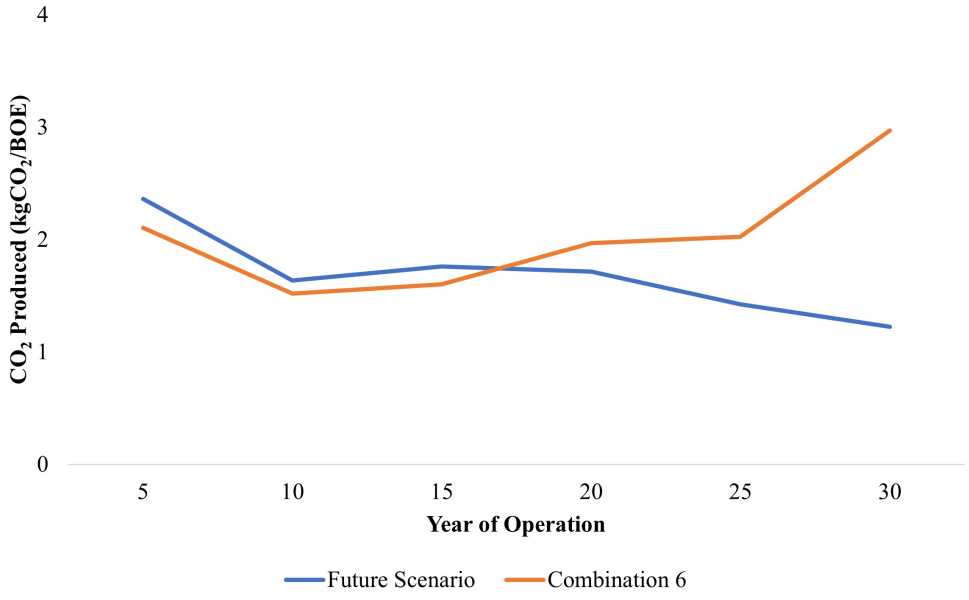

Figure 6.14 Carbon emissions for the future scenario compared against Combination 6

Figure 6.15 shows the breakdown of the operating costs of the future scenario. An important aspect to note here is that before year 20, the amount of CO_2 tax is steadily increasing, but as soon as H_2 is introduced this trend ceases. With the use of high levels of H_2 as a fuel in year 30, the total operating costs decrease; which is an outcome not seen in any of the other scenarios. The cost of H_2 in this year is far greater than any other cost, but when compared to the carbon tax paid in the 25th year, it is lower.

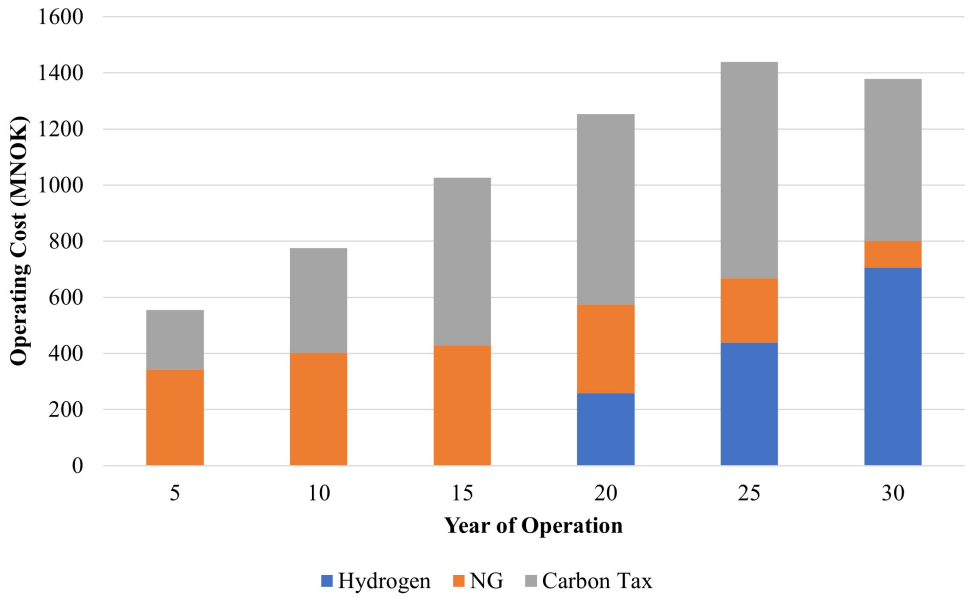

Figure 6.15 Breakdown of the operating costs for the future scenario. Note the costs for each point are a sum of the past 5 years of operation

The operating costs for this future scenario are then compared against the best performer from the previous section in this regard, Combination 8. This combination utilised wind energy with a steam bottoming cycle. There was no H_2 utilised - which is a key explanation for its lower operating costs. This comparison can be seen in Figure 6.16. For years 5 to 15, the results are identical as they both feature the same system. In year 20, when hydrogen is introduced for the future scenario, the operating costs are slightly higher. However, the following years are notably lower. As is previously mentioned, the future scenario breaks the upward trend for the costs incurred between year 25 and 30. This feature is not seen for Combination 8, whose costs increase drastically in the same time frame under consideration.

These results illustrate several positive features for the future scenario. From year 5 to 15, the scenario has the lowest costs obtainable, with slightly higher CO_2 emissions. Once the use of H_2 becomes economically viable, it is introduced in the scenario. The amount of CO_2 produced falls significantly, with only slightly more costs incurred. In the following years where the platform is meant to be the most expensive to operate, the use of hydrogen breaks this trend. At this point, the scenario has far lower costs and CO_2 emissions than any combination simulated in the previous

sections. These outcomes illustrate the importance of using certain technologies at certain points in time. If H_2 was to be used at the beginning of the platforms lifespan, the CO_2 emissions would drop, but the additional operating costs would be tremendous.

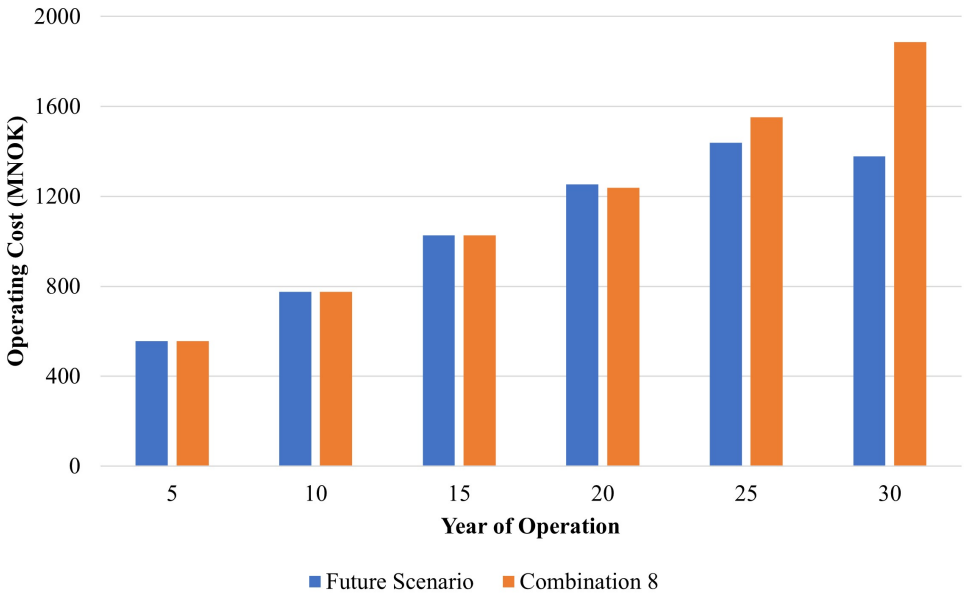

Figure 6.16 Operating costs for the future scenario compared against Combination 8. Note the costs for each point are a sum of the past 5 years of operation

The last two figures in this section compare the future scenario against the base case combination, Combination 1. This combination just uses a single gas turbine with no additional technology. Figure 6.17 shows the cumulative emissions throughout the platforms life. Here, it is seen that the total emissions from Combination 1 at year 30 are more than double that of the future scenario.

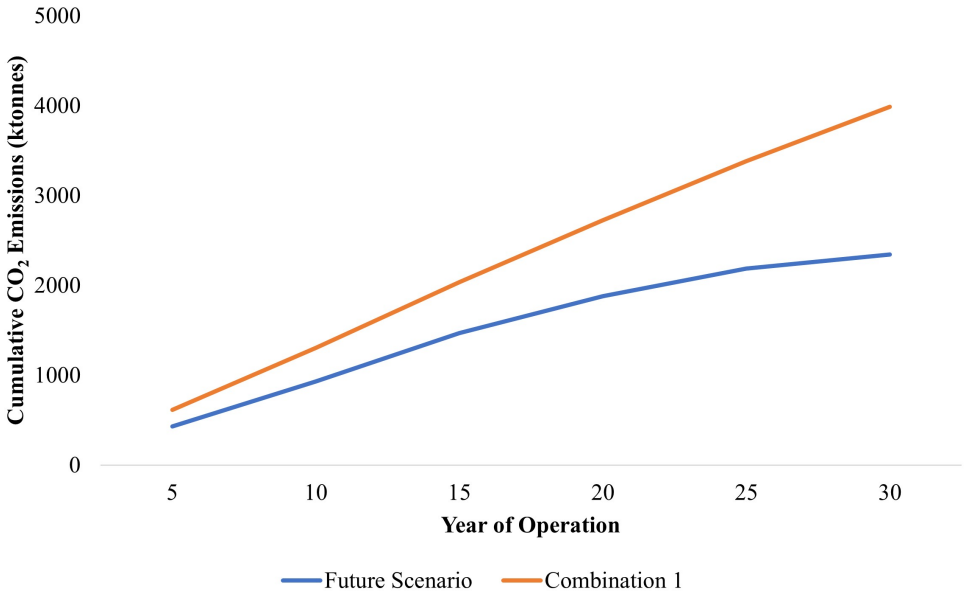

Figure 6.17 Cumulative carbon emissions for the future scenario compared against Combination 1

Figure 6.18 displays the cumulative operating costs for both schemes. As seen with the previous figure, there is a large difference between the two scenarios. Essentially, at year 30, the difference between the two schemes is the amount of savings with regard to the cost of operation. This value is just shy of 3.5 billion NOK over a period of 30 years - equating to over 100 million NOK per annum. These are significant savings, which could potentially pay off the required capital costs. However, this is something that is not investigated in this analysis, making this more of a speculative statement.

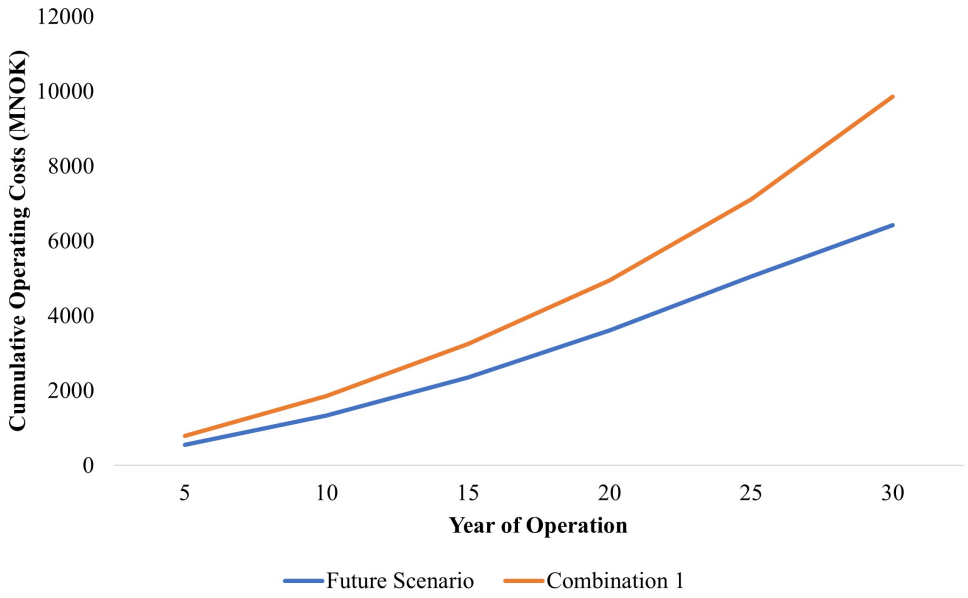

Figure 6.18 Cumulative operating costs for the future scenario compared against Combination 1

6.6 Sensitivity Analysis

In this section a sensitivity analysis is performed on the future low emission scenario. A rigorous analysis will not be conducted, rather the procedure will be simplified.

The goal of a sensitivity analysis is to illustrate how much a key result changes when an assumed variable is adjusted. In this scenario there were two aspects to the model: economic and operational. Thus, the sensitivity analysis will be divided into two separate subsections. The range and selected variables for the conducted sensitivity analyses are shown in Table 6.6

Table 6.6: Variable for the sensitivity analysis

Variable	Unit	Lower Value	Upper Value	Base Value
H_2 Price	NOK/kg	8.10	24.3	16.2
NG Price	NOK/kg	1.08	3.23	2.15
Rate of CO_2 Tax Increase	%/5 Years	1.00	2.00	1.50
Compressor Isentropic Efficiency	%	50.0	85.0	-

6.6.1 Economic Aspects

One of the key tools for comparing the results of the model was the KPI concerning operating costs. In this indicator three variables were assumed: purchase price of hydrogen; purchase price of natural gas; and carbon tax rates. The cost of hydrogen and natural gas will be varied ± 50 % in comparison to the original price (as shown in Table 6.6).

The carbon tax rate will be varied in a different manner. Initially, it was assumed that carbon tax would increase 50 % every 5 years. In this analysis, carbon tax will increase from 0 % to 100 %, i.e. if it is 0 % the price will remain constant throughout the lifespan scenario. In all cases, the variation will be represented on a percentage change basis.

The first figure (6.19) illustrates the variation of the total operating cost with the changing hydrogen fuel price. In the first 15 years there is no impact as hydrogen is not included. In the following 15 years, the dependence on the price of hydrogen increases steadily. This is not inherently positive nor negative. As mentioned before, the price of hydrogen is expected to decrease over the coming years as the technology becomes more commercialised. Thus, there is a potential to reduce operating costs by 25 % in the best case scenario.

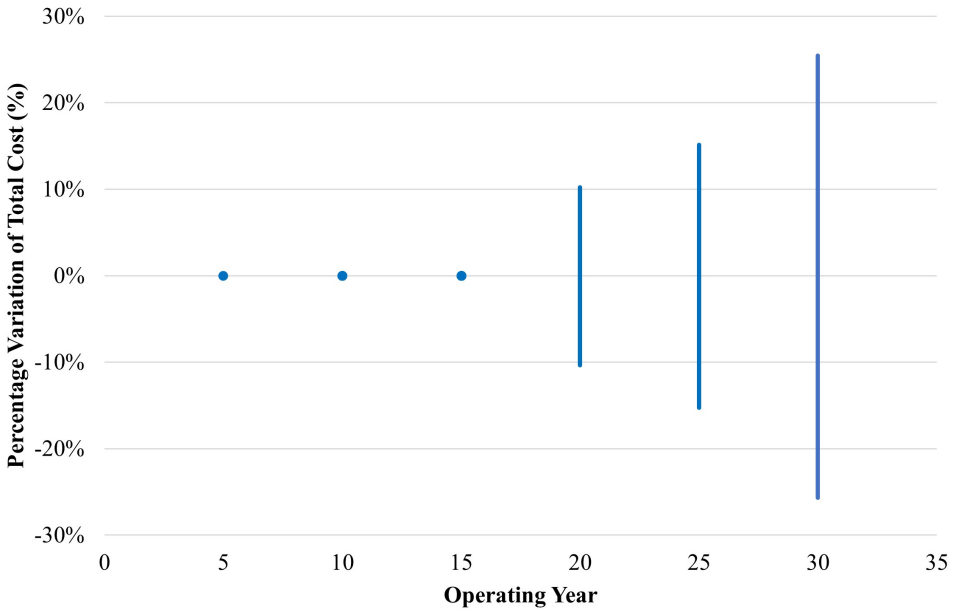

Figure 6.19 Effect of changing the purchase price of hydrogen (-50 % to 50 % change compared to the original price) on the total operating costs throughout the platform lifespan

Figure 6.20 shows the varying operating costs with the changing natural gas price. Comparing this figure with the previous one, the opposite trend is seen. In the first 15 years, the operating costs vary largely with the changing natural gas price. However, this value becomes relatively small in the last year of operation, where it varies between ± 5 %. Again, there are no obvious positive or negative aspects associated with this result.

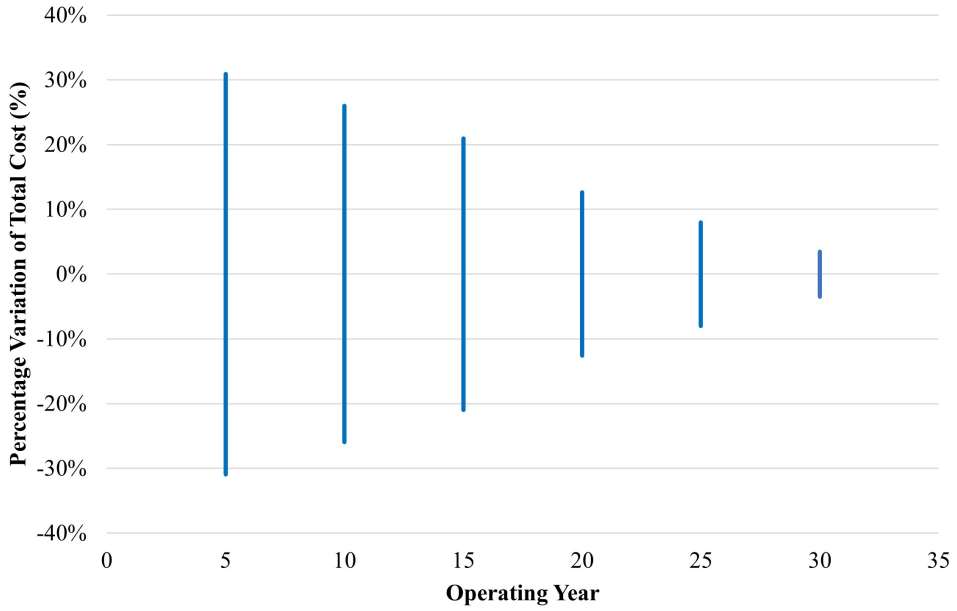

Figure 6.20 Effect of changing the purchase price of natural gas (-50 % to 50 % change compared to the original price) on the total operating costs throughout the platform lifespan

The last figure (6.21) illustrates the impact of the carbon tax price. As expected there is a relatively large dependence on this variable. On the upper part of the scale, if carbon tax is increased at a rate of 100 % every 5 years, then operational costs in the last year can increase up to just under 140 %. Whilst, if carbon tax is not changed there is a smaller decrease of up to 40 % in the same year (year 30).

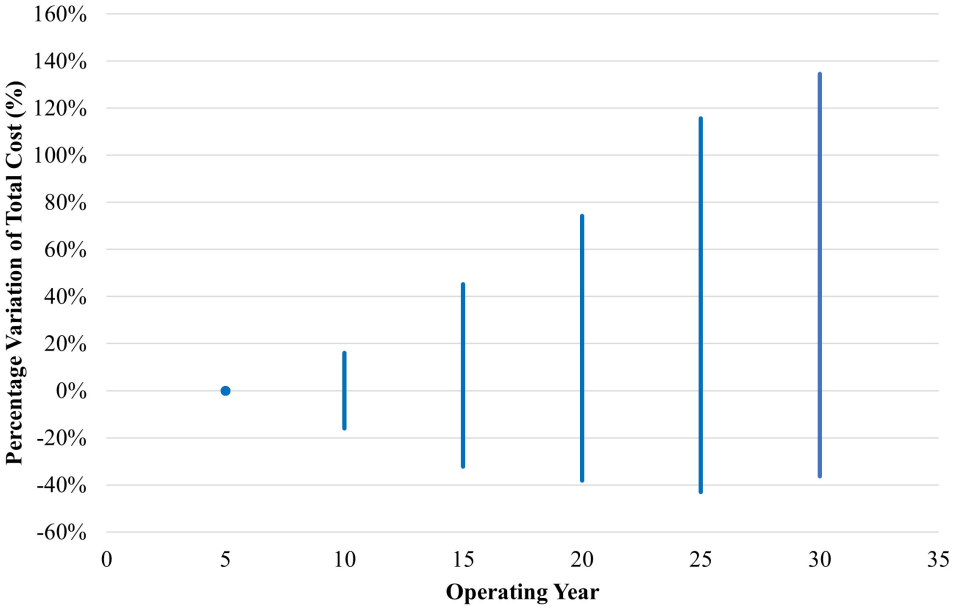

Figure 6.21 Effect of changing the carbon tax price (0 % increase per 5 years to 100 % increase per 5 years) on the total operating costs throughout the platform lifespan

Again this is not inherently positive nor negative. If carbon tax prices are going to increase to

a higher degree then there will be more incentive to implement carbon-efficient technologies. Whilst, on the opposite side, if carbon tax is not raised to the expected rate there is less of a notable impact on the operating costs. Perhaps this may have implications for the use of hydrogen, but the use of bottoming cycles and wind energy will remain highly beneficial.

6.6.2 Operational Aspects

Throughout the development of the model there were several assumptions made. However, the assumption that could impact this lifespan analysis to the highest degree is the assumed isentropic efficiency values for the utilised compressors. The reason for solely focusing on this aspect is that the power demand is highly dependant on the compression requirement - which is directly linked to this efficiency value. The range for this sensitivity analysis is shown in Table 6.6. The reason that a base value is not shown is because there are several different compression values assumed. However, all the assumed values fall within the range of 50 % to 85 %.

The resultant illustration from the sensitivity analysis can be seen in Figure 6.22. It should be noted that in general the platform power demand ranges between 22MW to 32MW within this time-span. An additional consideration to be taken to account is that the pipeline compressor is not included in this analysis. This is because this value highly dictates the overall power demand, as it has a demand in the range of 10MW to 20MW. Due to high compression demand this unit is normally specifically designed to run at high efficiencies. Thus, to take this into account would be unnecessary in this context.

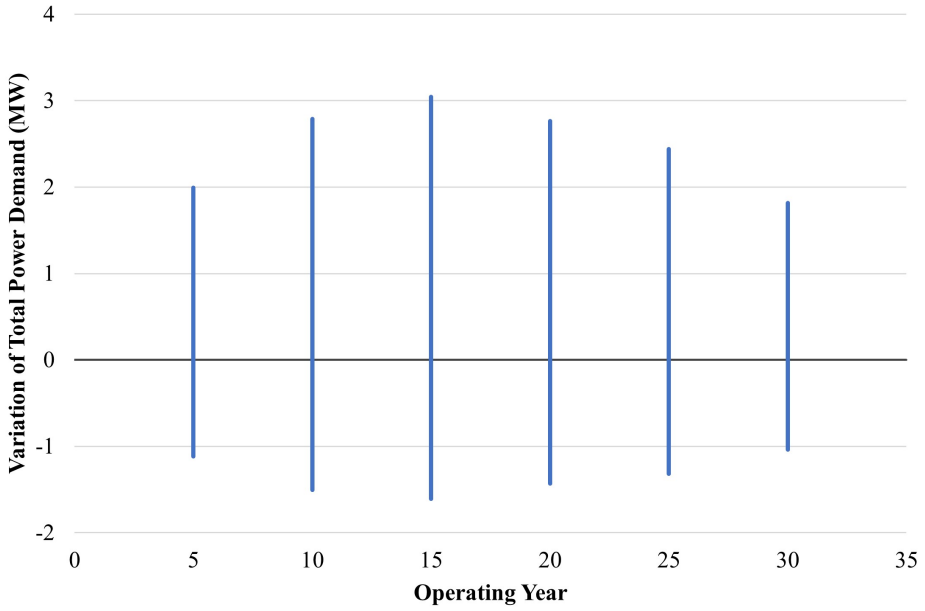

Figure 6.22 Effect of changing the isentropic efficiency of the compressors in the gas recompression train (50 % to 85 %) on the total power demand throughout the platform lifespan

As it can be seen from the figure, the power demand increases within the range of about 10 % for the lower efficiency values and decrease about half that amount for the higher efficiency values.

This implies that the compressors run closer to the higher efficiency values than the lower ones. This is a relatively general statement, but it implies that there could be a notable change to the power demand if the compressor efficiencies were over-estimated.

Chapter 7

Discussion and Conclusion

The purpose of this study was to develop an efficient and reliable computational model that can simulate an offshore oil and gas platform and determine how various energy-efficient technologies and/or practices can be implemented.

A literature study on the Norwegian petroleum industry identified the following subsystems for improvements: the production manifold; the recompression train; the gas treatment sector; and the power generation system. To improve energy usage in these areas, several technologies and practices were investigated for implementation. These being:

- Multi-phase expanders to replace inlet well throttling valves (production manifold)
- CO_2 Rankine Cycles for compressor waste heat recovery (recompression and gas treatment sections)
- CO_2 and H_2O bottoming cycles to recover waste heat from the gas turbine flue gas (power generation)
- Appropriate sizing of the utilised gas turbine (power generation)
- Wind energy (power generation)
- H_2 to replace natural gas as a fuel (power generation)

To test what technologies were most applicable, the developed model was tested over a 30 year time period with varying inlet conditions. From the initial comparisons, it was shown that the use of a steam bottoming cycle, H_2 fuel and wind energy were the most effective options in the context of this analysis. Thus, only these technologies were compared over the entire platform lifespan - mostly focusing on improving the energy efficiency of the power generation sector.

It is found that the use of a steam bottoming cycle results in a large decrease in carbon emissions. In comparison to the worst-case considered, there is a 36 % reduction in CO_2 emitted over the 30-year time period. Whilst only emitting 0.06 % more than the combination which uses H_2. However, when operating costs are considered, the bottoming cycle has 21 % fewer costs than the H_2 scenario. Similar benefits are seen when compared to wind energy, as the BC reduces both CO_2 emissions and costs by approximately 15 %. Thus, given this, it is concluded that within the scope of this model and platform, it is more beneficial to implement either wind energy or H_2 fuel if a bottoming cycle is already present. However, if the implementation of a bottoming cycle is not feasible, the use of either hydrogen or wind energy can still reduce both CO_2 emissions and operating costs to a notable extent. It should be noted that this statement is based on the conducted analysis, where capital costs and platform weight constraints are not considered.

To show the potential of combining these technologies a low emission scenario was proposed. For the first 15 years of operation, a smaller more efficient gas turbine was utilised with a steam bottoming cycle and wind energy. After the fifteenth year of operation, H_2 fuel was introduced and the blend fraction was increased from 50 molar % to 90 molar % in the last period analysed. Over the entire 30 year lifespan, compared to the worst case, this scenario reduced CO_2 emissions by 2.7 Mtonnes and saved 6.0 billion NOK, translating to a 54 % and 48 % reduction respectively. This scenario illustrates the potential of combining all these systems and the use of hydrogen when the cost of carbon tax becomes significant.

For the more immediate future, these reductions are critical to achieving the various carbon emission goals set by oil and gas companies. The obtained operational savings can be utilised to install a bottoming cycle and further investigate additional energy-efficient technologies. Although a large amount of work and research still needs to go into achieving net-zero production, this is a worthwhile starting point that should be taken into account for application.

Aside from obtaining information regarding low-emission technology, a key goal of this study was to develop a computational model that can be used as a method of analysis for low emission oil and gas scenarios. From the obtained results and performed analyses, it can be concluded that this model is flexible to changes in operating conditions and capable of outputting reliable data for additional investigation into low emissions scenarios - making it a useful tool for further research.

Chapter 8

Recommendations for Future Work

For further work the following aspects are recommended for consideration:

- Add additional KPIs that relate to capital costs or platform weight. This way a full picture can be drawn with regard to the implementation of certain technologies. Aspects such as the cost of electrifying compressors and process units should also be investigated
- Investigate the possibility of a central power distribution hub. A decommissioned offshore platform could be utilised in this study. Essentially, the gas turbines and bottoming cycles could be installed and electricity can then be distributed to the various platforms. This can reduce the frequency of gas turbines being run with a low efficiency and load. Additionally, this can reduce the weight on a production platform and can allow for the technologies such as transcritical CO_2 Rankine Cycles to be implemented
- Include operational costs for the use of wind energy
- Perform a more dynamic analysis to investigate how the variation of wind energy supply impacts CO_2 emissions
- More energy-efficient technologies can be investigated to recover waste energy on the platform, such as the use of low-temperature heat pumps
- Perform an exergy analysis on the power generation system

Bibliography

[1] Norwegian Petroleum Directorate, "Resource report - discoveries and fields 2019", Stavanger, Norway, Tech. Rep., 2019, ch. Emissions, discharges and the environment, pp. 48–53.

[2] Equinor. (2020). "Equinor sets ambition to reach net-zero emissions by 2050", [Online]. Available: https://www.equinor.com/en/news/20201102-emissions.html (visited on 11/23/2020).

[3] Norwegian Petroleum Directorate. (2020). "Norway's petroleum history", [Online]. Available: https://www.norskpetroleum.no/en/framework/norways-petroleum-history/ (visited on 11/25/2020).

[4] ——, (2020). "Recent activity", [Online]. Available: https://www.norskpetroleum.no/en/developments-and-operations/recent-activity/ (visited on 11/24/2020).

[5] ——, (2021). "Emissions to air", [Online]. Available: https://www.norskpetroleum.no/en/environment-and-technology/emissions-to-air/ (visited on 05/04/2021).

[6] M. Voldsund, I. S. Ertesvåg, W. He, and S. Kjelstrup, "Exergy analysis of the oil and gas processing on a north sea oil platform a real production day", *Energy*, vol. 55, pp. 716–727, 2013, ISSN: 0360-5442. DOI: https://doi.org/10.1016/j.energy.2013.02.038.

[7] M. Voldsund, T.-V. Nguyen, B. Elmegaard, I. S. Ertesvåg, A. Røsjorde, K. Jøssang, and S. Kjelstrup, "Exergy destruction and losses on four north sea offshore platforms: A comparative study of the oil and gas processing plants", *Energy*, vol. 74, pp. 45–58, 2014, ISSN: 0360-5442. DOI: https://doi.org/10.1016/j.energy.2014.02.080.

[8] M. J. Mazzetti, P. Nekså, H. T. Walnum, and A. K. T. Hemmingsen, "Energy-efficiency technologies for reduction of offshore CO_2 emissions", *Oil and gas facilities*, vol. 3, no. 1, pp. 89–96, 2014, ISSN: 0149-2136. DOI: https://doi.org/10.2118/169811-PA.

[9] T.-V. Nguyen, L. Pierobon, B. Elmegaard, F. Haglind, P. Breuhaus, and M. Voldsund, "Exergetic assessment of energy systems on north sea oil and gas platforms", *Energy*, vol. 62, pp. 23–36, 2013, ISSN: 0360-5442. DOI: https://doi.org/10.1016/j.energy.2013.03.011.

[10] L. O. Nord and O. Bolland, "Steam bottoming cycles offshore - challenges and possibilities", *Journal of power technologies*, vol. 92, no. 3, pp. 201–207, 2012, ISSN: 2083-4187.

[11] E. R. Følgesvold, H. S. Skjefstad, L. Riboldi, and L. O. Nord, "Combined heat and power plant on offshore oil and gas installations", *Journal of power technologies*, vol. 97, no. 2, pp. 117–126, 2017, ISSN: 2083-4187.

[12] H. T. Walnum, P. Nekså, L. O. Nord, and T. Andresen, "Modelling and simulation of CO_2 (carbon dioxide) bottoming cycles for offshore oil and gas installations at design and off-design conditions", *Energy*, vol. 59, pp. 513–520, 2013, ISSN: 0360-5442. DOI: https://doi.org/10.1016/j.energy.2013.06.071.

[13] T.-V. Nguyen, Y. M. Barbosa, J. A. da Silva, and S. de Oliveira Junior, "A novel methodology for the design and optimisation of oil and gas offshore platforms", *Energy*, vol. 185, pp. 158–175, 2019, ISSN: 0360-5442. DOI: https://doi.org/10.1016/j.energy.2019.06.164.

[14] T.-V. Nguyen, M. Voldsund, P. Breuhaus, and B. Elmegaard, "Energy efficiency measures for offshore oil and gas platforms", *Energy*, vol. 117, pp. 325–340, 2016, The 28th International Conference on Efficiency, Cost, Optimization, Simulation and Environmental Impact of Energy Systems - ECOS 2015, ISSN: 0360-5442. DOI: https://doi.org/10.1016/j.energy.2016.03.061.

[15] D. Rohde, H. T. Walnum, T. Andresen, and P. Nekså, "Heat recovery from export gas compression: Analyzing power cycles with detailed heat exchanger models", *Applied Thermal Engineering*, vol. 60, no. 1, pp. 1–6, 2013, ISSN: 1359-4311. DOI: https://doi.org/10.1016/j.applthermaleng.2013.06.027.

[16] L. Riboldi, S. Völler, M. Korpås, and L. O. Nord, "An integrated assessment of the environmental and economic impact of offshore oil platform electrification", *Energies (Basel)*, vol. 12, no. 11, p. 2114, 2019, ISSN: 1996-1073. DOI: https://doi.org/10.3390/en12112114.

[17] T.-V. Nguyen, L. Tock, P. Breuhaus, F. Maréchal, and B. Elmegaard, "CO_2-mitigation options for the offshore oil and gas sector", *Applied Energy*, vol. 161, pp. 673–694, 2016, ISSN: 0306-2619. DOI: https://doi.org/10.1016/j.apenergy.2015.09.088.

[18] W. He, G. Jacobsen, T. Anderson, F. Olsen, T. D. Hanson, M. Korpås, T. Toftevaag, J. Eek, K. Uhlen, and E. Johansson, "The potential of integrating wind power with offshore oil and gas platforms", *Wind engineering*, vol. 34, no. 2, pp. 125–137, 2010, ISSN: 0309-524X.

[19] Equinor. (2020). "Hywind tampen: The world's first renewable power for offshore oil and gas", [Online]. Available: https://www.equinor.com/en/what-we-do/hywind-tampen.html (visited on 11/28/2020).

[20] J. I. Marvik, E. V. Øyslebø, and M. Korpås, "Electrification of offshore petroleum installations with offshore wind integration", *Renewable Energy*, vol. 50, pp. 558–564, 2013, ISSN: 0960-1481. DOI: https://doi.org/10.1016/j.renene.2012.07.010.

[21] S. Oliveira-Pinto, P. Rosa-Santos, and F. Taveira-Pinto, "Electricity supply to offshore oil and gas platforms from renewable ocean wave energy: Overview and case study analysis", *Energy Conversion and Management*, vol. 186, pp. 556–569, 2019, ISSN: 0196-8904. DOI: https://doi.org/10.1016/j.enconman.2019.02.050.

[22] F. Haces-Fernandez, H. Li, and D. Ramirez, "Assessment of the potential of energy extracted from waves and wind to supply offshore oil platforms operating in the gulf of mexico", *Energies (Basel)*, vol. 11, no. 5, p. 1084, 2018, ISSN: 1996-1073. DOI: https://doi.org/10.3390/en11051084.

[23] S. Roussanaly, A. Aasen, R. Anantharaman, B. Danielsen, J. Jakobsen, L. Heme-De-Lacotte, G. Neji, A. Sødal, P. Wahl, T. Vrana, and R. Dreux, "Offshore power generation with carbon capture and storage to decarbonise mainland electricity and offshore oil and gas installations: A techno-economic analysis", *Applied Energy*, vol. 233-234, pp. 478–494, 2019, ISSN: 0306-2619. DOI: https://doi.org/10.1016/j.apenergy.2018.10.020.

[24] Equinor. (2020). “Carbon capture, utilisation and storage”, [Online]. Available: https://www.equinor.com/en/what-we-do/carbon-capture-and-storage.html (visited on 11/29/2020).

[25] I. Gökalp and E. Lebas, “Alternative fuels for industrial gas turbines (aftur)”, *Applied Thermal Engineering*, vol. 24, no. 11, pp. 1655–1663, 2004, Industrial Gas Turbine Technologies, ISSN: 1359-4311. DOI: https://doi.org/10.1016/j.applthermaleng.2003.10.035.

[26] W. D. York, W. S. Ziminsky, and E. Yilmaz, “Development and Testing of a Low NOx Hydrogen Combustion System for Heavy-Duty Gas Turbines”, *Journal of Engineering for Gas Turbines and Power*, vol. 135, no. 2, Jan. 2013, ISSN: 0742-4795. [Online]. Available: https://doi.org/10.1115/1.4007733.

[27] Y. Koç, H. Yağlı, A. Görgülü, and A. Koç, “Analysing the performance, fuel cost and emission parameters of the 50 mw simple and recuperative gas turbine cycles using natural gas and hydrogen as fuel”, *International Journal of Hydrogen Energy*, vol. 45, no. 41, pp. 22 138–22 147, 2020, ISSN: 0360-3199. DOI: https://doi.org/10.1016/j.ijhydene.2020.05.267.

[28] S. Meziane and A. Bentebbiche, “Numerical study of blended fuel natural gas-hydrogen combustion in rich /quench /lean combustor of a micro gas turbine”, *International Journal of Hydrogen Energy*, vol. 44, no. 29, pp. 15 610–15 621, 2019, ISSN: 0360-3199. DOI: https://doi.org/10.1016/j.ijhydene.2019.04.128.

[29] G. Juste, “Hydrogen injection as additional fuel in gas turbine combustor. evaluation of effects”, *International Journal of Hydrogen Energy*, vol. 31, no. 14, pp. 2112–2121, 2006, ISSN: 0360-3199. DOI: https://doi.org/10.1016/j.ijhydene.2006.02.006.

[30] D. Todd and R. Battista, “Demonstrated applicability of hydrogen fuel for gas turbines”, 2001. [Online]. Available: http://citeseerx.ist.psu.edu/viewdoc/summary?doi=10.1.1.140.7410.

[31] S. Holum, personal communication, Aug. 17, 2020.

[32] E. C. Carlson, “Don’t gamble with physical properties for simulations”, *Chemical Engineering Progress*, vol. 92, pp. 35–46, 1996.

[33] J. M. Campbell, “Gas conditioning and processing : Vol. 2”, in, 8th. Norman, Okla: Campbell Petroleum Series, 2002, vol. 2, ch. 18, pp. 333–394.

[34] R. Chebbi, M. Qasim, and N. Abdel Jabbar, “Optimization of triethylene glycol dehydration of natural gas”, *Energy Reports*, vol. 5, pp. 723–732, 2019, ISSN: 2352-4847. DOI: https://doi.org/10.1016/j.egyr.2019.06.014.

[35] L. Riboldi and L. Nord, “Offshore power plants integrating a wind farm: Design optimisation and techno-economic assessment based on surrogate modelling”, *Processes*, vol. 6, no. 12, p. 249, 2018, ISSN: 2227-9717. DOI: https://doi.org/10.3390/pr6120249.

[36] Norwegian Petroleum Directorate. (2021). “Abc of oil”, [Online]. Available: https://www.npd.no/en/about-us/information-services/abc-of-oil/ (visited on 04/05/2021).

[37] S. Gardarsdottir, M. Voldsund, and S. Roussanaly, *Comparative techno-economic assessment of low-co2 hydrogen production technologies*, 2019. [Online]. Available: https://www.sintef.no/globalassets/project/hyper/presentations-day-1/day1_1200_gardarsdottir_comparative-techno-economic-assessment-of-low-co2-hydrogen-production-technologies_sintef.pdf (visited on 04/05/2021).

[38] M. Höök, B. Söderbergh, K. Jakobsson, and K. Aleklett, "The evolution of giant oil field production behavior", *Natural Resources Research*, vol. 18, pp. 39–56, 2009. DOI: 10.1007/s11053-009-9087-z.

[39] Journal of Petroleum Technology. (2021). "Life extension of mature facilities through robust engineering and chemistry solutions", [Online]. Available: https://jpt.spe.org/life-extension-mature-facilities-through-robust-engineering-and-chemistry-solutions (visited on 04/05/2021).

Chapter A

Model Development

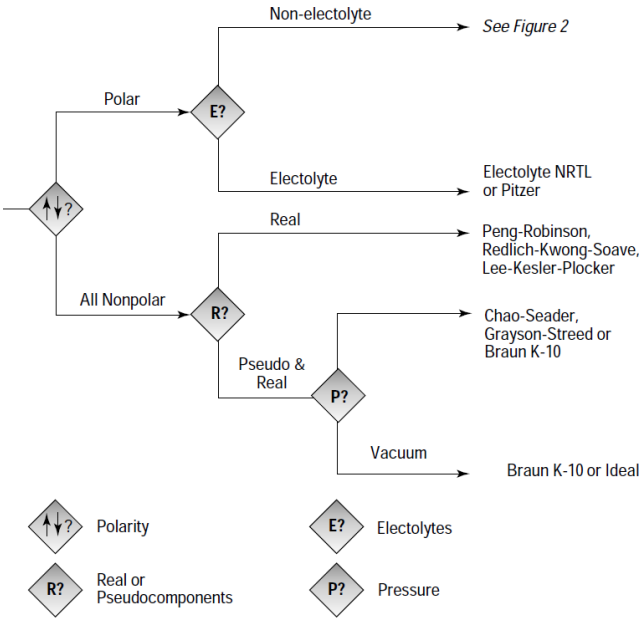

Figure A.1 Equation of state decision tree [32]

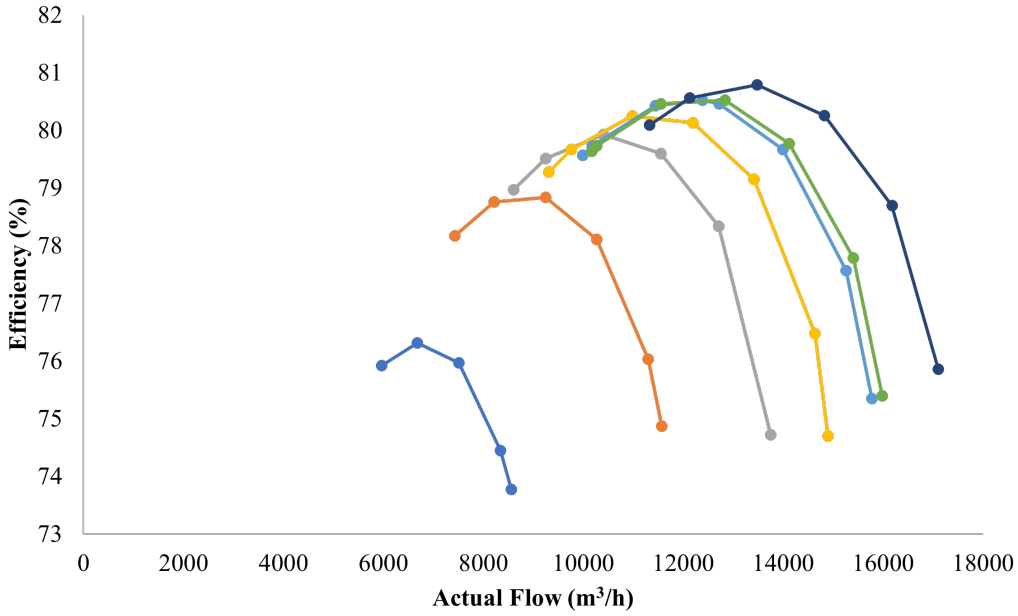

Figure A.2 Sample compressor map, developed on Aspen HYSYS

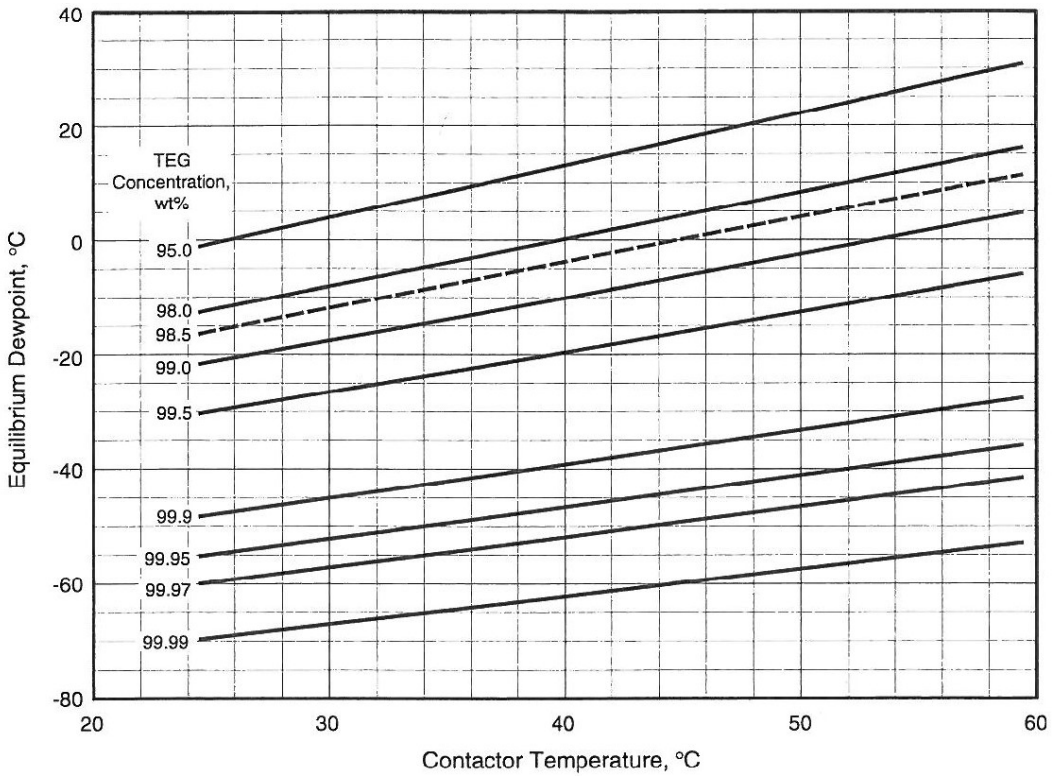

Figure A.3 Equilibrium water dewpoint at various contactor temperatures and TEG concentrations, taken from [33]

Table A.1: Full comparison between developed model and the control model outlet streams for Platform A

Stream	Variable	HYSYS Model	UniSim Model	Percentage Difference
Gas Export	Mass Flowrate (kg/s)	87.7	87.9	0.232%
	Pressure (bar)	167	167	0.000%
	Temperature (°C)	50.0	50.0	0.000%
	MW (g/mol)	19.4	19.4	0.0526%
Oil Export	Mass Flowrate (kg/s)	94.8	94.8	0.0431%
	Pressure (bar)	1.90	1.90	0.000%
	Temperature (°C)	15.0	15.0	0.000%
	MW (g/mol)	188	187	0.267%
Gas Reinjection	Mass Flowrate (kg/s)	75.8	75.9	0.0430%
	Pressure (bar)	432	432	0.000%
	Temperature (°C)	53.0	53.0	0.000%
	MW (g/mol)	19.4	19.4	0.0492%
Fuel Gas	Mass Flowrate (kg/s)	6.41	6.41	0.0480%
	Pressure (bar)	30.5	30.5	0.000%
	Temperature (°C)	37.0	37.0	0.000%
	MW (g/mol)	18.7	18.7	0.00657%
Produced Water	Mass Flowrate (kg/s)	194	194	0.00226%
	Pressure (bar)	19.0	19.0	0.000%
	Temperature (°C)	57.4	56.9	0.9034%

Table A.2: Full comparison between developed model and the control model compressor requirements for Platform A

Unit	Variable	HYSYS Model	UniSim Model	Percentage Difference
1st Gas Recompressor	Duty (kW)	1082	969	10.4%
	η_{np} (%)	67	63	5.02%
	Pressure Ratio	5.85	5.24	10.3%
	Mass Flow (kg/s)	3.84	3.86	0.59%
2nd Gas Recompressor	Duty (kW)	588	635	7.93%
	η_{np} (%)	43	42	1.68%
	Pressure Ratio	2.15	2.33	8.38%
	Mass Flow (kg/s)	3.18	3.19	0.18%
3rd Gas Recompressor	Duty (kW)	2914	2860	1.8%
	η_{np} (%)	64	60	6.2%
	Pressure Ratio	3.2	3.2	0.00%
	Mass Flow (kg/s)	11.9	11.8	0.86%
3rd Gas Recompressor	Duty (kW)	33237	33207	0.09%
	η_{np} (%)	80.2	77.9	2.86%
	Pressure Ratio	3.2	3.2	0.02%
	Mass Flow (kg/s)	164	164	0.13%
Gas Reinjection Compressor	Duty (kW)	15125	15202	0.51%
	η_{np} (%)	70.9	70.5	0.51%
	Pressure Ratio	2.7	2.7	0.48%
	Mass Flow (kg/s)	82	82	0.1%

Table A.3: Full comparison between developed model and the control model heating and cooling requirements for Platform A

Unit	Variable	HYSYS Model	UniSim Model	Percentage Difference
Gas Export Compressor Aftercooler	Duty (kW)	42718	42694	0.1%
	T_{supply}	137	136	0.4%
	T_{target}	50	50	0.0%
	Mass Flow (kg/s)	164	164	0.1%
Gas Dehydration Cooler 1	Duty (kW)	7385	7033	4.8%
	T_{supply}	54	52	3.8%
	T_{target}	30	30	0.0%
	Mass Flow (kg/s)	113	107	5.5%
Gas Dehydration Cooler 2	Duty (kW)	3649	4086	12.0%
	T_{supply}	55	55	0.0%
	T_{target}	30	30	0.0%
	Mass Flow (kg/s)	56	62	11.2%
Recompression Aftercooler 1	Duty (kW)	706	715	1.3%
	T_{supply}	111	99	10.4%
	T_{target}	30	30	0.0%
	Mass Flow (kg/s)	3.90	3.97	1.7%
Recompression Aftercooler 2	Duty (kW)	1003	972	3.1%
	T_{supply}	152	144	5.4%
	T_{target}	30	30	0.0%
	Mass Flow (kg/s)	3.45	3.45	0.2%
Recompression Aftercooler 3	Duty (kW)	1417	1610	13.6%
	T_{supply}	77	84	9.1%
	T_{target}	30	30	0.0%
	Mass Flow (kg/s)	12	12	0.8%
Gas Reinjection Cooler	Duty (kW)	15876	15961	0.5%
	T_{supply}	113	116	3.0%
	T_{target}	53	53	0.0%
	Mass Flow (kg/s)	82	82	0.1%
Gas Reinjection Aftercooler	Duty (kW)	3848	3886	1.0%
	T_{supply}	47	47	0.2%
	T_{target}	33	33	0.0%
	Mass Flow (kg/s)	82	82	0.1%
Export Crude Cooler	Duty (kW)	7869	7889	0.3%
	T_{supply}	54	58	7.4%
	T_{target}	15	15	0.0%
	Mass Flow (kg/s)	95	95	0.0%
Inlet Crude Heater	Duty (kW)	6035	6111	1.3%
	T_{supply}	50	50	0.4%
	T_{target}	78	78	0.5%
	Mass Flow (kg/s)	95	95	0.3%

Chapter B

Model Analysis

Table B.1: Volumetric flowrates for the oil, gas and water components over the platform lifespan

Year of Operation	Unit	Water	Gas	Oil	Inerts	Total
0	Sm^3/h	0	0	0	0	0
5	Sm^3/h	100	350	650	3.73	1104
10	Sm^3/h	200	500	1100	7.45	1807
15	Sm^3/h	264	561	1093	9.85	1928
20	Sm^3/h	450	500	850	16.8	1817
25	Sm^3/h	600	425	775	22.4	1822
30	Sm^3/h	750	300	450	28.0	1528

Table B.2: Assumed values for the operating costs of the platform throughout the entire lifespan

Year	Unit	5	10	15	20	25	30
Cost of H_2	NOK/kg	16.2	16.2	16.2	16.2	16.2	16.2
Cost of NG	NOK/kg	2.15	2.15	2.15	2.15	2.15	2.15
Carbon Tax	NOK/kg CO_2	493	740	1109	1664	2496	3744

Table B.3: Complete results for the initial comparison of the various technologies

Year	Unit	Combination A	Combination B	Combination C	Combination D	Combination E	Combination F
Gas Turbine	-	LM2500 G4 +	LM2500 G4 +	LM2500 G4 +	LM2500 G4 +	LM2500 G4 +	LM2500 G4 +
Technology	-	-	H_2O BC	CO_2 BC	H_2O BC	H_2O BC	H_2O BC & CO_2 RC
Wind	-	x	x	x	x	✓	x
Wind Farm Size	kW	0	0	0	0	4000	0
Hydrogen	-	x	x	x	✓	x	x
H_2 Composition	mol %	0	0	0	50	0	0
H_2 Flowrate	kg/s	0	0	0	0.116	0	0
NG Flowrate	kg/s	1.63	1.36	1.38	1.06	1.28	1.31
Power Demand	kW	29172	29172	29172	29172	29172	29172
Gas Turbine Power	kW	29172	20347	20906	20347	18107	18900
Wind Farm Actual Supply	kW	0	0	0	0	2240	0
BC Power	kW	0	8825	8266	8825	8825	8825
CO_2 RC Power	kW	0	0	0	0	0	1448
Power Generation Efficiency	%	37.95%	45.48%	44.91%	45.40%	44.48%	44.83%
CO_2 Produced from GT	kg/s	4.39	3.66	3.71	2.87	3.46	3.53
CO_2 Produced from H_2	kg/s	0	0	0	0.093	0	0
Total CO_2 Produced	kg/s	4.39	3.66	3.71	2.96	3.46	3.53
CO_2 Produced	ktonnes/annum	138	116	117	93.4	109	111
CO_2 Produced	kgCO2/BOE	2.25	1.88	1.90	1.52	1.77	1.81
Cost of H_2	MNOK/annum	0	0	0	59.5	0	0
Cost of NG	MNOK/annum	111	92.4	93.6	72.3	87.1	89.0
Cost of CO_2 Tax	MNOK/annum	68.2	57.0	57.7	46.0	53.7	54.9
Total Operating Cost	MNOK/annum	179	149	151	178	141	144

Table B.4: Full results for platform lifespan analysis - Combination 1

Combination 1							
Year	-	**5**	**10**	**15**	**20**	**25**	**30**
Gas Turbine	-	LM2500 G4	LM2500 G4	LM2500 G4	LM2500 G4	LM2500 G4	LM2500 G4
Technology	-	x	x	x	x	x	x
Wind	-	x	x	x	x	x	x
Wind Farm Size	kW	0	0	0	0	0	0
H_2 Composition	mol %	0	0	0	0	0	0
H_2 Flowrate	kg/s	0	0	0	0	0	0
NG Flowrate	kg/s	1.45	1.63	1.72	1.62	1.54	1.42
Power Demand	kW	23295	29172	31244	29069	26732	22279
Gas Turbine Power	kW	23295	29172	31244	29069	26732	22279
Power Generation Efficiency	%	0.34	0.38	0.38	0.38	0.37	0.33
CO_2 Produced	kg/BOE	3.38	2.25	2.39	2.91	3.03	4.79
CO_2 Produced from GT	kg/s	3.90	4.39	4.64	4.38	4.16	3.82
CO_2 Produced from H_2	kg/s	0	0	0	0	0	0
Total CO_2 Produced	kg/s	3.90	4.39	4.64	4.38	4.16	3.82
CO_2 Produced	ktonnes/5 years	615	692	731	691	656	603
Cumulative Sum	ktonnes	615	1307	2038	2729	3385	3988
Cost of H_2	MNOK/5 years	0	0	0	0	0	0
Cost of NG	MNOK/5 years	492	553	585	552	525	482
Cost of CO_2 Tax	MNOK/5 years	303	512	811	1149	1638	2257
Total Sum	MNOK/5 years	795	1065	1396	1701	2162	2738
Cumulative Cost Sum	MNOK	795	1859	3255	4956	7118	9857

Table B.5: Full results for platform lifespan analysis - Combination 2

Combination 2							
Year		**5**	**10**	**15**	**20**	**25**	**30**
Gas Turbine		LM2500	LM2500	LM2500	LM2500	LM2500	LM2500
Technology	-	x	x	x	x	x	x
Wind	-	x	x	x	x	x	x
Wind Farm Size	kW	0	0	0	0	0	0
H_2 Composition	mol %	0	0	0	0	0	0
H_2 Flowrate	kg/s	0	0	0	0	0	0
NG Flowrate	kg/s	1.83	2.07	2.13	2.07	1.99	1.76
Power Demand	kW	23295	29172	31244	29069	26732	22279
Gas Turbine Power	kW	23295	29172	31244	29069	26732	22279
Power Generation Efficiency	%	27.0%	29.8%	31.0%	29.8%	28.5%	26.8%
CO_2 Produced	kg/BOE	4.27	2.86	2.97	3.70	3.90	5.95
CO_2 Produced from GT	kg/s	4.92	5.58	5.75	5.57	5.36	4.75
CO_2 Produced from H_2	kg/s	0	0	0	0	0	0
Total CO_2 Produced	kg/s	4.92	5.58	5.75	5.57	5.36	4.75
CO_2 Produced	ktonnes/5 years	776	880	906	879	846	749
Cumulative Sum	ktonnes	776	1657	2563	3442	4288	5037
Cost of H_2	MNOK/5 years	0	0	0	0	0	0
Cost of NG	MNOK/5 years	621	704	724	702	676	599
Cost of CO_2 Tax	MNOK/5 years	383	651	1005	1462	2111	2805
Total Sum	MNOK/5 years	1003	1355	1730	2165	2787	3404
Cumulative Cost Sum	MNOK	1003	2358	4088	6253	9040	12444

Table B.6: Full results for platform lifespan analysis - Combination 3

Combination 3							
Year		**5**	**10**	**15**	**20**	**25**	**30**
Gas Turbine	-	LM2500 G4	LM2500 G4	LM2500 G4	LM2500 G4	LM2500 G4	LM2500 G4
Technology	-	H_2O BC	H_2O BC	H_2O BC	H_2O BC	H_2O BC	H_2O BC
Wind	-	x	x	x	x	x	x
Wind Farm Size	kW	0	0	0	0	0	0
H_2Composition	mol %	0	0	0	0	0	0
H_2 Flowrate	kg/s	0	0	0	0	0	0
NG Flowrate	kg/s	1.11	1.36	1.42	1.36	1.28	1.09
Power Demand	kW	23295	29172	31244	29069	26732	22279
Gas Turbine Power	kW	23295	29172	31244	29069	26732	22279
Power Generation Efficiency	%	44.2%	45.5%	46.6%	45.4%	44.4%	43.5%
CO_2 Produced	kg/BOE	2.60	1.88	1.98	2.43	2.50	3.67
CO_2 Produced from GT	kg/s	3.00	3.66	3.83	3.66	3.44	2.93
CO_2 Produced from H_2	kg/s	0	0	0	0	0	0
Total CO_2 Produced	kg/s	3.00	3.66	3.83	3.66	3.44	2.93
CO_2 Produced	ktonnes/5 years	473	578	604	577	542	461
Cumulative Sum	ktonnes	473	1050	1654	2231	2774	3235
Cost of H_2	MNOK/5 years	0	0	0	0	0	0
Cost of NG	MNOK/5 years	378	462	482	461	434	369
Cost of CO_2 Tax	MNOK/5 years	233	427	670	960	1354	1727
Total Sum	MNOK/5 years	611	889	1152	1422	1787	2096
Cumulative Cost Sum	MNOK	611	1500	2652	4074	5861	7957
Savings related to C1	MNOK	184	360	603	883	1257	1900

Table B.7: Full results for platform lifespan analysis - Combination 4

Combination 4							
Year		**5**	**10**	**15**	**20**	**25**	**30**
Gas Turbine		LM2500 G4	LM2500 G4	LM2500 G4	LM2500 G4	LM2500 G4	LM2500 G4
Technology	-	x	x	x	x	x	x
Wind	-	x	x	x	x	x	x
Wind Farm Size	kW	0	0	0	0	0	0
H_2Composition	mol %	50	50	50	50	50	50
H_2 Flowrate	kg/s	0.12	0.14	0.15	0.14	0.13	0.12
NG Flowrate	kg/s	1.14	1.28	1.35	1.28	1.34	1.23
Power Demand	kW	23295	29172	31244	29069	26732	22279
Gas Turbine Power	kW	23295	29172	31244	29069	26732	22279
Power Generation Efficiency	%	34.0%	37.9%	38.4%	37.9%	36.6%	33.2%
CO_2 Produced	kg/BOE	2.74	1.82	1.94	2.36	2.45	3.88
CO_2 Produced from GT	kg/s	3.07	3.44	3.64	3.44	3.27	3.00
CO_2 Produced from H_2	kg/s	0.10	0.11	0.12	0.11	0.11	0.10
Total CO_2 Produced	kg/s	3.16	3.56	3.76	3.55	3.37	3.10
CO_2 Produced	ktonnes/5 years	499	561	593	560	532	488
Cumulative Sum	ktonnes	499	1060	1653	2213	2744	3233
Cost of H_2	MNOK/5 years	316	356	376	355	337	310
Cost of NG	MNOK/5 years	386	434	459	434	457	419
Cost of CO_2 Tax	MNOK/5 years	246	415	658	932	1327	1829
Total Sum	MNOK/5 years	949	1204	1493	1721	2121	2558
Cumulative Cost Sum	MNOK	949	2153	3646	5367	7488	10046
Savings related to C1	MNOK	-154	-294	-391	-410	-370	-189

Table B.8: Full results for platform lifespan analysis - Combination 5

Combination 5							
Year		**5**	**10**	**15**	**20**	**25**	**30**
Gas Turbine		LM2500 G4	LM2500 G4	LM2500 G4	LM2500 G4	LM2500 G4	LM2500 G4
Technology	-	x	x	x	x	x	x
Wind	-	✓	✓	✓	✓	✓	✓
Wind Farm Size	kW	4000	4000	4000	4000	4000	4000
H_2Composition	mol %	0	0	0	0	0	0
H_2 Flowrate	kg/s	0	0	0	0	0	0
NG Flowrate	kg/s	1.38	1.55	1.62	1.55	1.48	1.34
Power Demand	kW	23295	29172	31244	29069	26732	22279
Gas Turbine Power	kW	21055	26932	29004	26829	24492	20039
Power Generation Efficiency	%	32.3%	36.8%	38.0%	36.8%	35.1%	31.6%
CO_2 Produced	kg/BOE	3.23	2.14	2.25	2.77	2.90	4.53
CO_2 Produced from GT	kg/s	3.72	4.17	4.37	4.17	3.99	3.62
CO_2 Produced from H_2	kg/s	0	0	0	0	0	0
Total CO_2 Produced	kg/s	3.72	4.17	4.37	4.17	3.99	3.62
CO_2 Produced	ktonnes/5 years	587	658	689	658	629	571
Cumulative Sum	ktonnes	587	1245	1934	2592	3220	3791
Cost of H_2	MNOK/5 years	0	0	0	0	0	0
Cost of NG	MNOK/5 years	469	526	551	526	503	456
Cost of CO_2 Tax	MNOK/5 years	289	487	764	1095	1569	2137
Total Sum	MNOK/5 years	759	1013	1315	1620	2072	2594
Cumulative Cost Sum	MNOK	759	1771	3086	4706	6778	9371
Savings related to C1	MNOK	36	88	169	250	341	485

Table B.9: Full results for platform lifespan analysis - Combination 6

Combination 6							
Year		**5**	**10**	**15**	**20**	**25**	**30**
Gas Turbine		LM2500 G4	LM2500 G4	LM2500 G4	LM2500 G4	LM2500 G4	LM2500 G4
Technology	-	H_2O BC	H_2O BC	H_2O BC	H_2O BC	H_2O BC	H_2O BC
Wind	-	x	x	x	x	x	x
Wind Farm Size	kW	0	0	0	0	0	0
H_2Composition	mol %	50	50	50	50	50	50
H_2 Flowrate	kg/s	0.09	0.12	0.12	0.12	0.11	0.09
NG Flowrate	kg/s	0.87	1.06	1.11	1.07	1.00	0.85
Power Demand	kW	23295	29172	31244	29069	26732	22279
Gas Turbine Power	kW	23295	29172	31244	29069	26732	22279
Power Generation Efficiency	%	44.2%	45.4%	46.5%	45.3%	44.3%	43.4%
CO_2 Produced	kg/BOE	2.11	1.52	1.60	1.97	2.03	2.97
CO_2 Produced from GT	kg/s	2.35	2.87	3.00	2.87	2.70	2.30
CO_2 Produced from H_2	kg/s	0.08	0.09	0.10	0.09	0.09	0.07
Total CO_2 Produced	kg/s	2.43	2.96	3.10	2.96	2.79	2.37
CO_2 Produced	ktonnes/5 years	383	467	489	468	439	374
Cumulative Sum	ktonnes	383	850	1339	1807	2246	2620
Cost of H_2	MNOK/5 years	243	297	311	296	279	238
Cost of NG	MNOK/5 years	297	362	379	362	340	290
Cost of CO_2 Tax	MNOK/5 years	189	345	542	778	1096	1400
Total Sum	MNOK/5 years	729	1004	1232	1436	1716	1927
Cumulative Cost Sum	MNOK	729	1733	2965	4401	6117	8044
Savings related to C1	MNOK	66	127	290	555	1001	1812

Table B.10: Full results for platform lifespan analysis - Combination 7

Combination 7							
Year		**5**	**10**	**15**	**20**	**25**	**30**
Gas Turbine		LM2500 G4	LM2500 G4	LM2500 G4	LM2500 G4	LM2500 G4	LM2500 G4
Technology	-	H_2O BC	H_2O BC	H_2O BC	H_2O BC	H_2O BC	H_2O BC
Wind	-	✓	✓	✓	✓	✓	✓
Wind Farm Size	kW	4000	4000	4000	4000	4000	4000
H_2Composition	mol %	0	0	0	0	0	0
H_2 Flowrate	kg/s	0	0	0	0	0	0
NG Flowrate	kg/s	1.05	1.28	1.35	1.28	1.19	1.02
Power Demand	kW	23295	29172	31244	29069	26732	22279
Gas Turbine Power	kW	21055	26772	28844	26669	24332	19879
Power Generation Efficiency	%	42.6%	44.5%	45.4%	44.5%	43.7%	41.9%
CO_2 Produced	kg/BOE	2.45	1.77	1.88	2.29	2.33	3.43
CO_2 Produced from GT	kg/s	2.83	3.46	3.65	3.45	3.20	2.74
CO_2 Produced from H_2	kg/s	0	0	0	0	0	0
Total CO_2 Produced	kg/s	2.83	3.46	3.65	3.45	3.20	2.74
CO_2 Produced	ktonnes/5 years	446	545	576	544	505	432
Cumulative Sum	ktonnes	446	991	1566	2110	2615	3047
Cost of H_2	MNOK/5 years	0	0	0	0	0	0
Cost of NG	MNOK/5 years	356	436	460	435	403	345
Cost of CO_2 Tax	MNOK/5 years	220	403	639	905	1260	1617
Total Sum	MNOK/5 years	576	839	1099	1340	1663	1962
Cumulative Cost Sum	MNOK	576	1415	2513	3854	5517	7479
Savings related to C1	MNOK	219	445	742	1103	1602	2378

Table B.11: Full results for platform lifespan analysis - Combination 8

Combination 8							
Year		**5**	**10**	**15**	**20**	**25**	**30**
Gas Turbine		LM2500	LM2500	LM2500	LM2500	LM2500	LM2500
Technology	-	H_2O BC	H_2O BC	H_2O BC	H_2O BC	H_2O BC	H_2O BC
Wind	-	✓	✓	✓	✓	✓	✓
Wind Farm Size	kW	4000	4000	4000	4000	4000	4000
H_2Composition	mol %	0	0	0	0	0	0
H_2 Flowrate	kg/s	0	0	0	0	0	0
NG Flowrate	kg/s	1.01	1.19	1.27	1.18	1.11	0.98
Power Demand	kW	23295	29172	31244	29069	26732	22279
Gas Turbine Power	kW	21055	26772	28844	26669	24332	19879
Power Generation Efficiency	%	44.1%	48.1%	48.5%	48.1%	46.9%	43.5%
CO_2 Produced	kg/BOE	2.36	1.64	1.76	2.12	2.17	3.30
CO_2 Produced from GT	kg/s	2.73	3.19	3.41	3.19	2.99	2.63
CO_2 Produced from H_2	kg/s	0	0	0	0	0	0
Total CO_2 Produced	kg/s	2.73	3.19	3.41	3.19	2.99	2.63
CO_2 Produced	ktonnes/5 years	430	504	538	503	471	415
Cumulative Sum	ktonnes	430	933	1471	1975	2445	2861
Cost of H_2	MNOK/5 years	0	0	0	0	0	0
Cost of NG	MNOK/5 years	344	403	430	402	376	332
Cost of CO_2 Tax	MNOK/5 years	212	372	597	837	1175	1554
Total Sum	MNOK/5 years	555	775	1027	1239	1552	1886
Cumulative Cost Sum	MNOK	555	1331	2357	3597	5148	7034
Savings related to C1	MNOK	239	529	898	1360	1970	2823

Table B.12: Full results for low emission future scenario

Year	Unit	5	10	15	20	25	30
Gas Turbine	-	LM2500	LM2500	LM2500	LM2500	LM2500	LM2500
H_2O BC	-	✓	✓	✓	✓	✓	✓
Wind Energy	-	✓	✓	✓	✓	✓	✓
H_2 Fuel	-	x	x	x	✓	✓	✓
H_2 Fuel Percentage	mol. %	0	0	0	50	70	90
Wind Farm Size	kW	4000	4000	4000	4000	4000	4000
Actual Wind Farm Size	kW	2240	2240	2240	2240	2240	2240
H_2 Flowrate	kg/s	0	0	0	0.101	0.171	0.276
NG Flowrate	kg/s	1.01	1.19	1.27	0.930	0.676	0.281
Total Power Demand	kW	23295	29172	31244	29069	26732	22279
Gas Turbine Power	kW	21055	26932	29004	26829	24492	20039
Power Generation Efficiency	%	44.1%	48.1%	48.5%	48.0%	47%	43.3%
CO_2 Produced (KPI)	kg/BOE	2.36	1.64	1.76	1.72	1.43	1.22
CO_2 Produced from GT	kg/s	2.73	3.19	3.41	2.51	1.82	0.756
CO_2 Produced from H_2	kg/s	0	0	0	0.0808	0.137	0.221
Total CO_2 Produced	kg/s	2.73	3.19	3.41	2.59	1.96	0.977
Total CO_2 Produced	ktonnes/5 years	430	504	538	408	309	154
Cumulative Sum of CO_2	ktonnes	430	933	1471	1879	2188	2342
Cost of H_2	MNOK/5 years	0	0	0	259	439	706
Cost of NG	MNOK/5 years	344	403	430	316	230	95.3
Cost of CO_2 Tax	MNOK/5 years	212	372	597	679	771	577
Total Cost	MNOK/5 years	555	775	1027	1253	1440	1378
Cumulative Cost Sum	MNOK	555	1331	2357	3611	5050	6428

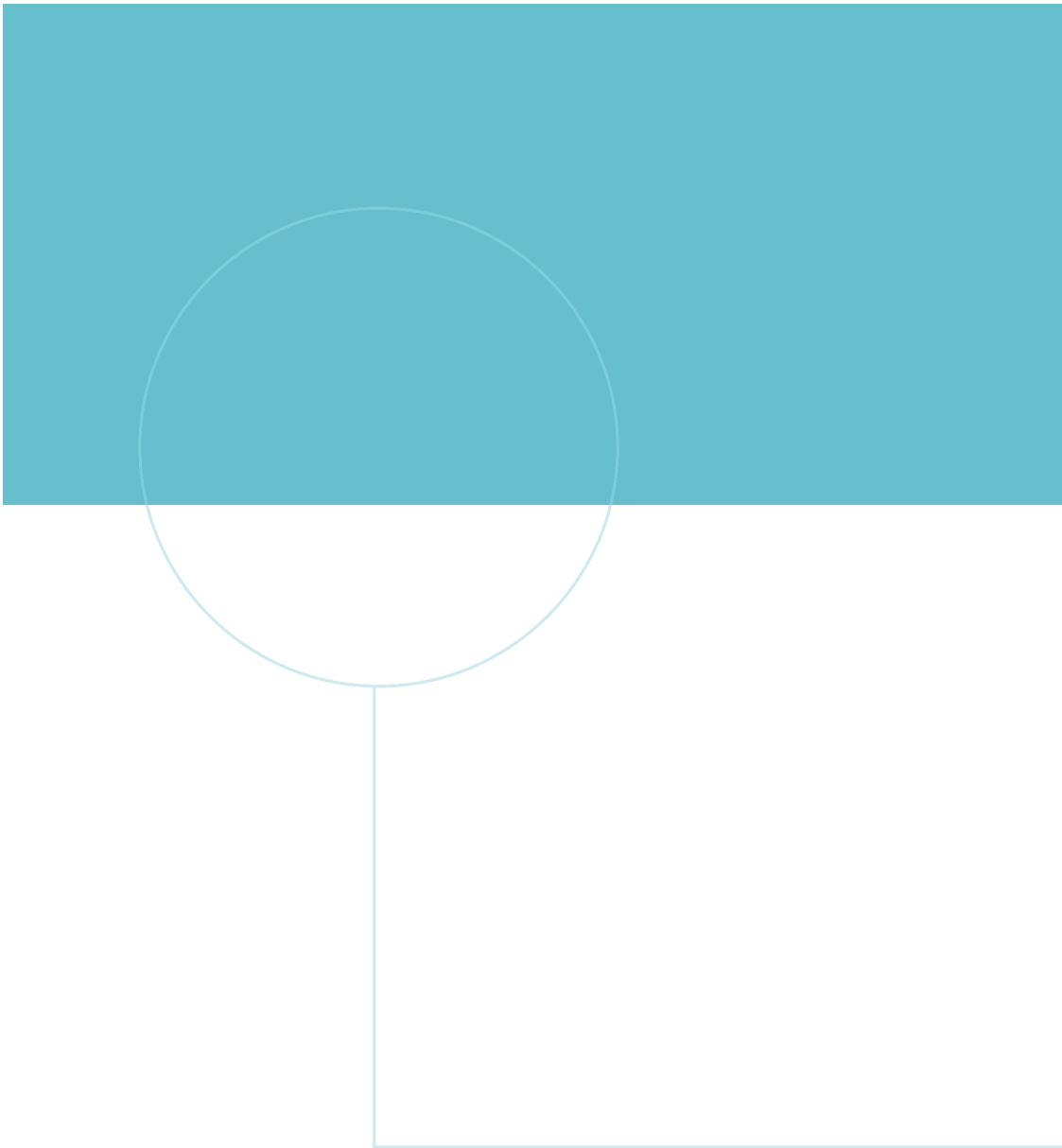

NTNU

Kunnskap for en bedre verden